2018

Phytochemical Investigation of a Native North American Species, "*Acer saccarinum*" and an Endemic Saudi Arabian Species, "*Euphorbia saudiarabica*"

Abdullatif Bin Muhsinah
University of Rhode Island, pharmakku@hotmail.com

PHYTOCHEMICAL INVESTIGATIONS OF A NATIVE NORTH AMERICAN SPECIES, "*ACER SACCHARINUM*" AND AN ENDEMIC SAUDI ARABIAN SPECIES, "*EUPHORBIA SAUDIARABICA"*

BY

ABDULLATIF BIN MUHSINAH

A DISSERTATION SUBMITTED IN PARTIAL FULFILLMENT OF THE REQUIREMENTS FOR THE DEGREE OF

DOCTOR OF PHILOSOPHY

IN

PHARMACEUTICAL SCIENCES

UNIVERSITY OF RHODE ISLAND

2018

DOCTOR OF PHILOSOPHY DISSERTATION

OF

ABDULLATIF BIN MUHSINAH

APPROVED:

Dissertation Committee

Major Professor

Navindra P. Seeram

Nasser Zawia

Brenton DeBoef

Nasser Zawia

DEAN OF THE GRADUATE SCHOOL

UNIVERSITY OF RHODE ISLAND

2018

ABSTRACT

The objectives of this work are the isolation, purification, structure elucidation, and biological evaluation of bioactive secondary metabolites, primarily tannins and diterpenoids, of two plant species: silver maple (*Acer saccharinum*) and *Euphorbia saudiarabica,* respectively.

Based on the ethnopharmacological literature, *Acer saccharinum* is a traditional medicinal plant that has been used by the people of North America. According to previous phytopharmacological studies by our group, over 70 phytochemicals, primarily tannins and flavonoids, have been discovered from three different maple species, including sugar (*Acer saccharum*), red (*Acer rubrum*), and sycamore (*Acer pseudoplatanus*) maples. Remarkably, the red maple species yielded very interesting bioactive (α-glucosidase inhibitors) glucitol-core containing gallotannins (GCGs). Therefore, to gain a better understanding of the phytochemical composition of other maple species, such as silver maple, the fresh leaves of silver maple were collected and extracted. Following this, the crude extracts of different polarities were prepared, and then all extracts initially screened using reversed-phase high-performance liquid chromatography (RP-HPLC) and thin-layer chromatography (TLC), and the Folin-Ciocalteau assay for quantifying polyphenol contents. Then, the isolation procedure was carried out using multiple techniques, including open column chromatography (OCC), TLC, and RP-HPLC on the highest total polyphenol content extract (which was the ethyl acetate [EtOAc] extract). Using high-performance liquid chromatography with diode-array detector (HPLC-DAD) analyses using previously isolated standards, nine compounds, including six GCGs, were identified as ginnalins A–C (**1**–**3**), maplexins B,

D, and F (**4–6**), methyl syringate (**7**), methyl gallate (**8**), and 3-methoxy-4-hydroxyphenol-1-β-D-(6-galloyl)-glucopyranoside (**9**). Additionally, pubineroid A (**10**), a sesquiterpenoid, was isolated and identified (by NMR).

The *Euphorbia* genus is one of the six largest genera of flowering plants which are known to produce several bioactive secondary metabolites, primarily diterpenes such as jatrophane and lathyrane-type. *Euphorbia saudiarabica*, which is endemic to Saudi Arabia, is well characterized by the production of a milky irritant latex. It is one of the plant species in the region that has not been studied. To increase the knowledge of the constituents of *E. saudiarabica*, a comprehensive phytochemical investigation was conducted, leading to the isolation of five new lathyrane-type diterpenoids (**1-5**) named saudiarabicain **A–E**. These compounds were evaluated for their cytotoxic activities against three cell lines, including, murine B16F10 melanoma cells, human HaCat keratinocytes, and human SH-SY5Y neuroblastoma cells. In B16F10 melanoma cells, only compounds **2**, **3**, and **4** induced significant toxicity, with compound **2** having the greatest range of toxicity from 100 μM (49.63% decrease) to 20 μM (14.69% decrease). In human keratinocytes (HaCat), each compound caused a decrease in cell viability with concentrations above 40 μM. At a concentration of 30 μM, compounds **3** and **4** caused reductions in cell viability by approximately 12.42% and 17.92%, respectively. Compound **3** was able to decrease viability by as much as 93.63% at 50 μM. Lastly, in SH-SY5Y cells, all of thecompounds (**1–5**) induced a cytotoxic effect at concentrations of 50 μM and above.

Lastly, for the first time, a qualitative analysis of the flavonoids present in a methanol extract of the aerial parts of *E. saudiarabica* using LC-ESI-TOF-MS/MS was

conducted. This led to the identification of 36 flavonoids including 7 flavonoids based on the galangin aglycon, 9 flavonoids based on the apigenin aglycon, and 20 flavonoids originated from luteolin.

In conclusion, this dissertation provids insights about the phenolic constituents, primarily tannins, of silver maple (*Acer saccharinum*), compared to other common maple species, mainly the sugar (*A. saccharum*), red (*A.rubrum*), and sycamore *(A. pseudoplatanus*) maples which were previously investigated by our group. In addition, the endemic *Euphorbia saudiarabica* species from Saudi Arabia yielded five new lathyrane-type of diterpenoids. All compounds evaluated for their cytotoxicity showed moderate effects. Lastly, a rapid and reliable method employing LC-ESI-TOF-MS/MS was developed for the identification of flavonoids in the aerial parts of *E. saudiarabica.*

ACKNOWLEDGMENTS

Without the guidance and blessing of Allah (Almighty God) and the kindness, understanding, and support of many people, this work would not have been possible.

I would like to thank my advisor, Dr. Navindra Seeram, for providing me with the opportunity to work on these projects. I would like to thank him for believing in me and helping to guide me to become a scientist from the very beginning of my time at the University of Rhode Island. I am grateful that he has worked with me, challenged me, and helped me to become a better scientist and a better person.

I would like to thank my family (mother, father, brothers, and sisters) in Saudi Arabia for their support, which made my graduate studies possible in the USA at URI. Moreover, my deepest gratitude to my wife (Aeshah) for her continuous support of me and our three beautiful kids (Ghaida, Naif, and Bayan). Without them, my research would not have been possible. I would like to thank my committee members, Dr. Brenton DeBoef, Dr. Koray Özpolat, and last but not least, graduate school dean, Dr. Nasser Zawia, for their review and contribution to my dissertation. I am thankful to have their wisdom and guidance to help me develop my thinking and approach to science in the academic sphere and beyond.

I would like to thank Dr. Yongqiang Liu, Dr. Tao Yuan, and Dr. Hang Ma, post-doctoral fellows in Dr. Seeram's group, for their patience and quality of time and instruction on the finer points of the practice of natural products chemistry in the laboratory. I will always remember their humility, strength, and perseverance; their conduct serves as an example of integrity that I will always remember, as well. I would also like to sincerely thank Dr. Al Bach for his guidance and his thoughtfulness in

patiently guiding me through experiments in NMR and their interpretation. I would like to thank Dr. David Rowley, department chair, for his teaching, advising, and his great support. All his lab members have done an excellent job helping me.

My warm thanks to Peter Morgan, master gardener and director of the College of Pharmacy's Medicinal Plant Garden, for the inspiration he has provided both with his words and his beautiful gardens, but mostly for his kindness and continued faith in me. Also, I would like to thank all of the Muslim community members in Kingstown for their help and guidance and warm friendships. I would like to thank my extended family and friends, for all of their love and support. Lastly, I am grateful to lab members and colleagues, especially Daniel Niesen, Craig Hessler, Nicholas A. DaSilva, and Shelby Johnson, for all their help and kind words to keep me working towards my goal.

PREFACE

This dissertation is written based on the University of Rhode Island "Guidelines for the Format of Thesis and Dissertations" standards for the manuscript format. This dissertation is composed of three manuscripts to satisfy the requirements of the Department of Biomedical and Pharmaceutical Sciences, College of Pharmacy, University of Rhode Island.

MANUSCRIPT I: **Bioactive Glucitol-Core Containing Gallotannins and Other Phytochemicals from Silver Maple (*Acer saccharinum*) Leaves.**

This manuscript was published in *Natural Products Communication*, 2017.

The objective of this work was to investigate the secondary metabolites, primarily polyphenolic compounds, and especially, gallotannins. The presence of unique gallotannins-type compounds in several maple species, including sugar, red, and sycamore species, and their bioactivities, prompted us to seek for new gallotannin compounds and/or known compounds from silver maple leaves.

MANUSCRIPT II: Saudiarabicain A–E, Macrocyclic Diterpenoids from *Euphorbia saudiarabica*.

This manuscript will be submitted to the *Journal of Natural Products*.

In this work, we investigated the phytochemical constituents of an endemic species from Saudi Arabia called *Euphorbia saudiarabica*. The genus *Euphorbia* is well known for its richness of secondary metabolites, primarily diterpenes, in their latex. The aerial parts of the plant were collected in 2014 in Saudi Arabia, where they are located in a colony close to the Red Sea. Next, it was extracted using methanol and sent to our laboratory

for further investigation. Several steps of purification and structure characterization were conducted, resulting in the isolation of five new diterpenoids compounds named saudiarabicains **A**–**E**. These compounds were evaluated for their cytotoxicity against three cell lines including murine B16F10 melanoma cells, human HaCat keratinocytes, and human SH-SY5 neuroblastoma cells.

MANUSCRIPT III. Liquid Chromatography Coupled with Time-of-Flight Mass Spectrometry for Rapid Identification of Flavonoids from Aerial Parts of *Euphorbia saudiarabica*

This manuscript will be submitted to the *Journal of Separation Science.*

This work focused on the phenolic contents, mainly flavonoids, of *Euphorbia saudiarabica*. The methanol extract of the plant was investigated using LC-ESI-TOF-MS/MS.

TABLE OF CONTENTS

INTRODUCTION

MANUSCRIPTS

MANUSCRIPT II:

MANUSCRIPT III:

LIST OF TABLES

Introduction

TABLE **PAGE**

Manuscript I

Manuscript II

TABLE **PAGE**

Manuscript III

TABLE **PAGE**

LIST OF FIGURES

Introduction

FIGURE **PAGE**

Manuscript I.

FIGURE **PAGE**

Manuscript II

FIGURE **PAGE**

Manuscript III

Figure **PAGE**

INTRODUCTION

All organisms are required to produce many organic compounds to enable them to live, grow, and reproduce. These organisms, such as plants, need to supply themselves with energy and sufficient amounts of building blocks to build up their tissues. Vast quantities of enzymes are involved in accelerating and regulating the chemical reactions that take place in organisms, and the pathways involved are called metabolic pathways. Carbohydrates, proteins, fats, and nucleic acids are some of the essential molecules for all organisms. Organisms differ broadly in their ability to synthesize and transform chemicals; plants are well known for their highly efficient synthesis of organic molecules. They produce these molecules through photosynthesis, a process through which light energy is converted into chemical energy that can be used to fuel energy transformations when they are needed later on. This diverse array of organic molecules, essential to plants, are called metabolites [(1)].

There are two types of metabolites: primary and secondary. The primary metabolites are all those organic compounds that are primarily involved in synthesizing and modifying the fundamental compounds of the plants including carbohydrates, proteins, fats, and nucleic acids, which are essential for vital processes such as glycolysis, fatty acid oxidation, carbohydrate degradation, etc. They, in other words, are all the metabolites that are directly involved in a plant's normal growth, reproduction, and development. By contrast, the secondary metabolites have a much more limited distribution within the plant kingdom [(2)]. Moreover, these types of metabolites are not necessarily produced in all plants because they are not directly involved in the plants' vital processes. Although the benefits of these compounds are not yet known, there are nonetheless some plausible

reasons for plants to have these types of metabolites. They include providing defense against predators by producing toxic compounds and warning other species by producing coloring agents. Biosynthetically, secondary metabolites are derived from primary metabolites through many complex biochemical pathways. These metabolites can be found in any of the plants' organs, such as their leaves, stem, bark, or roots. However, they may vary in their concentration based on their location in the plant. The secondary metabolites are also known as natural products [3].

Most of the pharmacological effects of a specific plant on humans or animals are due to the presence of one or more of these natural products, which are called bioactive natural products. The pharmacological effects of these products are many, such as therapeutic activities for diseases, or toxic activities responsible for human or animal illnesses. Furthermore, based on the secondary metabolites' biosynthetic origins and their chemical structure, there are three main classes of compounds: terpenes and steroids, phenolics, and nitrogen-containing compounds **(Fig. 1)** [1,3,4].

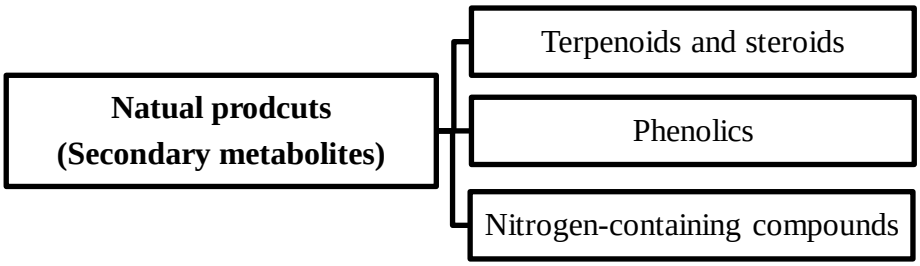

Figure 1. The main classes of natural products.

1- Phenolic compounds

Plants produce a vast variety of natural products such as phenolics, which contain a phenolic group that is chemically heterogeneous. Some of them are water soluble, others are soluble in organic solvents, and some are insoluble polymers. These phenolics have a very broad range of physiological roles in plants. For instance, some phenolics serve as a defense system against environmental stresses, including herbivores, pathogens, low temperatures, and nutrient deficiency. Phenolics arise biosynthetically via several different routes; however, the most important ones are the shikimic acid and malonic acids pathways. The shikimic acid pathway is the main route to produce most of the plant phenolics. It begins with a coupling of two start molecules: phosphoenolpyruvate (PEP) from the glycolytic pathway, and D-erythrose 4-phosphate from the pentose phosphate cycle. These two molecules produce a six-cyclic carbon compound with one carbon (COOH) side chain, namely shikimate, through an aldol-type condensation reaction. Then, several other complex transformations are formed to produce many different phenolic types (**Fig. 2**) [(5)].

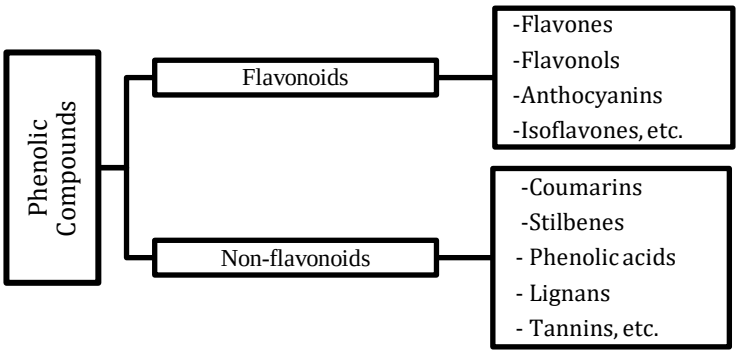

Figure 2. The main classes of phenolic compounds.

Tannins are a unique group of phenolic compounds called non-flavonoids, which have the capability to bind strongly with other secondary metabolites such as alkaloids, polysaccharides, and proteins. There are four main kinds of tannins, including:

1. Gallotannins, which are hydrolyzable tannins that galloyl units are attached to via several polyol residues.
2. Ellagitannins, which are hydrolyzable tannins. At least two galloyl units are attached to each other (C-C coupled) and are linked to D-glucosyl units.
3. Complex tannins, which are built up from a combination of either a gallotannin, a ellagitannin unit, or both, and a catechin unit.
4. Condensed tannins, which are polymers of polyhydroxy-flavan-3-ol monomers (also known as proanthocyanidins). [6,7]

Many of these tannins can be found in grape seeds, apple juice, strawberries, raspberries, pomegranates, walnuts, muscadine grapes, peaches, blackberries, etc.

Flavonoids and their conjugate forms are one of the most abundant polyphenols; over 8000 different flavonoids have been reported. In addition, they are considered to be the most plentiful of natural products in human diet since they are found in many plant tissues, including fruits and vegetables. The basic chemical structure of flavonoids is a skeleton of diphenylpropane connected by a three-carbon chain “bridge” which is biosynthetically derived from two different pathways: the shikimic acid pathway and malonic acid pathway. The three carbon chain bonds with one oxygen linked to form a pyran ring (heterocyclic ring) with one phenyl ring (malonic acid derived) to eventually form the benzopyrano ring moiety. Therefore,

the skeletal structure of the flavonoid can be abbreviated C6-C3-C6 (**Fig. 3**). Thus, according to the position of the bond of the aromatic ring to the

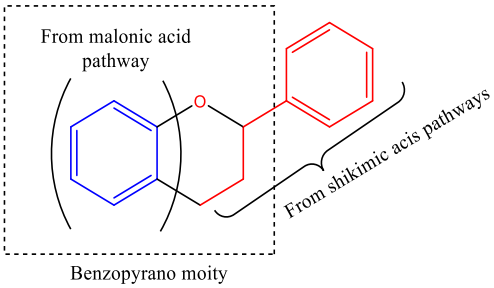

Figure 3. The skeletal structure of the flavonoids.

benzopyrano moiety and the degree of oxidation of the three-carbon chain, this flavonoid can be divided into four main classes: the anthocyanins, the flavones, the flavonols, and the isoflavones (**Fig. 4**) [8].

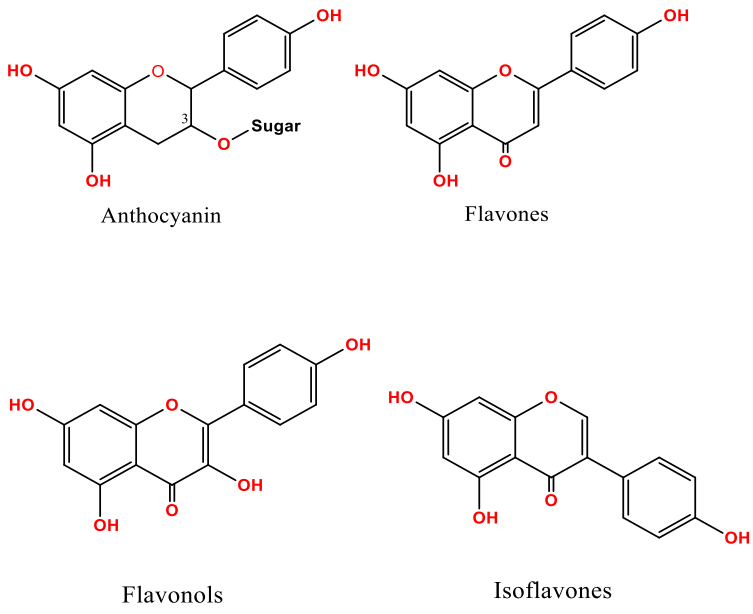

Figure 4. The skeletal structure of the four main classes of the flavonoid compounds.

2- Terpenoid compounds

The terpenoids, or the terpenes, are one of the most diverse classes of secondary metabolites. Most of them are known for their water insolubility. All terpenoids are

synthesized from acetyl-CoA or its glycolytic intermediates. Based on the number of isoprene units (C5) that are linked to each other, several sub-class of terpenes are produced as follows:

A- Monoterpene compounds (C10) are formed from an infusion of two isoprene units such as menthol and linalool.

B- Sesquiterpene compounds (C15) are composed of three isoprene units.

C- Diterpene compounds (C20) are formed from four isoprene units.

D- Triterpene compounds (C30) are formed from six isoprene units.

E- Tetraterpene compounds (C40) are composed by the fusion of eight isoprene units.

These terpenes are synthesized from primary metabolites by either the mevalonic acid pathway (MVA) or the methylerythritol phosphate (MEP) pathway. Most of the plant diterpenes, such as *Euphorbia* genus diterpenes, are produced through the MEP pathway. Most of the terpenes are known for their vital roles in plant growth, development, and defensive systems. Some of them are considered primary metabolites rather than secondary metabolites due to their fundamental role in plant life. For instance, sterols are essential components of cell membranes [9].

Diterpenes biosynthetically arise from their geranylgeranyl diphosphate (GGPP) precursors, which are initially derived from four isoprene units. They can be found in two main types, which are:

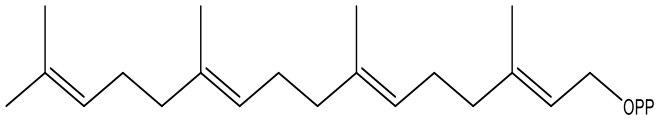

geranylgeranyl PP
(GGPP)

Figure 5. The chemical structure of geranylgeranyl diphosphate (GGPP) precursor.

- **Acyclic diterpenoids,** such as phytol, the reduced form of geranylgeraniol that form the side-chain of the chlorophylls, and phytyl, which is found in vitamin K.
- **Cyclic diterpenoids,** which are also subdivided into different types based on the number of rings systems present. For example, there are bicyclic diterpenoids such as labdane, tricyclic diterpenoids such as taxadiene, and tetracyclic diterpenoids such as stemodene (**Fig. 6**) [10].

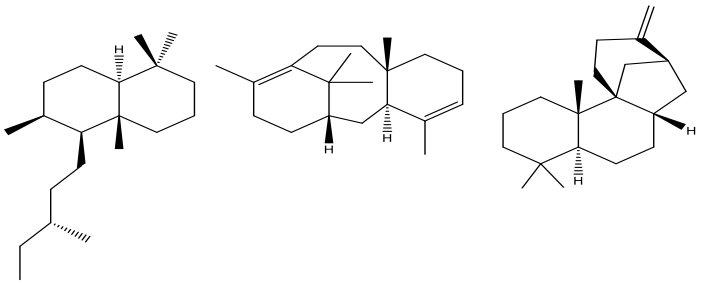

Labdane Taxadiene Stemodene

Figure 6. Different type of cyclic diterpenoids.

These different types of cyclized diterpenoids are generated through different cyclization reactions of GGPP, which are mediated by carbocation formation, as well as by the potential of Wagner-Meerwein rearrangements. For instance, paclitaxel (an anti-cancer drug) starts by generating carbocation form at the beginning of the reaction (**Fig. 7**).

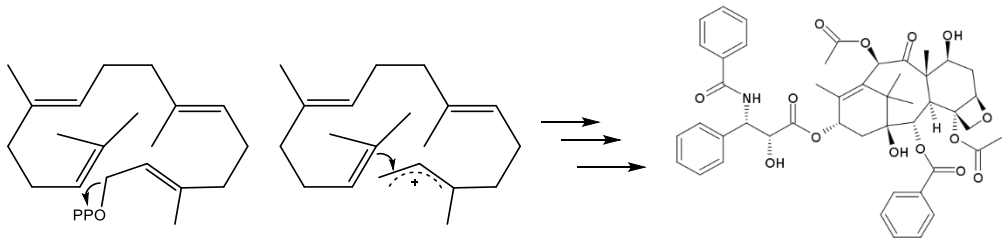

Figure 7. Reaction mechanism for the cyclization of GGPP

Diterpenoids can be found either in higher plants or fungi. For example, phytol is widespread in higher plants, where it binds to chlorophyll structures. Most diterpenoids are restrictively distributed and are rarely attached to sugar moieties to form glycosidic diterpenoids. If it is present, it is recognized as a sweetening agent.

3- Nitrogen-containing compounds

Many secondary metabolites have a nitrogen atom as part of their chemical structure. They include alkaloids, cyanogenic glycosides, glucosinolates, and non-protein amino acids. Alkaloids**,** the most abundant N-containing natural products, and are found in more than 20% of plants. Usually, the nitrogen atom is part of the cyclic rings. Alkaloids synthesized mainly from amino acids are mostly lysine, tryptophan, or tyrosine. Furthermore, the carbon skeleton of many alkaloids can be derived biosynthetically from a terpene pathway. They can be produced by different organisms such as fungi, bacteria, and animals. Depending on the chemical features of the compounds, alkaloids can be classified into seven main types (**Fig. 8**) [(2)].

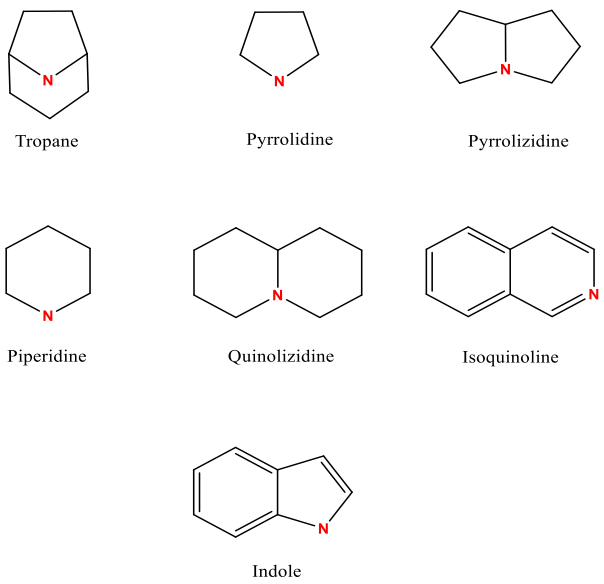

Figure 8. The main classes of alkaloids.

Phytopharmacological investigation of maple (*Acer*) species

Our laboratory has previously isolated a series of natural α-glucosidase inhibitory gallotannins, named maplexins A–I, from the red maple (*Acer rubrum*) species [11,12]. These compounds contained mono-, di-, and trigalloyl substituents located at different positions on a 1,5-anhydro-D-glucitol moiety. Interestingly, the α-glucosidase inhibitory activities of these maplexins increased with the number of galloyl substituents, and a trigalloyl-substituted maplexin (maplexin E) was 20-fold more potent than the clinical drug acarbose (**Fig. 9**) [12].

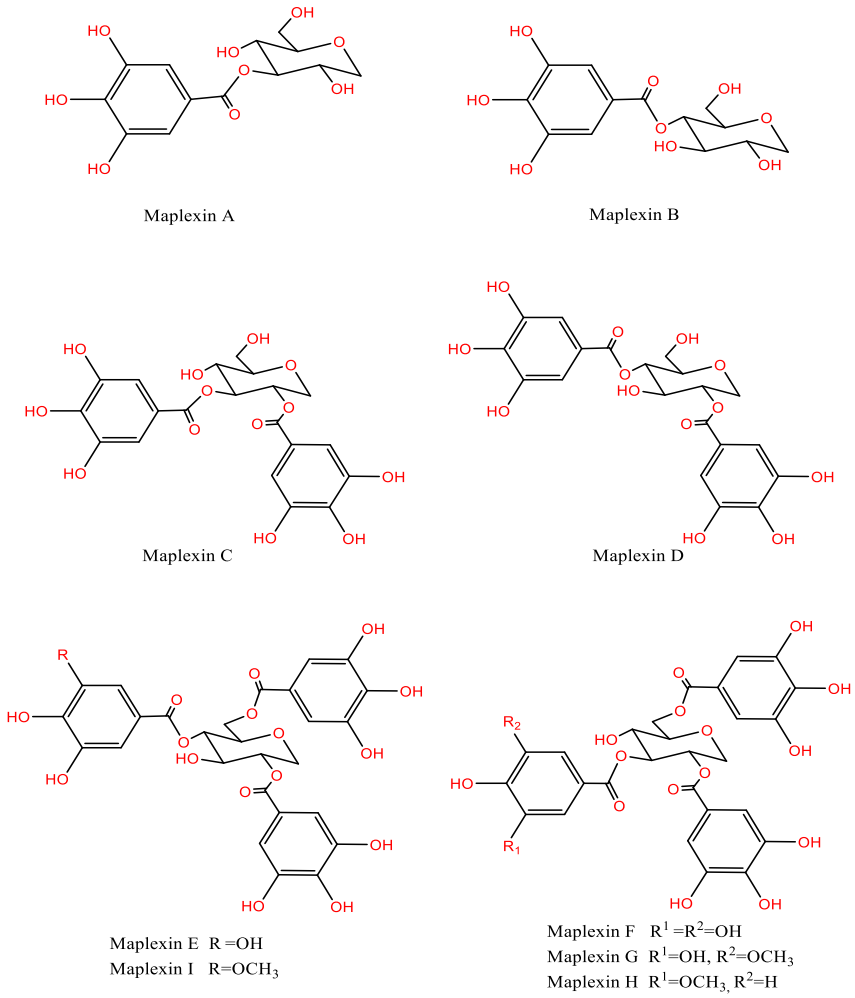

Figure 9. The chemical structure of maplexins A–I

Phytopharmacological investigation of *Euphorbia* species

The Euphorbiaceae family is among the most prominent families of the higher plants, and is composed of more than 300 genera and 7000 species subdivided into many subgenera and sections [(13)]. Among this family, the *Euphorbia* genus is one of the three largest genera of flowering plants, with approximately 2000 species [(14)]. The *Euphorbia* species all produce a mostly white latex, which is often rich in secondary metabolites, some of which are considered toxic. Several *Euphorbia* species have been used in ethnomedicine as purgatives and as treatments for asthma, tumors, and warts. [(13)] It is also well known for producing various types of secondary metabolites, primarily diterpenes, with immense chemical diversity [(15)]. Diterpenes occurring in the *Euphorbia* species are of considerable interest from the perspective of natural product drug discovery because of their wide range of unique biological activities and their high structural diversity. They have been reported to show a broad range of in vitro and in vivo biological properties, including multidrug resistance (MDR) modulator, antimicrobial, and anticancer agents. The importance of diterpenes from the Euphorbiaceae family is highlighted by the approval granted by the US Food and Drug Administration in 2012 for the treatment of actinic keratosis, a precancerous skin condition, of ingenol 3-angelate (ingenol mebulate, PEP005, Picato®, LEO pharma) [(16)]. Ingenol mebutate is a substance derived from the sap of the plant *Euphorbia peplus*. The high presence of active diterpenes in the latex of many *Euphorbia* species is well known. Diterpenoids are the majority secondary metabolites of the *Euphorbia* genus with many different skeletons, such as jatrophanes, ingenane, and lathyranes (**Fig. 10**), as well as sesquiterpenoids, flavonoids, and steroids. Previous publications on diterpenoids isolated from *Euphorbia* species have revealed novel compounds with promising cytotoxicity and

MDR modularity effects, such as macrocyclic lathyrane and jatrophane diterpenes [13]. Also, several structure-activity relationship studies on *Euphorbia* species have revealed that the diterpenoids with the jatrophanes and lathyrane pharmacophore are very active MDR modulators due to the high conformational flexibility of their 11, 12-membered rings (**Fig. 10**) [17]. A recent study also has shown that some *Euphorbia* species like *E. resinifera* and *E. bicolor* possess different structural compounds with various biological properties, such as an analgesic activity [18].

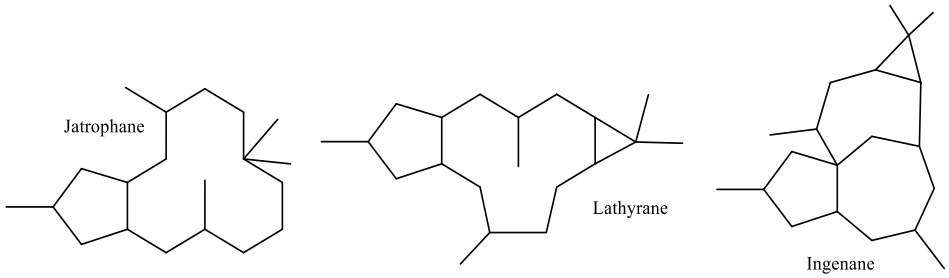

Figure 10. The skeletal structure of three types of *Euphorbia* diterpenoids.

A recent study has shown that the number of publications on the *Euphorbia* species increased by about 40% from 2012 to 2013 [14]. In the past few years, several researchers have revealed that *Euphorbia* diterpenes with different skeletal types (such as tigliane, lathyrane, myrsinane, and jatrophane) have exhibited moderate or strong antiproliferative effects on different human cell lines (e.g., pancreatic, lung, skin, ovarian, and colon carcinomas). Some of these diterpenes have been demonstrated as cytotoxic compounds, and other as apoptosis inducers. For example, several lathyrane diterpenoids isolated from *Euphorbia nivulia* exhibited strong cytotoxicity effects against Colo205, MT2, and CEM cell lines [19]. Many other diterpenes types, such as jatrophane, ingenane, premyrsinane and cyclomyrsinane derivatives, have shown potent cytotoxicity effects against various human cancer cell lines. A recent study has indicated that some jatrophane

diterpenes showed synergistic interactions with the anticancer drug doxorubicin [20]. This dual action was the result of the high flexibility of this macrocyclic diterpene.

Several *Euphorbia* diterpenes have been proposed to circumvent MDR to enhance the efficacy of drugs. Among those, the jatrophane- and lathyrane-type macrocyclic diterpenes from *Euphorbia* species have been described as strong MDR-reversing compounds by the modulation of the P-gp protein [21]. These promising findings led to the development in the in silico studies, as well as structure-activity relationship studies, to identify their pharmacophore structure and to optimize their efficacy. Findings indicate that P-gp inhibition contributes to the mechanisms of P-gp translocation, thereby enhancing the drug accumulation inside the cells. Therefore, the discovery of MDR modulators becomes a valuable therapeutic target for combating the progression of cancer diseases by enhancing the efficacy of anticancer agents and reducing the side effects that come with long chemotherapy treatments or ineffective treatments [22].

2. The Justification and Significance of the Study

Natural products are continuously inspiring new drug targets and synthetic scaffolds. Between 1940 and 2010, a total of 175 small-molecule, anti-cancer therapeutics have been accepted by the Food and Drug Administration. Of those 175 approved therapies, 49% were either discovered or derived directly from a natural product [23]. Even with natural products providing such significant impacts towards the generation of new pharmaceuticals, there is still a growing demand for the discovery of new lead compounds. This cycle puts continuous pressure on finding novel compounds and sources for drug candidates.

A- Silver maple (*Acer saccharinum)*

The incidence of type 2, or non-insulin dependent, diabetes mellitus is increasing rapidly worldwide and has become a significant public health burden [24]. Among various strategies used for type 2 diabetes management, clinical α-glucosidase inhibitory drugs, such as acarbose, are used to block the activity of carbohydrate-hydrolyzing enzymes thus decreasing postprandial hyperglycemia [25].

Over the past years, there has been renewed scientific attention in identifying natural plant-based α-glucosidase inhibitors for the treatment and management of diabetes. Therefore, silver maple has not been previously investigated for all of its polyphenolics content. Only two compounds were identified previously from silver maple which are Gramine and methyl-gallate (**Fig. 11**). As the total polyphenolic content level in silver maple leaves is high, it seems reasonable to investigate the chemical constituents in the leaves, which could also serve as α-glucosidase inhibitors. Therefore, a phytochemical study is proposed to isolate and identify known or undiscovered phenolic compounds from silver maple leaves and evaluate

these compounds for antioxidant and anti-diabetic activities. This study also proposes to elucidate the chemical structures of new compounds by using various techniques.

Scientific classification of silver maple	
Kingdom	Plantae
Order:	Sapindales
Family:	Sapindaceae
Genus:	*Acer*
Species:	*A. saccharinum*

Table 1. The scientific classification of silver maple.

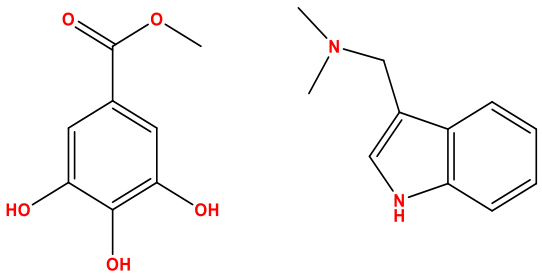

Methyl Gallate Gramine

Figure 11. Structures of chemical constituents previously identified in silver maple.

B- *Euphorbia saudiarabica.*

The importance of *Euphorbia* species has increased in the last five years, and the number of publications in this period has shown that this genus is producing a large number of promising bioactive compounds, mainly diterpenoids. Few of the *Euphorbia* species have been investigated thus far. In Saudi Arabia, for example, there are about 40 *Euphorbia* species, of which many are uninvestigated or poorly investigated; five of these are endemic, such as *E. saudiarabica* [26]. Therefore, the *Euphorbia saudiarabica* species was chosen for investigation of its phytochemical and biological activities.

Euphorbia saudiarabica was identified in 2007 and is endemic to the southwestern region of Saudi Arabia along the Albirk-Jazan road (**Fig. 12**) [27]. It is a small tree that resembles as a candelabra-like succulent spiny shrub and does not exceed 3 meters in length. It produces a strong, white, skin-irritant latex. The aerial part of the plant was collected, dried, and extracted with methanol in order to screen their phytopharmacological properties. Approximately 123 g of methanolic extract was obtained from King Khalid University through a Materials Transfer Agreement with the University of Rhode Island.

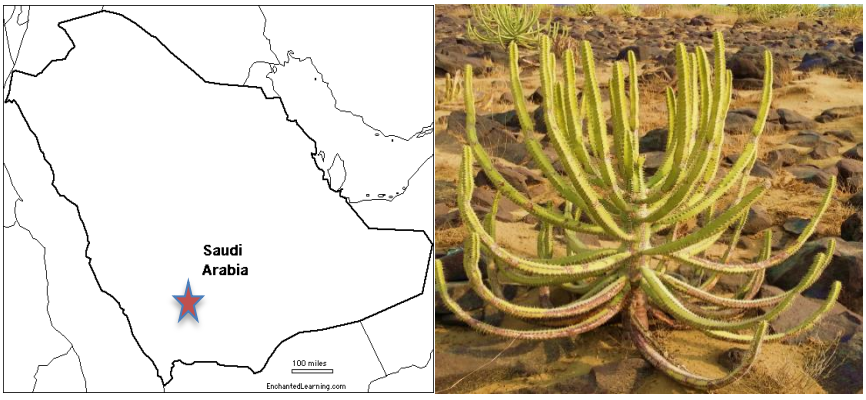

A **B**

Figure 12. (**A**) Map of Saudi Arabia (**B**) The aerial part of *Euphorbia saudiarabica*

3. The Objectives of the Study

The objective of this study is to isolate and evaluate the phytochemical compositions and the pharmacological properties of two higher plants, silver maple (*Acer saccharinum*) and *Euphorbia saudiarabica,* through the following aims:

- **Aim 1** Phytochemical investigation of the silver maple leaves and the aerial part of *Euphorbia saudiarabica* using different isolation and purification processes, such as open column chromatography (OCC), thin layer chromatography (TLC), medium pressure liquid chromatography (MPLC), and high-performance liquid chromatography (HPLC), etc.

- **Aim 2** The pure compounds will be isolated, and then the structure of all compounds will be elucidated using several techniques, including IR, UV, HR-ESIMS, NMR, and experimental ECD.

- **Aim 3** Biological activities evaluation of all isolated phytochemicals will be conducted using different bioassays, such as cytotoxicity.

- **Aim 4** The flavonoids composition of *Euphorbia saudiarabica* crude extract will be examined using LC-ESI-TOF-MS/MS.

References

1. McMurry, J. *Organic Chemistry: With Biological Applications*. 2nd ed. Cengage Learning, Science, Belmont, CA; **2010**. 598.
2. Taiz, L. Zeiger, E., Moller, I.M. and Murphy, A. *Plant Physiology and Development*. 6th ed. Sinauer Associates, Sunderland, CT; **2015**.
3. Wink, M. *Introduction: Biochemistry, Physiology and Ecological Functions of Secondary Metabolites*, in Annual Plant Reviews Volume 40: Biochemistry of Plant Secondary Metabolism. 2nd ed. Wiley-Blackwell, Oxford, UK; **2010**.
4. Dewick, P.M. *Medicinal Natural Products: A Biosynthetic Approach*. 2nd ed. John Wiley and Sons Ltd, Chichester, UK; **2002**.
5. B. Buchanan, W. Gruissem, R. Jones, eds. *Biochemistry and Molecular Biology of Plants*. American Society of Plant Physiologists, Rockville, MD; **2015**. 1250–1268.
6. Ozcan T., Bayizit A.A., Ersan L.Y., & Delikanli B. Phenolic in human health. *International Journal of Chemical Engineering and Applications*; **2014**. 5: 393-395.
7. Khanbabaee, K., van Ree, T. Tannins: classification and definition. *Nat. Prod. Rep*; **2001**. 18, 641-649.
8. Lattanzio, V. *Phenolic Compounds: Introduction. In Handbook of Natural Products*; Ramawat, K.G., Merillon, J.M., Eds.; Springer-Verlag: Berlin Heidelberg, Germany; **2013**. 1543–1580.
9. Agostini-Costa, T.d.S., Vieira, R.F., Bizzo, H.R., Silveira, D., Gimenes, M.A. *Secondary metabolites*. In: Dhanarasu, S, ed. Chromatography and its Application: InTech; **2012**.
10. Crozier, A, Yokota, T, Jaganath, I.B., et al. *Secondary metabolites as dietary components in plant-based foods and beverages*. In Plant Secondary Metabolites. Occurrence, Structure, and Role in the Human Diet; **2006**. 47–90.

11. Wan, C., Yuan, T., Li, L., Kandhi, V., Cech, N.B., Xie, M., Seeram, N.P. Maplexins, new α-glucosidase inhibitors from red maple (*Acer rubrum*) stems. *Bioorg Med. Chem Lett*; **2012**. 22, 597-600.
12. Yuan, T., Wan, C., Liu, K., and Seeram, N.P. New maplexins F–I and phenolic glycosides from red maple (*Acer rubrum*) bark. *Tetrahedron*; **2012**. 68, 959-964.
13. Vasas, A., Hohmann, J. *Euphorbia* diterpenes: isolation, structure, biological activity, andsynthesis (2008–2012*). Chem.Rev*; **2014**. 114, 8579–8612.
14. Ernst, M., Saslis-Lagoudakis, C.H., Grace, O.M., Nilsson, N., Simonsen, H.T., Horn, J.W., Rønsted, N. Evolutionary prediction of medicinal properties in the genus *Euphorbia* L. *Scientific Reports;* **2016**. 6: 30531.
15. Ramsay, J.R., Suhrbier, A., Aylward, J.H., Ogbourne, S., Cozzi, S-J., Poulsen, M.G., Baumann, K.C., Welburn, P., Redlich, G.L., Parsons, P.G. The sap from *Euphorbia peplus* is effective against human nonmelanoma skin cancers. *Br. J. Dermatol*; **2011**. 164:633-6.
16. Lebwohl, M., Swanson, N., Anderson, L.L., Melgaard, A., Xu, Z., Berman, B. N. Ingenol Mebutate Gel for Actinic Keratosis. *Engl. J. Med*; **2012**, 366(11).
17. Corea, G., Fattorusso, E., Lanzotti, V., Motti, R., Simon, P. N., Dumontet, C., Di Pietro, A. Jatrophane diterpenes as modulators of multidrug resistance. Advances of structure−activity relationships and discovery of the potent lead pepluanin A. *J. Med. Chem*; **2004**, 47:988**–**992.
18. Basu, P., Harris, T., Tongkhuya, S., Riley, A., Wojtaszek, J., Granger, J., Maier, C., Averitt, D. Phytochemical analysis and analgesic properties of *Euphorbia bicolor* latex extract. *The Journal of Pain*; **2018**. 19:S97.
19. Shi, Q.-W., Su, X.-H., Kiyota, H. Chemical and Pharmacological Research of the Plants in Genus *Euphorbia*. *Chemical Rev*; **2008**, 108: 4295**–** 4327.

20. Reis M., Ahmed O., Spengler G., Molnár J., Lage H., Ferreira M. Jatrophane diterpenes and cancer multidrug resistance—ABCB1 efflux modulation and selective cell death induction. *Phytomedicine*; **2016**, 23:968-978.
21. Reis, M., Ferreira, R. J., Santos, M. M. M., dos Santos, D. J. V. A., Molnar, J., Ferreira, M.-J. U. Enhancing Macrocyclic Diterpenes as Multidrug-Resistance Reversers: Structure–Activity Studies on Jolkinol D Derivatives. *J. Med. Chem;* **2013**, 56, 748**–**760.
22. Kathawala, R.J., Gupta, P., Ashby, C.R., Jr., Chen, Z.-S. The modulation of ABC transporter-mediated multidrug resistance in cancer: a review of the past decade. *Drug Resist. Update*; **2015**, 18:1–17.
23. Cragg, G.M., and Newman, D.J.. Natural Products as Sources of New Drugs over the 30 Years from 1981 to 2010. *J. Nat. Prod;* **2012**. 60 (1): 52**–**60.
24. World Health Organization (WHO) Diabetes Fact Sheet. Updated January 2015. http://www.who.int/mediacentre/factsheets/fs312/en/.
25. Wardrop, D.J.; Waidyarachchi, S.L. Synthesis and biological activity of naturally occurring α-glucosidase inhibitors. *Nat. Prod. Rep;* **2010**. 27:1431.
26. Collenette, I..S. *Wildflowers of Saudi Arabia*. National Commission for Wildlife Conservation and Development, Riyadh; **1999**.
27. Fayed, A., AL-Zahrani, A. Three new spiny *Euphorbia* (Euphorbiaceae) species from western Saudi Arabia. *Edinburgh Journal of Botany*; **2007**. 64(2): 117**–**129.

Manuscript I

Bioactive Glucitol-Core Containing Gallotannins and Other Phytochemicals from Silver Maple (*Acer saccharinum*) Leaves

*Abdullatif Bin Muhsinah, Hang Ma, Nicholas A. DaSilva, Tao Yuan and Navindra P. Seeram**

Bioactive Botanical Research Laboratory, Department of Biomedical and Pharmaceutical Sciences,

College of Pharmacy, University of Rhode Island, Kingston, RI 02881, USA

nseeram@uri.edu

This manuscript is written and published in the *Natural Product Communications Journal*

Bin Muhsinah A, Ma H, DaSilva NA, Tuan T, Seeram NP (**2017**) Bioactive glucitol-core containing gallotannins and other phytochemicals from silver maple (*Acer saccharinum*) leaves. Nat Prod Commun 12:83–84.

Abstract

In the course of our group's investigation of members of the maple (*Acer*) genus, a series of glucitol-core containing gallotannins (GCGs) were isolated and identified (by NMR and HREISMS). Among higher plants, only certain maple species are known to produce GCGs, compounds with potential nutraceutical and cosmetic applications due to their reported antioxidant, antidiabetic, anti-α-glucosidase, anti-glycation, anticancer, and skin health promoting effects. Herein, we sought to investigate whether the previously un-investigated silver maple (*Acer saccharinum*) species was also a source of GCGs. Nine phenolic compounds, including six GCGs, were identified (by HPLC-DAD analyses using previously isolated standards) as ginnalins A-C (1-3), maplexins B, D, and F(4-6), methyl syringate (7), methyl gallate (8), and 3-methoxy-4-hydroxyphenol-1-β-D-(6 galloyl)-glucopyranoside (9). In addition, one sesquiterpenoid, namely, pubineroid A (10), was isolated and identified (by NMR).

Keywords: Silver maple, *Acer saccharinum*, Phenolic, Glucitol-core containing gallotannins (GCGs).

Introduction

The maple (*Acer*) genus contains thirteen species which are native to North America including the sugar (*A. saccharum*), red (*A. rubrum*), and silver (*A. saccharinum*) maples. Apart from sap which is primarily consumed as maple syrup [1], other maple plant parts (leaves, bark, etc.) have also been used as traditional medicines by the indigenous people of North America [2]. Our group has reported on the isolation and structure elucidation (by NMR and HREISMS) of over 70 phytochemicals, from the sugar, red, and sycamore (*A. pseudoplatanus*) maples [3-7]. Among these species, only the red maple yielded glucitol-core containing gallotannins (GCGs) [3, 4, 6]. These compounds have been reported, by our group [8-15], and others [16-20], to show a wide range of in vitro and in vivo biological effects including, antioxidant, anti-diabetic, anti-α-glucosidase, anti-glycation, anticancer, and skin-health promoting effects. Given the potential nutraceutical and cosmetic applications of these compounds, as well as our access to the aforementioned maple-derived phytochemical standards, herein, we sought to investigate whether the silver maple was a source of GCGs. Using authentic standards (previously isolated by our laboratory), nine phenolics, including six GCGs, were identified from silver maple leaves as ginnalins A-C (1-3), maplexins B, D, and F (4-6), methyl syringate (7), methyl gallate (8), and 3-methoxy-4-hydroxyphenol-1-β-D-(6-galloyl)-glucopyranoside (9) (by HPLCDAD analyses, see Supplementary data, Table S1) [6, 7]. In addition, one sesquiterpenoid, namely, pubinernoid A (10), was isolated and identified (by NMR; see Supplementary data, Figures S1 and S2). Pubinernoid A was obtained as a white amorphous powder and its ^{1}H and ^{13}C NMR data were consistent with the literature [7]. The chemical structures of the compounds identified from silver maple leaves are shown in Figure 1. In summary, this is the

first reported phytochemical investigation of the silver maple which led to the identification of nine phenolic compounds (six GCGs and three phenolics) and a sesquiterpenoid. Our findings add to the growing body of data of phytochemicals identified from the maple (*Acer*) genus, and more importantly, about which maple species produce GCGs, a promising class of bioactive plant polyphenols with nutraceutical and cosmetic applications.

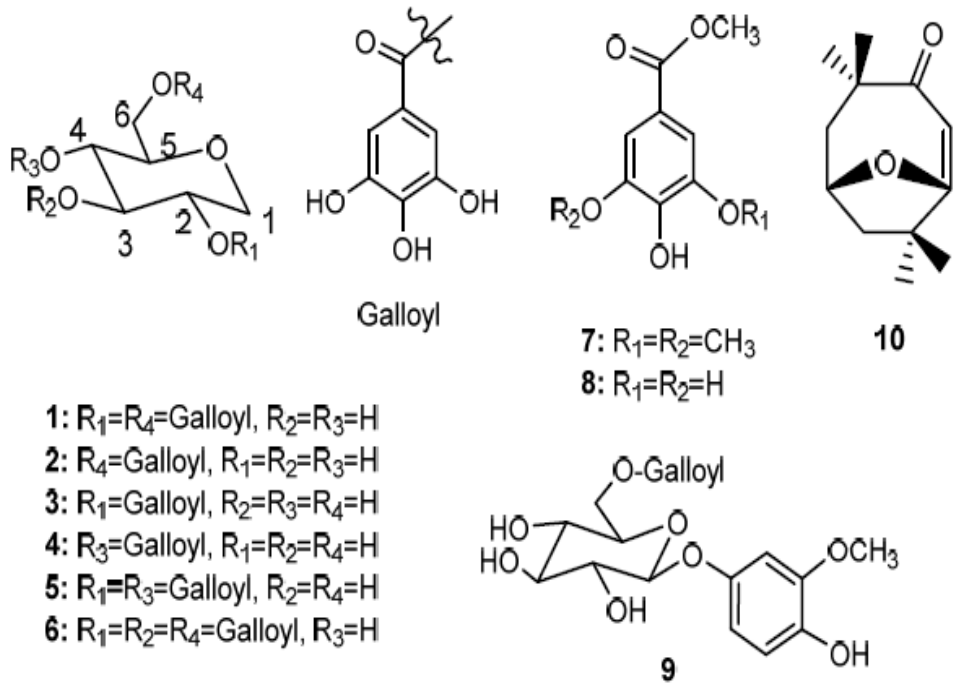

Figure 1: Chemical structures of compounds 1-10.

Experimental

General: High performance liquid chromatography (HPLC) analyses were performed on a Hitachi Elite LaChrom system consisting of a L-2130 pump, a L-2200 autosampler, and a L-2455 Diode Array Detector. All 1H and 13C NMR spectra were acquired on a Bruker 300 MHz spectrometer using MeOD4 as solvent.

Plant material: Silver maple (*Acer saccharinum*) leaves were collected on the Kingston campus of the University of Rhode Island (Kingston, RI, USA) in the summer of 2010 and were botanically authenticated by Mr. J. Peter Morgan. Voucher specimens (16JPM1-APS6310) are deposited in the Heber-Youngken Garden and Greenhouse at the College of Pharmacy, University of Rhode Island.

Extraction of plant material: Air-dried silver maple leaves (1007.8 g) were macerated for 9 days with MeOH (5.5 L× 3). The filtrate was concentrated under reduced pressure to afford a dried methanol extract (250 g). This was suspended in distilled water and successively partitioned to yield n-hexanes (67.5 g), ethyl acetate (EtOAc; 28.7 g), and n-butanol (37.5 g) extracts after solvent removal in vacuo. The EtOAc extract, which contained the highest total polyphenol content (58.8% GAEs based on the Folin-Ciocalteau assay, see Supplementary data, Table S2), was selected for further phytochemical investigation (described below).

Identification of compounds 1-9 in the EtOAc extract of silver maple leaves by HPLC-DAD analyses: The EtOAc extract (5 mg) was analyzed on a Phenomenex C18 column (250 × 4.6 mm, i.d. 5 μm). The injection volume was 10 μL and the flow rate was 0.75 mL/min. A gradient mobile phase solvent system consisting of solvent A (0.1% aqueous trifluoroacetic acid) and solvent B (MeOH) was used as follows: 0-50 min, 5%-46% B. The HPLC profile was monitored at 220 nm and

compounds 1-9 were identified by comparison of their retention times to authentic standards previously isolated by our laboratory from red maple [3, 4, 6].

Isolation of compound 10 from the EtOAc extract of silver maple leaves: Having identified the major constituents in the EtOAc extract which were phenolics (1-9), we attempted to isolate the (minor) non-phenolic constituent/s (based on UV absorbance; see Supplementary Data, Table S1) present in the extract. Briefly, the EtOAc extract (28.2 g) was purified on a silica gel column eluted with a gradient solvent system of chloroform/MeOH (50:1 - 1:1; v/v) to afford 11 fractions (F1 - F11). Fraction F3 (440 mg) was chromatographed on a Sephadex LH-60 column eluting with MeOH to afford 6 sub-fractions (13A - 13F). Fraction 13B (340 mg) was chromatographed on a silica gel column eluting with a gradient solvent system of hexane/dichloromethane (10:0 - 0:10; v/v) to afford 5 fractions (16A - 17C). Fraction 16C (15 mg) was further purified by C18 reversed-phase semi-preparative HPLC with a mobile phase consisting of MeOH and 0.1% aqueous trifluoroacetic acid (60:40; v/v) to afford compound 10 (3.4 mg, tR =12.2 min).

Supplementary data: Supplementary data are available for this article and available free of charge.

References

[1] Ball DW. (**2007**) The chemical composition of maple syrup. *Journal of Chemical Education*, ***84***, 1647-1650.

[2] Arnason T, Hebda RJ, Johns T. (**1981**) Use of plants for food and medicine by Native peoples of eastern Canada. *Canadian Journal of Botany*, ***59***, 2189-2325.

[3] Wan C, Yuan T, Li L, Kandhi V, Cech NB, Xie M, Seeram NP. (**2012**) Maplexins, new α-glucosidase inhibitors from red maple (*Acer rubrum*) stems. *Bioorganic Medicinal Chemistry Letters*, ***22***, 597-600.

[4] Yuan T, Wan C, Liu K, Seeram NP. (**2012**) New maplexins F-I and phenolic glycosides from red maple (*Acer rubrum*) bark. *Tetrahedron*, ***68***, 959-964.

[5] Yuan T, Wan C, González-Sarrías A, Kandhi V, Cech NB, Seeram NP. (**2011**) Phenolic glycosides from sugar maple (*Acer saccharum*) bark. *Journal of Natural Products*, ***74***, 2472-2476.

[6] Zhang Y, Ma H, Yuan T, Seeram NP. (**2015**) red maple (*Acer rubrum*) aerial parts as a source of bioactive phenolics. *Natural Product Communications*, ***10***, 1409-1412.

[7] Zhang L, Tu Z, Yuan T, Ma H, Niesen DB, Wang H, Seeram NP. (**2015**) New gallotannin and other phytochemicals from sycamore maple (*Acer pseudoplatanus*) leaves. *Natural Product Communications*, ***10***, 1977-1980.

[8] Seeram NP, Xu J, Li L, Slitt A. (**2012**) Mining red maple (*Acer rubrum*) trees for novel therapeutics to manage diabetes. *Medicine and Health, Rhode Island*, ***95***, 283-284.

[9] Ma H, Wang L, Niesen DB, Cai A, Cho BP, Tan W, Gu Q, Xu J, Seeram NP. (**2015**) Structure activity related, mechanistic, and modeling studies of

gallotannins containing a glucitol-core and α-glucosidase. *RSC Advances*, ***5***, 107904-107915.

[10] Ma H, Liu W, Frost L, Kirschenbaum LJ, Dain JA, Seeram NP. (**2016**) Glucitol-core containing gallotannins inhibit the formation of advanced glycation end-products mediated by their antioxidant potential. *Food & Function*, ***7***, 2213-2222.

[11] Ma H, Xu J, Guo L, Lu W, Seeram N. (**2016**) Bioactive glucitol-core containing gallotannins from red maple (*Acer rubrum*) inhibit melanogenesis via down-regulation of tyrosinase and melanogenic gene expression in B16F10 melanoma cells. American Chemical Society, 252nd ACS National Meeting & Exposition, Philadelphia, PA, United States, August 21-25, 2016, AGFD-12.

[12] González-Sarrías A, Ma H, Edmonds ME, Seeram NP. (**2013**) Maple polyphenols, ginnalins A-C, induce S-and G2/M-cell cycle arrest in colon and breast cancer cells mediated by decreasing cyclins A and D1 levels. *Food Chemistry*, ***136***, 636-642.

[13] González-Sarrías A, Li L, Seeram NP. (**2012**) Effects of maple (*Acer*) plant part extracts on proliferation, apoptosis and cell cycle arrest of human tumorigenic and non-tumorigenic colon cells. *Phytotherapy Research*, ***26***, 995-1002.

[14] Apostolidis E, Li L, Kang B, Lee CM, Seeram NP. (**2012**) Seasonal influence on phenolic-mediated antihyperglycemic properties of Canadian sugar and red maple leaves using *in vitro* assay models. *Food Science and Biotechnology*, ***21***, 753-760.

[15] González-Sarrías A, Yuan T, Seeram NP. (**2012**) Cytotoxicity and structure activity relationship studies of maplexins A-I, gallotannins from red maple (*Acer rubrum*). *Food and Chemical Toxicology*, ***50***, 1369-1376.

[16] Honma A, Koyama T, Yazawa K. (**2011**) Anti-hyperglycaemic effects of the Japanese red maple *Acer pycnanthum* and its constituents the ginnalins B and C. *Journal of Enzyme Inhibition and Medicinal Chemistry*, ***26***, 176-180.

[17] Bi W, Shen J, Gao Y, He C, Peng Y, Xiao P. (**2016**) Ku-jin tea (*Acer tataricum* subsp. *ginnala* or *A. tataricum* subsp. *theiferum*), an underestimated functional beverage rich in antioxidant phenolics. *Journal of Functional Foods*, ***24***, 75-84.

[18] Kamori A, Kato A, Miyawaki S, Koyama J, Nash RJ, Fleet GW, Miura D, Ishikawa F, Adachi I. (**2016**) Dual action of acertannins as potential regulators of intracellular ceramide levels. *Tetrahedron: Asymmetry*. doi.org/10.1016/j.tetasy.2016.09.006

[19] Lu RL, Hu FL, Xia T. (**2010**) Activity-guided isolation and identification of radical scavenging components in Gao-Cha tea. *Journal of Food Science*, ***75***, H239-H243.

[20] Honma A, Koyama T, Yazawa K. (**2010**) Anti-hyperglycemic effects of sugar maple *Acer saccharum* and its constituent acertannin. *Food Chemistry*, ***123***, 390-394.

Manuscript II

Saudiarabicain A—E, Macrocyclic Diterpenoids from *Euphorbia saudiarabica*

Abdullatif Bin Muhsinah[†,‡,§], Yongqiang Liu[‡,§], Nicholas A. DaSilva[‡], Navindra P. Seeram*[,‡]

[†] *Department of Pharmacognosy, College of Pharmacy, King Khalid University, P.O.Box # 641, Abha, Saudi Arabia*

[‡] *Bioactive Botanical Research Laboratory, Department of Biomedical and Pharmaceutical Sciences, College of Pharmacy, University of Rhode Island, Kingston, RI 02881, USA*

[§] *Abdullatif Bin Muhsinah and Yongqiang Liu contributed equally to this work.*

Supporting information

This manuscript is written in the style of the *Journal of Natural Products*

Abstract

Methanol extracts of aerial parts of *Euphorbia saudiarabica* afforded five new macrocyclic-lathyrane diterpenoids, named saudiarabicain **A–E** (**1–5**). **1** and **2** represent an unusual type of lathyrane diterpenoids. Structures of **1–5** were determined by analysis of extensive NMR and mass spectroscopic data, and the relative configuration of all compounds (**1–5**) were established by NOESY spectra analysis. Diterpenoid **2** showed a significant cytotoxicity effect against B16-F10 murine melanoma cells, while the remaining compounds exhibited only moderate or no cytotoxicity activity against B16F10, human HaCat keratinocytes, and human SH-SY5Y neuroblastoma cells.

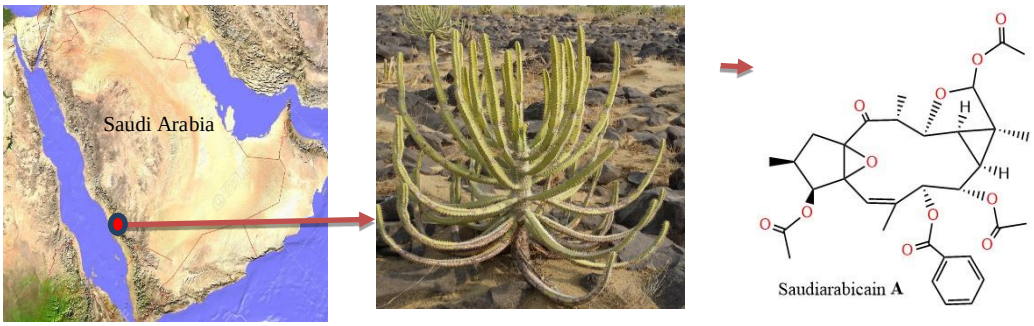

E. saudiarabica

Introduction

The Euphorbiaceae family is among the largest families of higher plants, composed of more than 300 genera and 7000 species subdivided into many subgenera and sections[1]. Among this family, the *Euphorbia* genus is one of the three largest genera of flowering plants, with approximately 2000 species[2]. The *Euphorbia* species all have milky irritant latex that is often rich in secondary metabolites; some of them are considered toxic. Several *E.* species have been used in ethnomedicine as purgatives and as treatments for asthma, tumors, and warts[1]. It is also well known for producing various types of secondary metabolites, primarily diterpenes, with immense chemical diversity[3]. Diterpenes occurring in the *Euphorbia* species are of considerable interest from the perspective of natural product drug discovery because of their wide range of unique biological activities and their high structural diversity.

The importance of diterpenes from the *Euphorbia* genus is highlighted by the approval granted by the US Food and Drug Administration in 2012 for the treatment of actinic keratosis, a precancerous skin condition, for ingenol 3-angelate (ingenol mebulate, PEP005, Picato®, LEO pharma)[4]. Diterpenoids are the majority secondary metabolites of the *Euphorbia* genus with many different skeletons such as jatrophanes, ingenane, and lathyranes, as well as sesquiterpenoids, flavonoids, and steroids[5]. Previous publications on diterpenoids isolated from *Euphorbia* species have revealed novel compounds with promising cytotoxicity and multi-drug resistance (MDR) modularity effects, such as macrocyclic lathyrane and jatrophane diterpenes[1]. Also, several structure-activity relationship studies on *Euphorbia* species have revealed that the diterpenoids with the jatrophanes and lathyrane pharmacophore are very active MDR modulators due to the high conformational

flexibility of their 11, 12-membered rings[6].

Herein, we report the isolation and characterization of five new lathyrane-type diterpenoids named saudiarabicain A–E (**1–5**) from the aerial part of *Euphorbia saudiarabica*. *E. saudiarabica* is an endemic plant in Saudi Arabia and mainly distributed in the southwestern area of that country, close to the Red Sea. Furthermore, we evaluated the cytotoxicity effects of these compounds using three different cell lines.

RESULTS AND DISCUSSION

Compound **1** was obtained as white amorphous powder and had molecular formula $C_{31}H_{40}O_{11}$ as deduced by (+)-HRESIMS ion at *m/z* 633.2332 $[M + Na]^+$ (calcd 633.2312). The ^1H NMR and ^{13}C NMR Data of compound **1** (**Table 1**) revealed three acetyl moieties and one benzoyl group (δ_C 170.5, 133.3, 129.5, 129.3, 128.5; δ_H 7.99, 7.55, 7.42). The remaining 20 carbons, building the lathyrane-type diterpene core structure, contained a rare oxymethine, four methyls, one *cis* C=C bond and one ketone carbonyl group[7]. Their connections were deduced from correlations observed in the ^1H-^1H COSY and HMBC spectrum. Three spin systems were established by ^1H-^1H COSY correlations: H-1/H-2/H-3, H20/H13/H12/H11/H9/H8/H7 and H4'/H3' (**Fig. 2A**). The carbonyl group at C-14 was determined by the long-range correlations of H-20 to C-14 and H-13 to C-14, which observed in the HMBC spectrum. The HMBC correlations of H-1 to C-4 and H-3 to C-15 supported the locations of the two oxygenated quaternary carbons: C-4 and C-15. The assignment of the olefinic proton H-5 at δ_H 5.43 was determined by the HMBC correlation of H-5 to C-15. The HMBC correlations of H-19 to C-9, C-12, and C-18, combined with the chemical shift of C-19 (103.1), supported the identification of the rare oxygenated C-19. The locations of the acetyl moieties were assigned by the HMBC correlations which showed in **Fig. 2A**. The planar structure of **1** was deduced as shown in **Fig. 2A**. The relative stereochemistry of **1** was assigned by NOESY correlations as shown in **Fig. 2B**. H-2, H-1α, H-3, H9, H-11, and H-19 were assigned randomly as α-oriented based on the NOESY correlations of H-2/H-1α, H-2/H-3, H-9/H-11, and H-11/H-19. Consequently, H-7, H-8, H-12,

and H-13 were assigned as *β*-oriented by NOESY correlations of H-7/H-8, H-8/H-12, and H-12/H-13 (**Fig. 2B**).

Compound **2** showed a (+)-HRESIMS $[M + Na]^+$ ion peak at *m/z* 611.2495 (calcd for $C_{33}H_{38}O_{11}Na$, 611.2468). Analysis of NMR spectra data suggested that the structure of compound **2** was closely related to compound **1** (**Table. 1**). The only major differences in the NMR data of compound **2** is the presence of angelate group signals instead of benzoyl group as it was in compound **1. (Fig. S1**, supporting information**).**

The HRESIMS of compound **3** showed a sodiated molecular ion at *m/z* 691.2751 $[M + Na]^+$, corresponding to the molecular formula of $C_{36}H_{44}O_{12}$ (calcd, 691.2730). The ^1H and ^{13}C NMR data (**Table 1**) of **3** revealed the lack of chemical shift of C-19 (103.1), which indicate that **3** is clearly different from **1** and **2**. Analysis of ^1H and ^{13}C NMR revealed four acetoxy groups and one benzyl group (δ_c 170.5, 134.1, 129.1, 128.2, 126.8, 40.7; δ_H 7.20, 3.65). The remaining 20 carbons, building the lathyrane-type diterpene core structure, contained one *cis* C=C and one ketone carbonyl group[8.] Their connections were deduced by ^1H-^1H COSY and HMBC spectra. Two spin systems were established by ^1H-^1H COSY correlations: H-1/H-2/H-3 and H-20/H13/H-12/H-11/H-9/H-8/H-7 (**Fig. 2C**). The carbonyl group at C-14 was determined by the long-range correlations of H-20 to C-14 and H-13 to C-14, which was observed in the HMBC spectrum. The HMBC correlations of H-1 to C-4, H-3 to C-15 supported the locations of the two oxygenated quaternary carbons: C-4 and C-15. The olefinic proton H-5 at the δ_H 5.43 location was determined by the HMBC correlation of H-5 to C-15. The correlations of H-7 to phenylacetoxy carbonyl (δ_C 170.5) revealed that the phenylacetoxy group was located at C-7. The presence of acetoxy groups at C-3, C-8, C-12, and C-19 was suggested by HMBC

correlations between acetoxy carbonyls and H-3, H-8, H-12, and H-19, respectively. (**Fig. 2C**). The relative configuration of **3** was established by NOESY correlations. H-2, H-1α, H-3, H-9, H-11, and H-18 were assigned randomly as α-oriented on the basis of NOESY correlations of H-2/H-1α, H-2/H-3, H-9/H-11, and H-9/H-18. Consequently, H-7, H-8, H-12, and H-13 were assigned as *β*-oriented by NOESY interactions of H-7/H-8, H-8/H-12, and H-12/H-13 (**Fig. 2D**).

Compound **4** was obtained as a white amorphous powder. The ^{1}H NMR and ^{13}C NMR data of **4** (**Table 2**) were quite similar to those of **3**. Comparison between the ^{1}H NMR spectrum of **3** and **4** showed a difference only in the ester moieties. The ^{1}H NMR and ^{13}C NMR spectrum of **4** revealed the presence of one benzoyloxy group, one angelate group, two acetoxy groups, and a free hydroxyl. In the HMBC spectrum, the carbonyls of the benzoyloxy, one angelate group, and two acetoxy groups displayed cross-peaks with H-8, H-7, H-12, and H-19, indicating the groups located at C-8, C-7, C-12, and C-19, respectively. The free hydroxyl was located at C-3 because of the HMBC correlation between the free hydroxyl and C-3. By comparing the NMR data of **5** (**Table 2**) with those of **4**, we deduced the structure of **5,** which is the same as that of compound **4** except for the benzoyloxy group at C-8 in **4** that is replaced by the angelate group in **5**.

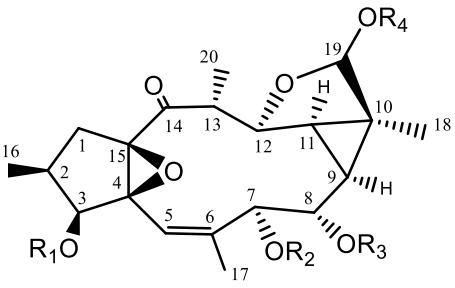

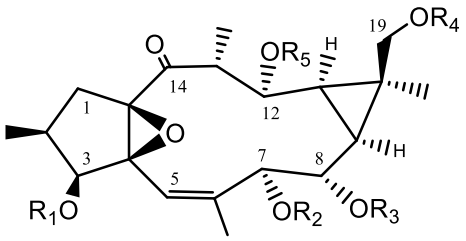

	R_1	R_2	R_3	R_4
1	Ac	Bz	Ac	Ac
2	Ac	Ang	Ac	Ac

	R_1	R_2	R_3	R_4	R_5
3	Ac	Bzl	Ac	Ac	Ac
4	H	Ang	Bz	Ac	Ac
5	H	Ang	Ang	Ac	Ac

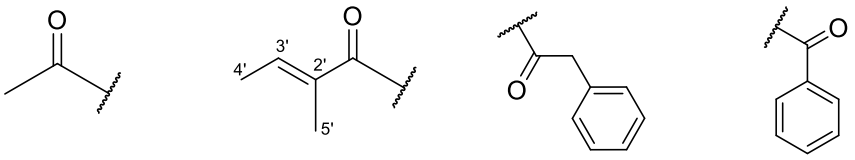

Ac Ang Bzl Bz

Figure 1: Chemical structures of compounds **1–5**.

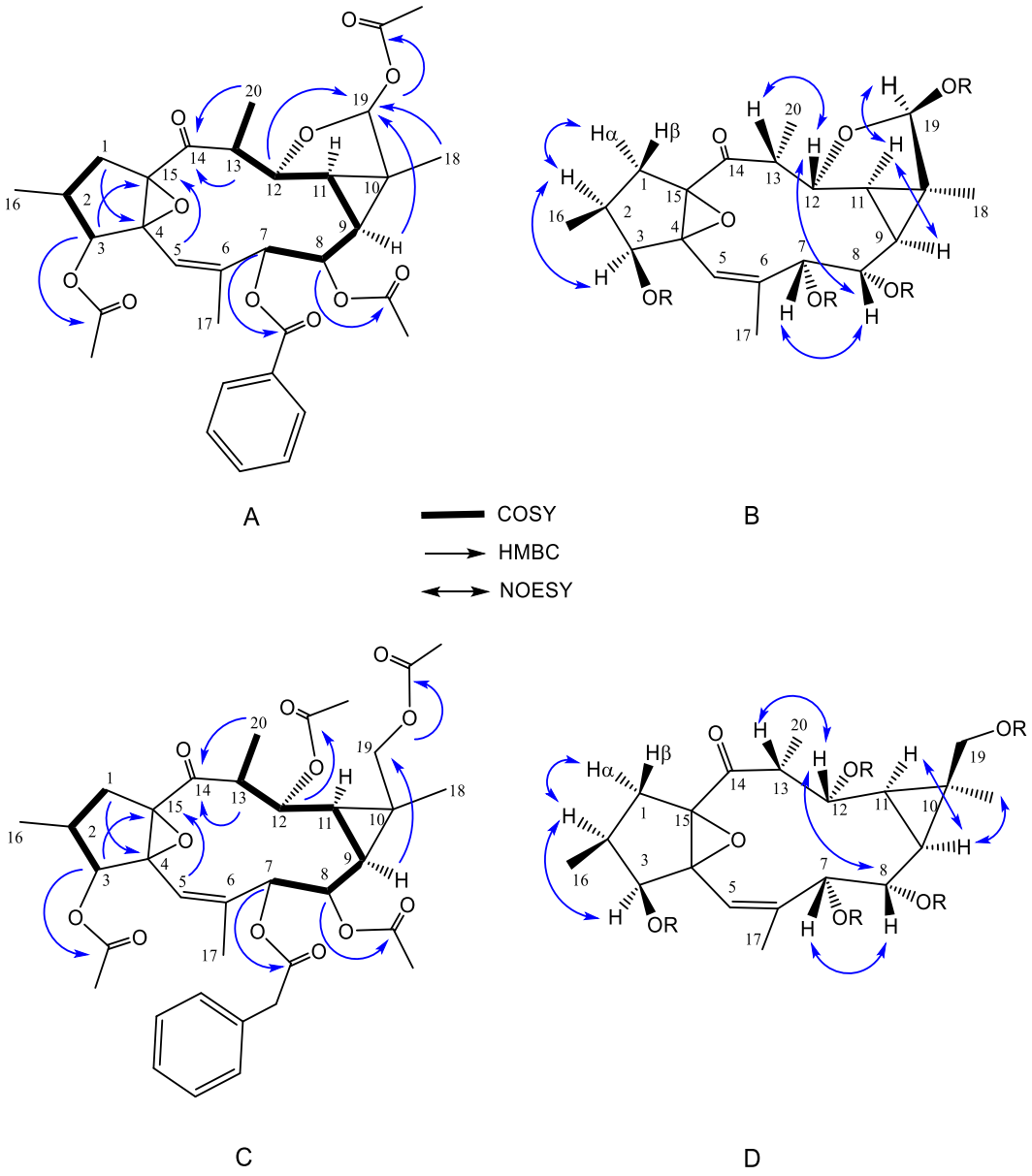

Figure 2. (A and C) Key HMBC and COSY (bold bonds) for compound **1** and **3**, respectively. (B and D) NOESY correlations for compound **1** and **3**, respectively.

Table 1. ^{1}H NMR and ^{13}C NMR data (300 and 75 MHz, CD_3OD) for compounds **1–3**

	1		**2**		**3**	
no.	δH (*J* in Hz)	δC	δH (*J* in Hz)	δC	δH (*J* in Hz)	δC
1*α*	2.56 dd (15.0, 9.0)	34.1	2.59 dd (14.7, 9.0)	34.1	2.70 dd (14.7, 9.0)	31.1
1*β*	1.67 d (15.0)		1.72 d (15.0)		1.60 d (14.7)	
2	2.34 m	29.2	2.36 m	29.3	2.41 m	29.3
3	5.03 d (8.4)	77.1	5.06 d (8.4)	77.1	5.13 d (8.7)	76.8
4		73.3		73.3		71.0
5	5.70 s	116.7	5.53 s	116.4	5.43 m	117.6
6		142.1		142.4		138.7
7	5.45 brs	77.2	5.22 brs	77.1	5.04 d (1.8)	76.4
8	5.02 dd (11.2, 1.2)	70.2	4.92 d (11.1)	70.2	4.54 dd (10.8, 1.8)	70.7
9	1.61 dd (10.8, 9.0)	27.2	1.46 dd (10.8, 9.0)	27.2	1.30 dd (10.8, 9.0)	25.0
10		33.0		32.7		21.6
11	1.34 dd (8.7, 1.5)	31.0	1.25 m	30.9	1.15 dd (11.1, 9.0)	30.9
12	4.65 dd (4.5, 1.5)	78.1	4.58 d (4.8)	78.0	4.84 dd (11.1, 7.8)	69.4
13	3.34 qd (6.6, 4.5)	48.7	3.30 qd (6.9, 5.1)	48.7	2.82 dq (7.5, 7.2)	43.0
14		206.4		206.4		207.0
15		72.9		72.9		73.4
16	0.84 d (7.2)	16.0	0.84 d (7.5)	16.0	0.84 d (7.5)	15.9
17	2.08 s	16.6	1.97 d (1.8)	16.5	1.96 d (1.5)	16.2
18	1.25 s	17.0	1.20 s	17.0	1.00 s	23.2
19	6.13 s	103.1	6.03 s	103.0	19*α*: 4.01 d (12.0) 19*β*: 3.46 d (12.0)	64.7
20	0.96 d (6.6)	6.8	0.93 d 6.6	6.8	0.92 d (7.2)	12.4
3-OAc		170.5		170.5		170.6
	1.99 s	19.1	1.97 s	19.0	2.00 s	19.7
8-OAc		170.6		170.7		170.4
	1.87 s	19.5	1.98 s	19.9	1.94 s	19.0
12-OAc						170.8
					1.89 s	19.33
19-OAc		170.8		170.6		171.3
	2.01 s	19.9	1.84 s	19.5	1.88 s	19.5
7-R		**O-Bz**		**O-Ang**		**O-Bzl**
C=O		170.5		166.5		170.5
1'		129.5				134.1
2'	7.99 m	129.3		128.0		129.1
3'	7.42 ddd (7.2, 7.2, 1)	128.5	6.86 q (6.6)	138.4	7.20 5H m	126.8
4'	7.55 dddd (7.5, 7.5, 1.5, 1.5)	133.3	1.74 d (6.6)	13.2		128.2
5'	7.42 ddd (7.2, 7.2, 1.5)	128.5	1.76 s	10.8		126.8
6'	7.99 m	129.3	-	-		129.1
7'	-	-	-	-	3.65 s	40.7

Table 2. ^{1}H NMR and ^{13}C NMR data (500 and 125 MHz) for compounds **4**–**5** (**4** in DMSO-d_6, **5** in CD_3OD).

	4		**5**	
no.	δH (*J* in Hz)	δC	δH (*J* in Hz)	δC
1α	2.03 dd (13.5, 10.5)	32.6	2.19, m	31.8
1β	1.85 d (14.0)		1.90, m	
2	1.84 m	33.2	1.90 m	33.0
3	3.83 dd (6.5, 5.5)	75.2	3.90 d (5.0)	75.7
4		73.3		73.2
5	6.11 q (1.5)	118.4	6.16 s	117.8
6		136.2		136.8
7	5.43 d (1.5)	75.9	5.29 d (1.5)	76.2
8	5.14 dd (11.0, 2.0)	72.5	4.82 dd (11.0, 1.5)	70.9
9	1.65 m	25.5	1.64 dd (11.0, 9.0)	25.6
10		21.7		21.6
11	1.37 dd (11.5, 9.0)	31.6	1.42 dd (11.0, 9.0)	31.3
12	5.08 dd (11.5, 3.5)	69.5	5.01 dd (11.5, 3.5)	69.5
13	2.94 qd (7.0, 3.5)	43.4	3.04 qd (7.0, 3.5)	43.2
14		207.8		207.8
15		73.2		73.0
16	0.88 d (7.0)	13.0	0.99 d (6.5)	11.0
17	2.11 d (1.5)	17.7	2.13 s	16.4
18	1.16 s	24.4	1.16 s	23.2
19α	3.88 d (12.0)	64.9	4.08 d (12.0)	64.8
19β	3.62 d (12.0)		3.60 d (12.0)	
20	0.95 d (7.0)	13.4	1.04 d (7.0)	12.3
3-OAc	3-OH: 5.32 d (6.5)			
12-OAc		170.3		170.8
	2.03 s	21.3	2.10 s	19.7
19-OAc		170.5		171.2
	1.64 s	20.5	1.93 s	19.3
7-R		**O-Ang**		**O-Ang**
C=O		166.3		166.6
1'				
2'		128.2		128.1
3'	6.89 q (7.0)	139.0	6.95 m	138.3
4'	1.79 d (7.0)	14.8	1.84 d (7.0)	13.1
5'	1.78 s	12.5	1.87 s	10.8
6'	-	-	-	-
8-R		**O-Bz**		**O-Ang**
C=O		165.2		166.9
1"		129.8		
2"	7.87 dd (7.5, 1.5)	129.6		128.0
3"	7.53 dd (7.5, 7.5)	129.4	6.83 m	138.3
4"	7.66 m	134.0	1.81 d (7.5)	13.1
5"	7.53 dd (7.5, 7.5)	129.4	1.80 s	10.6
6"	7.87 dd (7.5, 1.5)	125.6	-	-

All compounds (**1**–**5**) were evaluated for cytotoxicity in three cell lines. B16F10 murine melanoma cells are often used for their high metastatic potential and moreover their ability to express MDR1[9]. Similarly, HaCat, a line of immortalized human keratinocytes, were used to model one of the outermost layers of skin and thus serve as a significant site of action for this *Euphorbia* spp. based terpenoids[10]. Cell Titer Glo is a luminescence-based viability assay that utilizes luciferase and ATP from lysed cells to generate a positive correlation between viability and luminesce intensity. Viable cells which produce ATP will produce a higher luminescence signal as opposed to damaged (necrotic) or dying (apoptotic) cells[11]. As a cytotoxic control, etoposide, an MDR1 substrate and chemotherapeutic agent[12], at 50 μM decreased B16F10 cell viability by 25.16%. Only compounds **2**, **3,** and **4** induced significant toxicity. Moreover, compound **2** had the greatest range of toxicity from 100 μM (49.63% decrease) to 20 μM (14.69% decrease). In human keratinocytes (HaCat), each compound caused a decrease in cell viability above 40 μM. Compounds **3** and **4** caused reductions in cell viability by approximately 12.42% and 17.92%, respectively, at a concentration of 30 μM. Compound **3** was able to decrease viability by as much as 93.63% at 50 μM. SH-SY5Y cells are typically used in neuropharmacology and neurodegenerative studies to model the sensitive nature of neurons[13]. Specifically, undifferentiated SH-SY5Y cells serve as an in vitro model for cancer and Parkinson's disease due the dopaminergic receptors available[13]. Exposure to etoposide at 10 μM decreased viability by approximately 44.64% (as in agreement with literature[14]). The compounds induced a cytotoxic effect at concentrations at 50 μM and above.

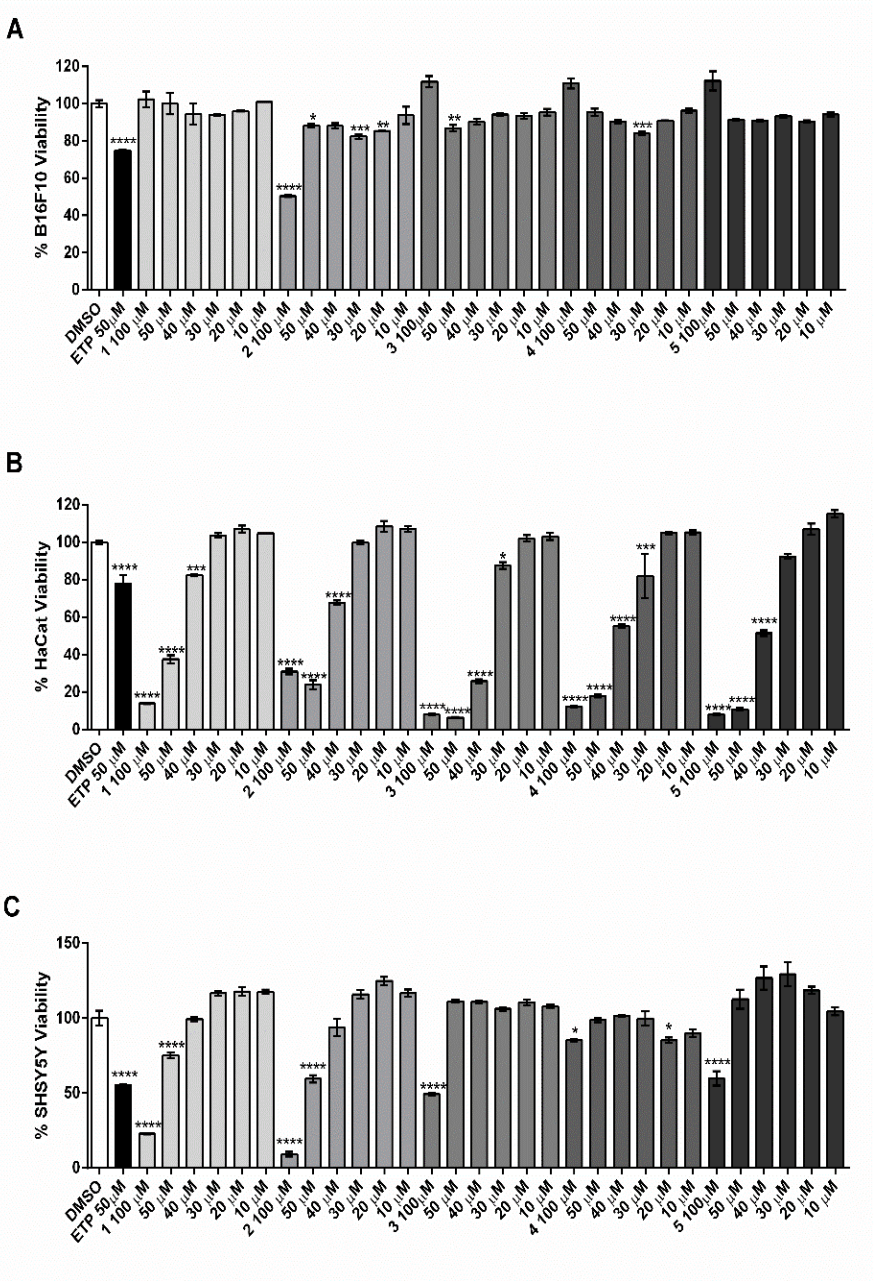

Figure 3. Cytotoxicity activities of **1–5.**

EXPERIMENTAL SECTION

General Experimental Procedures. The general experiments were completed according to the reported procedures with minor modification (General Experimental Procedures, Supporting Information).

Plant Material. Aerial parts of *E. saudiarabica* were collected in July 2015 in Thahban, Asir Province, Saudi Arabia. A.A. Fayed and D.A. Al-zahrani identified the plant species in 2007[15].

Extraction and Isolation. Air-dried powder of *E. saudiarabica* was macerated with methanol (3 × 15 L). The filtrate was concentrated under reduced pressure to afford a dried methanol extract (135 g). This was suspended in distilled water and successively partitioned to yield *n*-hexanes (66.6 g), ethyl acetate (3.32 g), and *n*-butanol (13.88 g) extracts after solvent removal in vacuo. The *n*-hexanes extract was dissolved in acetonitrile and successively partitioned again with *n*-hexanes to yield acetonitrile extract (22.1 g). Next, acetonitrile extract was fractioned using silica gel column eluted with *n*-hexanes/EtOAc (from 20:1 to 3:1) and then with $CHCl_3$/MeOH (from 40:1 to 1:1) to afford six major fractions (ES5–ES10). Fraction ES8 (1.07 g) was fractionated by semi-preparative HPLC (CH_3CN/H_2O) to afford two major fractions (ES8A and ES8B). Fraction ES8A (100 mg) was further purified by C_{18} reversed-phase semi-preparative HPLC (CH_3CN/H_2O) to give compound **1** (19.1 mg). Fraction ES6 (1.28 g) was chromatographed over MCI gel column chromatography eluting with H_2O/MeOH (9:1 to 1:9) to afford four major fractions (ES6A–ES6D). Fraction ES6C was purified by semi-preparative HPLC

(CH_3CN/H_2O 45:55, 2.5 mL/min) to obtain compounds **2** (6.2 mg) and **3** (5.5 mg). Fraction ES9 (1.3 g) afforded compounds **4** (3.5 mg) and **5** (2.6 mg) by repeated semi-preparative HPLC (CH_3CN/H_2O 35:65, 2.5 mL/min).

Saudiarabicain A **(1)** Reddish amorphous powder; $[\alpha]_D^{20}$ +78 (*c* 0.5, MeOH); UV (MeOH) λ_{max} (log ε) 208 (5.61), 272 (4.75) nm; IR (KBr) ν_{max} 2965, 1732, 1271, 1235, 1023, 989 cm^{-1}; ^1H and ^{13}C NMR (CD_3OD), see Table 1; (+)-HRESIMS *m/z* 633.2332 $[M + Na]^+$ (calcd for $C_{33}H_{38}O_{11}Na$, 633.2312).

Saudiarabicain B (**2**) *White* amorphous powder; $[\alpha]_D^{20}$ +78 (*c* 0.5, MeOH); UV (MeOH) λ_{max} (log ε) 203 (5.40), 270 (3.49) nm; IR (KBr) ν_{max} 1737, 1716, 1234, 1012, 988 cm^{-1}; ^1H and ^{13}C NMR (CD_3OD), see Table 1; (+)-HRESIMS *m/z* 611.2495 $[M + Na]^+$ (calcd for $C_{31}H_{40}O_{11}Na$, 611.2468).

Saudiarabicain C (**3**) White amorphous powder; $[\alpha]_D^{20}$ +78 (*c* 0.5, MeOH); UV (MeOH) λ_{max} (log ε) 210 (4.93), 270 (3.71) nm; IR (KBr) ν_{max} 2965, 1732, 1245 cm^{-1}; ^1H and ^{13}C NMR (CD_3OD), see Table 1; (+)-HRESIMS *m/z* 691.2751 $[M + Na]^+$ (calcd for $C_{36}H_{44}O_{12}Na$, 691.2730).

Saudiarabicain D (**4**) White amorphous powder; $[\alpha]_D^{20}$ +78 (*c* 0.5, MeOH); UV (MeOH) λ_{max} (log ε) 200 (4.56), 270 (3.20) nm; IR (KBr) ν_{max} 1716, 1299, 1243, 1180 cm^{-1}; ^1H and ^{13}C NMR (DMSO-d_6), Table 2; (+)-HRESIMS *m/z* 675.2785 $[M + Na]^+$ (calcd for $C_{36}H_{44}O_{11}Na$, 675.2781).

Saudiarabicain E (**5**) White amorphous powder; $[\alpha]_D^{20}$ +78 (*c* 0.5, MeOH); UV (MeOH) λ_{max} (log ε) 222 (3.92), 275 (2.84) nm; IR (KBr) ν_{max} 2958, 1344, 1241,1135 cm^{-1}; ^1H and ^{13}C NMR (CD_3OD), see Table 2; (+)-HRESIMS *m/z* 653.2953 $[M + Na]^+$ (calcd for $C_{34}H_{46}O_{11}Na$, 653.2938).

Cell Culture

Murine B16F10 melanoma cells and human HaCat keratinocytes were generously donated by Dr. Wen of Providence College. Human SH-SY5Y neuroblastoma cells were obtained from the European Collection of Authenticated Cell Cultures (ECACC; Porton Down, England UK). Melanoma cells and keratinocytes were maintained using DMEM supplemented with 10% fetal bovine serum (FBS) and 1% penicillin/streptomyces antibiotic cocktail. Neuroblastoma cells were maintained using DMEM/F12, also supplemented with 10% FBS and 1% pen/strep antibiotic cocktail. All cells were housed in a humidified incubator set to 37 °C under 5% CO_2. Cells were counted prior to seeded onto assay plates by using a hemocytometer and trypan blue dye. Following seeding, cells were allowed to incubate for at least 24 hours in serum-free media. Compounds were dissolved in DMSO (Sigma Aldrich, St. Louis, MO, USA) and diluted into serum-free media whereby the final DMSO content was less than 0.1% DMSO.

Cell Viability Assessment

Cell viability was determined using Cell Titer Glo 2.0 luminescence-based assay (Promega, Madison, WI, USA). As previously reported by our group[16], cells were seeded on white-walled 96-well plates at a density of either 100,000 cells/mL (B16F10 and SH-SY5Y) or 200,000 cells/mL (HaCat) to yield an 85% confluent plate following 24 hours. In brief, cells were treated with test compounds at 100, 50, 40, 30, 20, and 10 μM for 24 hours. Cell Titer Glo Reagent was then added directly to each well, mixed on an orbital shaker for approximately 2 minutes, and allowed to incubate at room temperature for 10 minutes prior to measuring luminescence using a Glomax Luminometer (Promega, Madison, WI, USA).

Statistical Analysis

Data are reported as mean ± standard error where each experiment was performed in triplicate. Statistical analysis was performed using Graphpad Prism Software (La Jolla, CA, USA) and significance was determined using one-way analysis of variance (ANOVA) using Dunnett's Correction for multiple comparisons. Calculated P values were determined to be as follows: P< 0.05*, P< 0.01**, P<0.001***, P<0.0001****.

ASSOCIATED CONTENT

Supporting Information: The Supporting Information is available free of charge on the ACS Publications website….

AUTHOR INFORMATION

Corresponding Author

(N.P.S.) Phone: +1 401-874-9367; Fax: 401-874-5787; Email: nseeram@uri.edu

ORCID

Navindra Seeram: 0000-0001-7064-2904

Author Contributions

§ Abdullatif Bin Muhsinah and Yongqiang Liu contributed equally to this work.

Notes: The authors declare no competing financial interest.

ACKNOWLEDGEMENTS

Research reported in this publication was made possible by the use of equipment and services available through the RI-INBRE Centralized Research Core Facility which is supported by the Institutional Development Award (IDeA) Network for Biomedical Research Excellence from the National Institute of General Medical Sciences of the National Institutes of Health under grant number P20GM103430.

REFERENCES

(1) Vasas, A.; Hohmann, J. *J. Chem. Rev.* **2014**, 114, 8579–8612

(2) Ernst, M.; Saslis-Lagoudakis, C. H.; Grace, O. M.; Nilsson, N.; Simonsen, H. T.; Horn, J. W.; Rønsted, N. *Scientific Reports*. **2016**, 6: 30531.

(3) Ramsay, J. R.; Suhrbier, A.; Aylward, J. H.; Ogbourne, S.; Cozzi, S. J.; Poulsen, M. G.; Baumann, K. C.; Welburn, P., Redlich, G. L., Parsons, P. G. *Br. J. Dermatol.* **2011**, 164: 633.

(4) Lebwohl, M.; Swanson, N.; Anderson, L. L.; Melgaard, A.; Xu, Z.; Berman, B. *N Engl J Med.* **2012**, 366: 1010–1019.

(5) Shi, Q.-W.; Su, Z.-H.; Kiyota, H. *Chemical Reviews.* **2008,** 108 (10), 4295–4327.

(6) Corea, G.; Fattorusso, E.; Lanzotti, V.; Motti, R.; Simon, P. N.; Dumontet, C.; Di Pietro, A. *J. Med. Chem.* **2004**, 47, 988–992.

(7) Fakunle, C. O.; Okogun, J. I., Ekong, D. E.; Connolly, J. D., Rycroft, D. S. *J. Chem. Soc., Perkin Trans. 1*. **1990**, 0, 727–730.

(8) Fatope, M. O.; Zeng, L.; Ohayagha, J. E.; McLaughlin, J. L. *Bioorg.Med. Chem. Lett*. **1996**, 4, 1679.

(9) He, X.; Wang, J.; Dou, J.; Yu, F.; Cai, K.; Li, X.; Gu, N. *Experimental and therapeutic medicine*. **2011**, 2(5), 911–916.

(10) Chudzik, M.; Korzonek-Szlacheta, I.; Król, W. *Molecules*. **2015,** 20(1), 1610–1625.

(11) Crouch, S. P., Kozlowski, R., Slater, K. J., and Fletcher, J. *J. Immunol. Methods*. **1993**, 160, 81–88.

(12) Krishna, R.; Mayer, L. D. *European Journal of Pharmaceutical Sciences*. **2000**, 11(4), 265–283.

(13) Xicoy, H.; Wieringa, B.; Martens, G. J. *Molecular Neurodegeneration*. **2017**,12(1),10.

(14) Cui, H., Schroering, A.; Ding, H. F. *Molecular Cancer Therapeutics*. **2002,** 1(9), 679–686.

(15) Fayed, A., Al-Zahrani, A. *Edinburgh J. of Bot.* **2007**, 64(2): 117–129.

(16) Ma, H., DaSilva, N. A., Liu, W., Nahar, P. P., Wei, Z., Liu, Y.; Shaikh, Z. A. *Neurochemical Research*. **2016**, 41(11), 2836–2847.

Manuscript III

Liquid Chromatography Coupled with Time-of-Flight Mass Spectrometry for Rapid Identification of Flavonoids from Aerial Parts of *Euphorbia saudiarabica*

Abdullatif Bin Muhsinah[§], Chunting Li[§], Navindra Seeram*

Bioactive Botanical Research Laboratory, Department of Biomedical and Pharmaceutical Sciences, College of Pharmacy, University of Rhode Island, Kingston, RI 02881, USA

[§] Abdullatif Bin Muhsinah and Chunting Li contributed equally to this work.

* Correspondence should be addressed to:

Navindra P. Seeram

Bioactive Botanical Research Laboratory, Department of Biomedical and Pharmaceutical Sciences, College of Pharmacy, University of Rhode Island, 7 Greenhouse Road, Kingston, RI 02881, USA

Tel: +1 401-874-9367; Fax: +1 401-874-5787; Email: nseeram@uri.edu

KEYWORDS:

Euphorbia saudiarabica, flavonoids, Tandem mass spectrometry

This manuscript is written in the style of the *Journal of Separation Science*

ABSTRACT

The dried methanolic extract of aerial parts of *Euphorbia saudiarabica* was subjected to investigate its flavonoid composition using LC-ESI-TOF-MS/MS. In the present study, 36 flavonoids were identified. The compounds constituted 7 flavonoids based on the galangin aglycon, 9 flavonoids based on the apigenin aglycon, and 20 flavonoids originated from luteolin. Among these, 3 compounds are malonyl substituted, and 13 compounds are acetyl substituted.

INTRODUCTION

Flavonoids and their conjugate forms are some of the most abundant polyphenols, and more than 8000 different flavonoids have been demonstrated so far. These flavonoids are considered to be the most plentiful natural products in the human diet since they are found in many plant tissues, including fruits and vegetables. In addition, the presence of flavonoids among plant genera, such as *Euphorbia* genus, are widely described. A literature review of the *Euphorbia* genus showed that many of its secondary metabolites, like diterpenoids and flavonoids, are highly bioactive [1]. *Euphorbia saudiarabica* is one of about 8000 species of the family Euphorbiaceae [2]. It is an endemic species to the southwest of Saudi Arabia close to the Red Sea [3]. This plant, like other *Euphorbia* species, is known for its a milky skin-irritant latex.

To our knowledge, the flavonoid content of *E. saudiarabica* have not been studied. Therefore, the objective of the present study was to determine the phytochemical profiles of the total flavonoid contents of this plant using the liquid chromatography-tandem mass spectrometry (LC-MS/MS) technique.

MATERIALS AND METHODS

Chemicals

LC-MS grade methanol was purchased from Sigma-Aldrich (St. Louis, MO, USA).

Sample preparation

Air-dried powder of *E. saudiarabica* (1 g) was macerated with methanol (3 × 15 mL). The filtrate was concentrated under reduced pressure to afford a dried methanol extract. The methanol extract was re-dissolved in 10 mL acetonitrile, then partitioned with hexane (3 × 10 mL). The acetonitrile layer was concentrated under reduced pressure and re-dissolved in methanol. The methanol solution was stored at −20 °C and filtered (0.22 μm) before analysis.

Liquid Chromatography-Mass Spectrometry Conditions

LC-ESI-TOF-MS/MS analyses were performed on a SHIMADZU Prominence UFLC system (Marlborough, MA, USA) consisting of two LC-20AD pumps, a DGU-20A degassing unit, a SIL-20AC auto sampler, a CTO-20AC column oven, and a CBM-20A communication bus module. Chromatographic separation was performed on a 150 mm × 4.6 mm i.d., 3 μm, Atlantis dC18 column (Waters, Milford, MA, USA). The mobile phase consisted of 0.1% formic acid/methanol (A) and 0.1% aqueous formic acid (B) with a gradient elution of 5% A from 0 to 5 min, 5%–95% A from 5 to 95 min. The column temperature was 40 °C, the flow rate was 0.50 mL/min, and the injection volume was 10 μL. Mass spectrometry was performed using a Triple TOF 4600 system from Applied Biosystems/MDS Sciex (Framingham, MA, USA) coupled with ESI interface. Nitrogen was used in all cases. In this study, the parameters were optimized as follows: ESI voltage, −4500

V; GS1, 40 psi; GS2, 55 psi; CUR, 30 psi; turbo gas temperature, 550 °C; declustering potential, −80 V; collision energy, 40 eV. Instrument calibration was carried out according to the manufacturer's instructions. The mass range was set from *m/z* 100 to 1250. The data were acquired and processed using Analyst TF 1.7 Software.

RESULTS AND DISCUSSION

Qualitative characterization of the flavonoids present in the methanol extract of aerial parts of *E. saudiarabica* was performed in ESI negative ionization mode, and all of the compounds showed $[M - H]^-$ ions (**Table 1**). Accurate mass data were then acquired in full scan analysis, and product ion mass data were acquired via the information dependent acquisition (IDA) method. An Atlantis dC18 column was used, and formic acid was introduced into the mobile phase (0.1%) to alleviate peak tailing and to produce better peak shapes. The acidic conditions did not significantly affect the ionization efficiency of the compounds in negative mode.

In the present study, 36 flavonoids were identified based on previously reported MS/MS fragmentation patterns for flavonoids [4]. The compounds constituted 7 flavonoids based on the galangin aglycon, 9 flavonoids based on the apigenin aglycon, and 20 flavonoids originated from luteolin (**Table 1**). Among these, 3 compounds are malonyl substituted, and 13 compounds are acetyl substituted. The total ion chromatograms profiles of the compounds are shown in **Figure**. **1**. Accurate mass measurements, retention times (tR), formula, errors, and main MS/MS product ions for all of the flavonoids are summarized in **Table 1**.

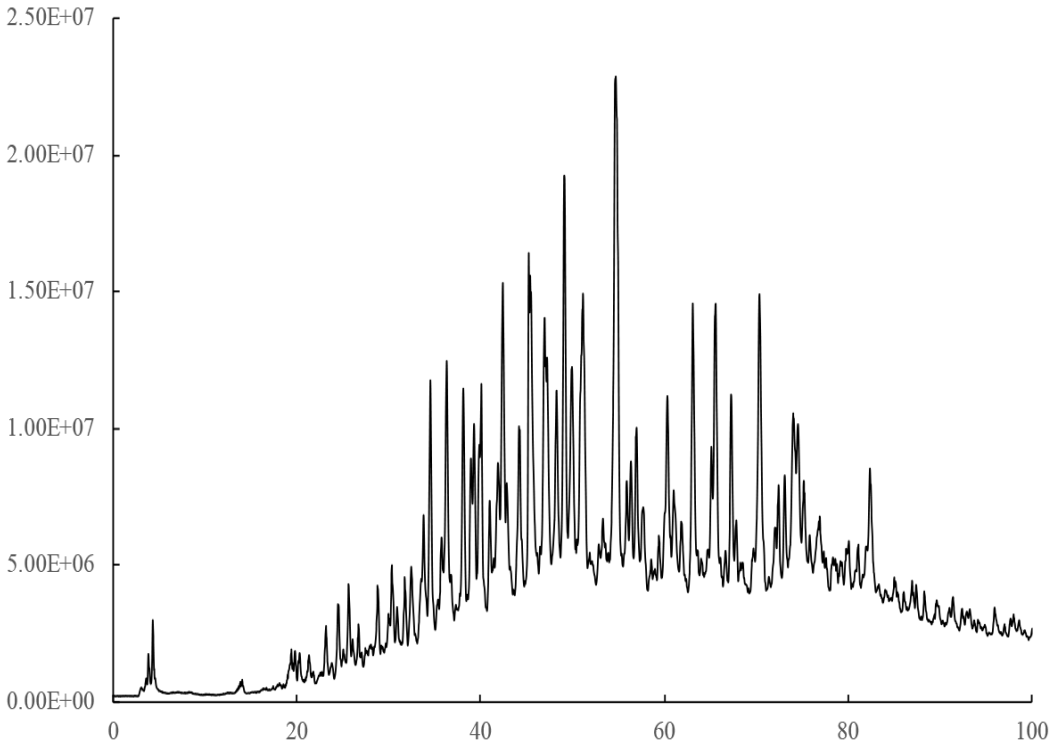

Figure 1. Total ion chromatogram of a methanol extract from aerial parts of *E. saudiarabica*.

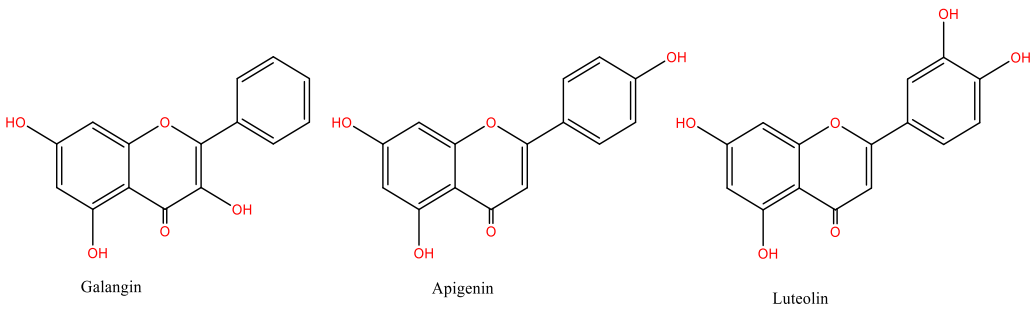

Figure 2. The skeletal structure of galangin, apigenin, and luteolin.

Table 1. LC-ESI-TOF-MS/MS data for flavonoids identified in a methanol extract from aerial parts of *E. saudiarabica*.

No.	tR (min)	Molecular formula	HR-ESI(-)-MS $[M-H]^-$ (m/z)	Error (ppm)	Major and important MS/MS ions	Identification
1	41.27	$C_{33}H_{38}O_{21}$	769.1844	1.4528	607, 431, 337, 311, 269, 175, 151, 149, 113	A-(GlcUA-Hex, Hex)
2	45.15	$C_{28}H_{30}O_{16}$	609.1460	-0.1789	447, 285, 199, 175, 151, 133	L-(Hex, Hex)
3	46.95	$C_{27}H_{28}O_{17}$	623.1272	2.9311	605, 561, 447, 357, 337, 327, 285, 199, 175, 151, 133	L-(Hex, GlcUA)
4	47.53	$C_{28}H_{30}O_{16}$	609.1487	4.2535	447, 285, 199, 175, 151, 133	L-(Hex-Hex)
5	48.32	$C_{27}H_{28}O_{17}$	623.1273	3.0916	447, 285, 199, 175, 151, 133	L-(Hex-GlcUA)
6	48.67	$C_{28}H_{30}O_{16}$	609.1476	2.4477	447, 357, 327, 285, 199, 175, 151, 133	L-(Hex-Hex)
7	50.12	$C_{27}H_{28}O_{16}$	607.1313	1.3853	431, 337, 315, 269, 225, 151, 149, 117, 113, 107	A-(Hex-GlcUA)
8	51.18	$C_{21}H_{20}O_{11}$	447.0942	2.0457	357, 327, 285, 199, 175, 151, 133	L-Hex
9	51.47	$C_{28}H_{30}O_{17}$	637.1434	3.7297	619, 461, 337, 299, 284, 199, 175, 151, 133	ML-(Hex-GlcUA)
10	51.77	$C_{28}H_{30}O_{16}$	609.1487	4.2535	447, 285, 199, 175, 151, 133	L-(Hex-Hex)
11	51.86	$C_{27}H_{30}O_{15}$	593.1525	2.2012	431, 269, 225, 151, 149, 117, 113, 107	A-(Hex-Hex)
12	52.08	$C_{28}H_{30}O_{17}$	637.1429	2.9449	461, 299, 284, 199, 175, 151, 133	ML-(Hex-GlcUA)
13	52.25	$C_{27}H_{28}O_{16}$	607.1312	1.2206	431, 357, 337, 269, 225, 151, 149, 117, 113, 107	A-(Hex-GlcUA)
14	52.67	$C_{29}H_{30}O_{17}$	649.1418	1.196	473, 269, 225, 151, 149, 117, 113, 107	A-(acetylHex-GlcUA)
15	54.03	$C_{28}H_{30}O_{16}$	621.1471	0.991	431, 269, 225, 201, 183, 181, 151, 149, 117, 113	A-(Hex-MethylGlcUA)
16	54.07	$C_{24}H_{22}O_{14}$	533.0937	0.0386	489, 285, 199, 175, 151, 133	L-(6-malonylHex)
17	54.20	$C_{30}H_{30}O_{20}$	709.1279	3.0071	665, 623, 603, 489, 447, 379, 357, 285, 199, 175, 151, 133	L-(malonylHex, GlcUA)
18	54.36	$C_{23}H_{22}O_{12}$	489.1058	3.9866	447, 429, 357, 327, 285, 256, 227, 199, 175, 151, 133	L-acetylHex
19	54.72	$C_{21}H_{20}O_{10}$	431.0976	-1.7878	269, 268, 240, 211, 151, 117	G-3-O-Hex

20	56.02	$C_{21}H_{20}O_{10}$	431.0990	1.4596	269, 268, 240, 211, 151, 117	G-3-O-Hex
21	56.41	$C_{21}H_{20}O_{11}$	447.0934	0.2563	285, 199, 175, 151, 133	L-Hex
22	56.96	$C_{24}H_{22}O_{14}$	533.0949	2.2896	489, 447, 285, 199, 175, 151, 133	L-malonylHex
23	56.99	$C_{23}H_{22}O_{12}$	489.1041	0.5109	447, 357, 327, 285, 256, 227, 199, 175, 151, 133	L-acetylHex
24	57.15	$C_{29}H_{30}O_{17}$	649.1408	-0.3444	473, 269, 225, 151, 149, 117, 113, 107	A-(acetylHex-GlcUA)
25	57.70	$C_{23}H_{22}O_{11}$	473.1095	1.1932	269, 268, 240, 211, 151, 117	G-3-O-acetylHex
26	58.38	$C_{23}H_{22}O_{11}$	473.1088	-0.2863	269, 268, 240, 211, 151, 117	G-3-O-acetylHex
27	58.59	$C_{21}H_{20}O_{11}$	447.0937	0.9273	285, 199, 175, 151, 133	L-Hex
28	59.02	$C_{23}H_{22}O_{11}$	473.1092	0.5591	269, 268, 240, 211, 151, 117	G-3-O-acetylHex
29	59.39	$C_{29}H_{30}O_{18}$	665.1350	-1.4106	489, 357, 327, 285, 199, 175, 151, 133	L-(acetylHex-GlcUA)
30	60.47	$C_{23}H_{22}O_{11}$	473.1096	1.4046	269, 268, 240, 211, 151, 117	G-3-O-acetylHex
31	61.79	$C_{23}H_{22}O_{12}$	489.1044	1.1243	447, 357, 327, 285, 256, 227, 199, 175, 151, 133	L-acetylHex
32	62.20	$C_{29}H_{30}O_{17}$	649.1419	1.35	473, 269, 225, 151, 149, 117, 113, 107	A-(acetylHex-GlcUA)
33	63.10	$C_{15}H_{10}O_{6}$	285.0401	-1.2692	199, 175, 151, 133	L
34	64.42	$C_{23}H_{22}O_{12}$	489.1044	1.1243	285, 199, 175, 151, 133	L-(6-acetylHex)
35	65.25	$C_{23}H_{22}O_{11}$	473.1096	1.4046	269, 268, 240, 211, 151, 117	G-3-O-acetylHex
36	67.36	$C_{15}H_{10}O_{5}$	269.0460	1.6832	227, 225, 201, 197, 183, 181, 159, 151, 149, 117, 107	A

Compounds **19** (t_R=54.72 min) and **20** (t_R=56.02 min) displayed same $[M-H]^-$ at *m/z* 431, and their MS/MS fragmentation all yielded the aglycone Y_0^- ion at *m/z* 269. This aglycone was further confirmed as galangin by the characteristic product ions at *m/z* 117, 151, 211, and 240 [4]. The product ion at *m/z* 269 $[M-H-162]^-$ also indicated the loss of a hexose group (162 Da). However, the nature of hexose could not be determined only by MS data. Therefore, compounds **19** and **20** were identified as galangin-*O*-hexosides. In their MS/MS spectrum, $[Y_0-H]^-$ ion at *m/z* 268 with high intensity was also observed. Flavonols substituted at the 3-OH position should yield a high-intensity fragment $[Y_0-H]^-$, sometimes higher than the Y_0^- ion [5]. Thus, the glycosylation position of compounds **19** and **20** should be at 3-OH. Therefore, compound **19** and **20** were further identified as galangin-3-*O*-hexosides.

Compounds **25**, **26**, **28**, **30** and **35** all produced the same $[M-H]^-$ ion at *m/z* 473 with different tR of 57.70, 58.38, 59.02, 60.47, and 65.25 min, respectively. In their MS/MS spectra, they all showed the same fragment ion at *m/z* 269 which was produced by the loss of an acetyl-hexose group (204 Da). Also, the characteristic fragment ions of galangin at *m/z* 117, 151, 211, and 240 were observed. Thus, these compounds were identified as galangin-*O*-(acetyl-hexoside). High-intensity radical aglycone $[Y_0-H]^-$ ion at *m/z* 268 was found in the MS/MS spectra of all compounds, indicating that they were galangin-3-*O*-(acetyl-hexoside).

Compound **36** (t_R=67.36 min) produced the $[M-H]^-$ ions at *m/z* 269. In the MS/MS spectrum, the typical product ions at *m/z* 107, 117, 149, 151, and 225 led to the identification of compound **36** as apigenin [6]. Compound **11** (t_R=51.86 min) displayed a pseudomolecule ion $[M-H]^-$ at *m/z* 593 and gave the aglycone Y_0^- ion at *m/z* 269 in its MS/MS spectrum. The typical product ions at *m/z* 107, 117, 149,

151, and 225 led to the identification of the aglycone as apigenin. The loss of 324 Da could be attributed to the loss of a caffeoyl-hexose unit or a di-hexose unit. It should be noted that deprotonated apigenin-*O*-caffeoylhexoside possesses the same nominal molecular weight of 593 as deprotonated apigenin-*O*-hexosylhexoside, but their accurate molecular weights are different, i.e., 593.1300 for apigenin-*O*-caffeoylhexoside and 593.1511 for apigenin-*O*-hexosylhexoside, and their molecular formulae are $C_{30}H_{26}O_{13}$ and $C_{27}H_{30}O_{15}$, respectively. According to the deprotonated molecular ion $[M - H]^-$ at *m/z* 593.1525 measured by TOF-MS, compound **11** was identified as apigenin-*O*-hexosylhexoside.

Compounds **7** (t_R=50.12 min) and **13** (t_R=52.25 min) produced the same $[M - H]^-$ ions at *m/z* 607. In their MS/MS spectra, they showed a same aglycone Y_0^- ion at *m/z* 269. In addition, the aglycone was determined as apigenin by the characteristic fragment ions at *m/z* 107, 117, 149, 151, and 225. A weak ion at *m/z* 431 arising from the loss of 176 Da was also observed in their MS/MS spectrum, which represents a loss of a glycuronic acid unit. Further loss of 162 Da ($[M - H -$ glycuronic acid unit $-$ hexose unit$]^-$) allowed us to infer that compounds **7** and **13** may consist of the apigenin moiety with a glycuronic acid group (176 Da) and a hexose group (162 Da), while the glycuronic acid group is in the external position. Thus, compounds **7** and **13** were identified as apigenin-*O*-hexosylglycuronides.

Compounds **14** (t_R=52.67 min), **24** (t_R=57.15 min), and **32** (62.20 min) all produced the same $[M - H]^-$ ions at *m/z* 649. In their MS^2 spectra, they all showed the same aglycone Y_0^- ions at *m/z* 269. In addition, the characteristic fragment ions of apigenin at *m/z* 107, 117, 149, 151, and 225 were observed. The weak ions at *m/z* 473 in their MS/MS spectrum indicated that compounds **14**, **24,** and **32** contained a glycuronic acid group (176 Da) and an acetyl-hexose group (204 Da), while the

glycuronic acid group is in the external position. Thus, compounds **14**, **24**, and **32** were identified as apigenin-*O*-acetylhexosylglycuronides.

Compounds **15** (t_R=54.03 min) displayed its $[M - H]^-$ ions at *m/z* 621. In the MS/MS spectra, the aglycone Y_0^- ion at *m/z* 269 was observed and was identified as apigenin by the characteristic fragment ions at *m/z* 107, 117, 149, 151, and 225. A weak ion at *m/z* 431 indicated a loss of a methyl-glycuronic acid unit (190 Da). Compound **15** was identified as apigenin-*O*-(hexosyl-methylglycuronide).

Compounds **1** (t_R=41.27 min) produced the $[M - H]^-$ ions at *m/z* 769. In the MS/MS spectra, it gave the aglycone Y_0^- ion at *m/z* 269. In addition, the aglycone was determined as apigenin by the characteristic fragment ions at *m/z* 107, 117, 149, 151, and 225. The loss of 500 Da allowed us to infer that compound **1** may consist of the apigenin moiety with a glycuronic acid group (176 Da) and two hexose groups (162 Da). The high-intensity ion at *m/z* 431 indicated a hexose group and a hexose-glycuronic acid group glycosylated to two different positions on the apigenin moiety of compound **1**. The weak ions at *m/z* 607 arising from the loss of 162 Da was also observed in MS/MS spectrum, which represents the hexose as in the external position of the hexose-glycuronic acid group. Thus, compound **1** was identified as apigenin-*O*-(hexoside, glucuronylhexoside).

Compound **33** (t_R=63.10 min) produced the $[M - H]^-$ ions at *m/z* 285. In the MS/MS sepectrum, the typical product ions at *m/z* 133, 151, 175, and 199 led to the identification of compound **33** was luteolin [4]. Compounds **8** (t_R=51.18 min), **21** (t_R=56.41 min), and (**27**) (t_R=58.59 min) displayed the same $[M - H]^-$ ions at *m/z* 447, and their MS/MS spectrum all yielded the aglycone Y_0^- ion at *m/z* 285. This aglycone was further confirmed as luteolin by the characteristic product ions at *m/z* 133, 151, 175, and 199. The product ion at *m/z* 285 $[M - H - 162]^-$ also indicated

the loss of a hexose group (162 Da). Therefore, compounds **8**, **21,** and **27** were identified as luteolin-*O*-hexosides.

Compounds **18** (t_R=54.36 min), **23** (t_R=56.99 min), **31** (t_R=61.79 min), and **34** (t_R=64.42 min) all produced the same $[M - H]^-$ ions at *m/z* 489. In their MS/MS spectra, they all showed the same aglycone Y_0^- ions at *m/z* 285. In addition, the characteristic fragment ions of luteolin at *m/z* 133, 151, 175, and 199 were observed. The loss of 204 Da indicated the existence of an acetyl hexose group in each compound. Thus, compounds **18**, **23**, **31,** and **34** were identified as luteolin-*O*-acetylhexosides. In the MS/MS spectrum, compounds **18**, **23**, and **31** gave the same weak ion at *m/z* 447 that indicated the loss of acetyl group. However, the ion at *m/z* 447 was not observed in the MS/MS spectrum of compound **34**. The acylation in position 6 of hexose is difficult to break in mass spectrometry [7]. Thus, compound **34** was further identified as luteolin-*O*-(6-acetylhexoside).

Compounds **16** (t_R=54.07 min) and **22** (t_R=56.96 min) produced the $[M - H]^-$ ions at *m/z* 533. In the MS/MS spectra, they all gave aglycone Y_0^- ions at *m/z* 285. In addition, the aglycone was determined as luteolin by the characteristic fragment ions at *m/z* 133, 151, 175, and 199. Their product ions at *m/z* 489 and 285 by the loss of 44 Da (CO_2) and 204 Da (acetyl-hexose group) indicated the existence of a malonyl-hexose group [7]. Therefore, compounds **16** and **22** were identified as luteolin-*O*-(malonylhexoside). In the MS/MS spectrum, compound **22** gave a weak ion at *m/z* 447, indicating the loss of an acetyl group (remains of malonyl after decarboxylation) from an ion at *m/z* 489. However, the ion at *m/z* 447 was not observed in the MS/MS spectrum of compound **16**. Therefore, compound **16** was further identified as luteolin-*O*-(6-malonylhexoside).

Compounds **2** (t_R=45.15 min), **4** (t_R=47.53 min), **6** (t_R=48.67 min), and **10** (t_R=51.77 min) displayed the same pseudomolecule ions $[M - H]^-$ at *m/z* 609. The aglycone Y_0^- ion at *m/z* 285 and typical product ions at *m/z* 133, 151, 175, and 199 in their MS/MS spectrum indicated the aglycone as luteolin. The loss of 324 Da could be attributed to the loss of a caffeoyl-hexose unit or a di-hexose unit. Their accurate molecular weights by TOF-MS supported their molecular formulae to be $C_{28}H_{30}O_{16}$. Thus, compounds **2**, **4**,**6**, and **10** consist of the luteolin moiety with two hexose groups (162 Da). In the MS/MS spectrum of compound **2**, the high-intensity product ion at *m/z* 447 indicated the two hexose groups substituted for different positions on the luteolin moiety. However, only the tiny peak of an ion at *m/z* 447 was observed in the MS/MS spectrum of compounds **4**, **6,** and **10**. Therefore, compounds **4**, **6,** and **10** were determined as luteolin-*O*-hexosylhexosides, and compound **2** was identified as luteolin-*O*-(hexoside, hexoside).

Compounds **3** (t_R=46.95 min) and **5** (t_R=48.32 min) exhibited the same $[M - H]^-$ ions at *m/z* 623. In their MS/MS spectra, the Y_0^- ions at *m/z* 285 and the characteristic fragment ions at *m/z* 133, 151, 175, and 199 were observed, suggested the aglycone was luteolin. The loss of 338 Da indicated ccompounds **3** and **5** consist of the luteolin moiety with a hexose group (162 Da) and a glucuronic acid group (176 Da). In the MS/MS spectrum of compound **3**, a high-intensity product ion at *m/z* 447 was observed, indicating the hexose and glucuronic acid groups substituted to different positions on the luteolin moiety. In the MS/MS spectrum of compound **5**, only a weak ion at *m/z* 447 arising from the loss of 176 Da was observed, indicating the existence of the hexose-glucuronic acid group and glucuronic acid in the external position. Thus, compounds **3** and **5** were identified as luteolin-*O*-(hexoside, glucuronide) and luteolin-*O*-hexosylglucuronide, respectively.

Compounds **9** (t_R=51.47 min) and **12** (t_R=52.08 min) gave the same $[M - H]^-$ ions at *m/z* 637. In the MS/MS spectra, they gave the aglycone Y_0^- ion at *m/z* 299. In addition, the aglycone was determined as methylluteolin by the characteristic fragment ions at *m/z* 133, 151, 175, 199, and 284. The loss of 338 Da suggested compounds **9** and **12** consist of the methylluteolin moiety with a glucuronic acid group (176 Da) and a hexose group (162 Da). In their MS/MS spectrum, the weak ions at *m/z* 461 arising from the loss of 176 Da were observed, representing glucuronic acid in the external position of the hexose-glucuronic acid group. Thus, compounds **9** and **12** were identified as methylluteolin-*O*-hexosylglucuronide.

Compounds **29** (t_R=59.39 min) and **17** (t_R=54.20 min) gave $[M - H]^-$ ions at *m/z* 665 and 709. The aglycone Y_0^- ion at *m/z* 285 was observed in both compounds, and the aglycone was identified as luteolin by MS/MS spectrum. The weak ion at *m/z* 489 ($[M - H -$ glucuronic acid group$]^-$) combined with the Y_0^- ion at *m/z* 285 ($[M - H - 176$ Da $- 204$ Da$]^-$) suggested compound **29** possessed an acetylhexose-glucuronic acid group and glucuronic acid was in the external position. Thus, compound **29** was identified as luteolin-*O*-acetylhexosylglucuronide. In the MS/MS spectrum of compound **17**, product ions of *m/z* 665 ($[M - H - 44$ Da$]^-$) and *m/z* 623 ($[M - H - 44$ Da $- 42$ Da$]^-$) indicated the existence of a malonyl group. The high intensity product ions of *m/z* 489 ($[M - H - 44$ Da $- 176$ Da$]^-$) and 285 ($[M - H - 176$ Da $- 44$ Da $- 204$ Da$]^-$) indicated that a glucuronic acid group and a malonylhexose group substituted to different positions of luteolin. Thus, compound **17** was identified as luteolin-*O*-(malonylhexoside, glucuronide).

CONCLUDING REMARKS

In summary, a rapid and reliable method employing LC-ESI-TOF-MS/MS was developed for the identification of flavonoids aerial parts of *E. saudiarabica*. Based on accurate mass measurement and characteristic fragmentation ions, 36 flavonoids, including 7 flavonoids originating from galangin, 9 from apigenin, and 20 from luteolin, were identified. Among these, 3 compounds are malonyl substituted and 13 compounds are acetyl substituted. The LC-ESI-TOF-MS/MS method established herein could be used for future characterization and standardization of *E. saudiarabica*.

ACKNOWLEDGEMENT

Research reported in this publication was made possible by the use of equipment and services available through the RI-INBRE Centralized Research Core Facility, which is supported by the Institutional Development Award (IDeA) Network for Biomedical Research Excellence from the National Institute of General Medical Sciences of the National Institutes of Health under grant number P20GM103430.

AUTHOR INFORMATION

Corresponding Author

(N.P.S.) Phone: +1 401-874-9367; Fax: 401-874-5787; Email: nseeram@uri.edu

ORCID

Navindra Seeram: 0000-0001-7064-2904

Author Contributions

§ Abdullatif Bin Muhsinah and Chunting Li contributed equally to this work.

CONFLICT OF INTEREST STATEMENT

The authors have declared no conflict of interest.

REFERENCES

[1] Shi Q-W., Su Z-H., Kiyota H. Chemical and pharmacological research of the plants in genus *Euphorbia. Chemical Reviews.* **2008,** *108 (10)*, 4295–4327.

[2] Vasas A., Hohmann J. *Euphorbia* diterpenes: isolation, structure, biological activity, and synthesis (2008–2012), *Chem. Rev.* **2014**, *114*, 8579–8612.

[3] Fayed A., Al-Zahrani A. Three new spiny *Euphorbia* (Euphorbiaceae) species from western Saudi Arabia. *Edinburgh J. of Bot.* **2007**, *64(2)*, 117–129.

[4] Gu D., Yang Y., Abdulla R., Aisa H. A., Characterization and identification of chemical compositions in the extract of *Artemisia rupestris* L. by liquid chromatography coupled to quadrupole time-of-flight tandem mass spectrometry. *Rapid Commun. Mass Spectrom.* **2012**, *26*, 83–100.

[5] Hvattum E., Ekeberg D., Study of the collision-induced radical cleavage of flavonoid glycosides using negative electrospray ionization tandem quadrupole mass spectrometry. *J. Mass Spectrom.* **2003**, *38*, 43–49.

[6] Hughes R. J., Croley T. R., Metcalfe C. D., March R. E., A tandem mass spectrometric study of selected characteristic flavonoids. *Int. J. Mass spectrom.* **2001**, 210/211, 371–385.

[7] Abu-Reidah I. M., Gil-Izquierdo A., Medina S., Ferreres F., Phenolic composition profiling of different edible parts and by-products of date palm (*Phoenix dactylifera* L.) by using HPLC-DAD-ESI/MS(n). *Food Res. Int.* **2017**, *100*, 494–500.

Conclusion and Future Plan

The aim of this work was the isolation and structure elucidation of the secondary metabolites from the crude extract of two plants: silver maple leaves *(Acer saccharinum*) and aerial parts of the species *Euphorbia saudiarabica*. First, the polyphenolic contents of the silver maple leaves were investigated by using TLC, RP-HPLC, and the Folin-Ciocalteau method for quantifying total polyphenols. Next, the isolation and purification process was carried out which led to **10** identified compounds by means of spectroscopic methods (NMR, and HPLC-DAD). These compounds, including six GCGs (ginnalins A-C [1-3], maplexins B, D, and F [4-6]), methyl syringate (**7**), methyl gallate (**8**), and 3-methoxy-4-hydroxyphenol-1-β-D-(6-galloyl)-glucopyranoside (**9**). Additionally, one sesquiterpenoid, namely, pubineroid A (**10**), was isolated and identified. Likewise, the diterpenoids contents of *Euphorbia saudiarabica* were investigated using HPLC-DAD and TLC techniques. Next, after multistep of the separation and purification, five new lathyrane-diterpenoid compounds were elucidated. Additionally, the cytotoxicity effects of these compounds were evaluated; all of them exhibited mild to moderate cytotoxicity effects. Next, a rapid and reliable method employing LC-ESI-TOF-MS/MS was developed for the identification of flavonoids from the aerial parts of *E. saudiarabica* which led to 36 reported flavonoid compounds. Finally, future plan will be focused on exploring the biological activities of the isolated diterpenoids (**1-5**) from *Euphorbia saudiarabica*, mainly for their multi-drug resistance (MDR) inhibitory effects. In addition, future goals will be focused on investigating other *Euphorbia* species endemic to Saudi Arabia to evaluate their cytotoxicity, as well as their antifungal and MDR-modulatory effects.

Appendix I

Saudiarabicain A-E, Macrocyclic Diterpenoids from *Euphorbia saudiarabica*

Abdullatif Bin Muhsinah[†,§], Yongqiang Liu[‡,§], Nicholas A. DaSilva[‡],Navindra Seeram*[,‡]

[†] *Department of Pharmacognosy, College of Pharmacy, King Khalid University, P.O.Box # 641, Abha, Saudi Arabia*

[‡] *Bioactive Botanical Research Laboratory, Department of Biomedical and Pharmaceutical Sciences, College of Pharmacy, University of Rhode Island, Kingston, RI 02881, USA*

[§] *Abdullatif Bin Muhsinah and Yongqiang Liu contributed equally to this work.*

Supporting information Available

Figures

Tables

Figures

1

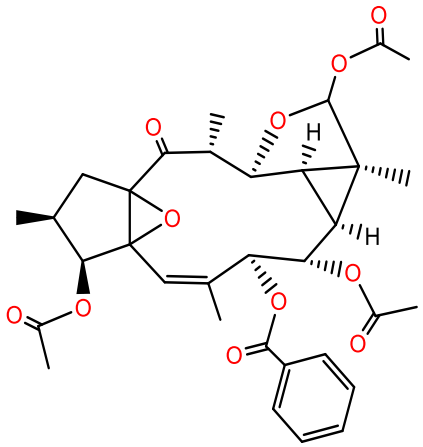

Chemical Formula: $C_{33}H_{38}O_{11}$
Exact Mass: 610.24

2

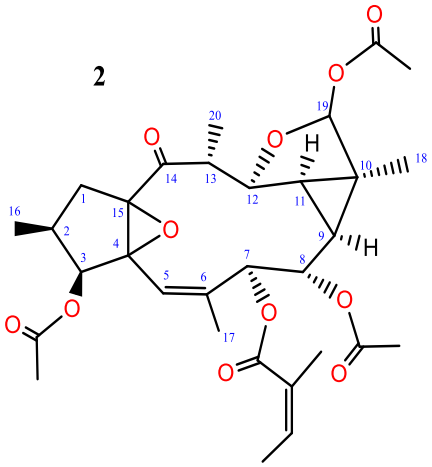

Chemical Formula: $C_{31}H_{40}O_{11}$
Molecular Weight: 588.65

3

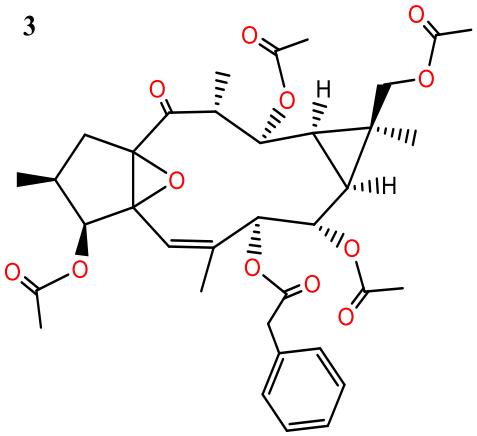

Chemical Formula: $C_{36}H_{44}O_{12}$
Exact Mass: 668.28

4

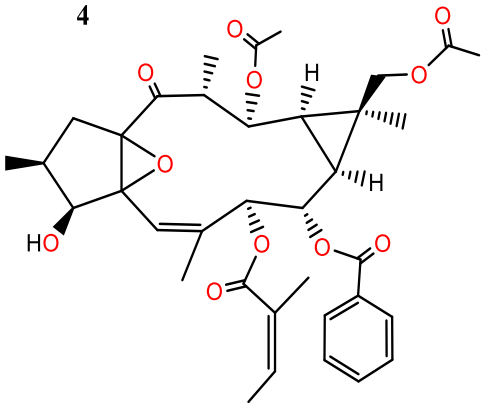

Chemical Formula: $C_{36}H_{44}O_{11}$
Exact Mass: 652.29

5

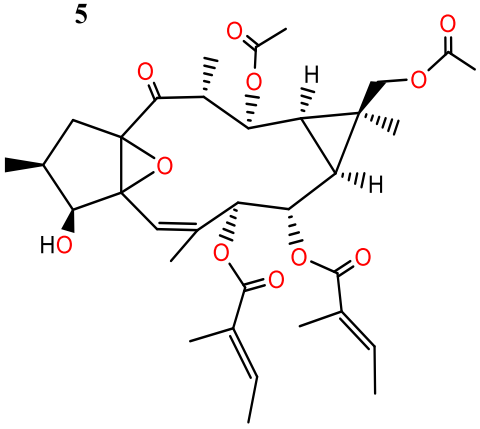

Chemical Formula: $C_{34}H_{46}O_{11}$
Exact Mass: 630.30

Figure S1. Structures of the isolated compounds (**1-5**) .

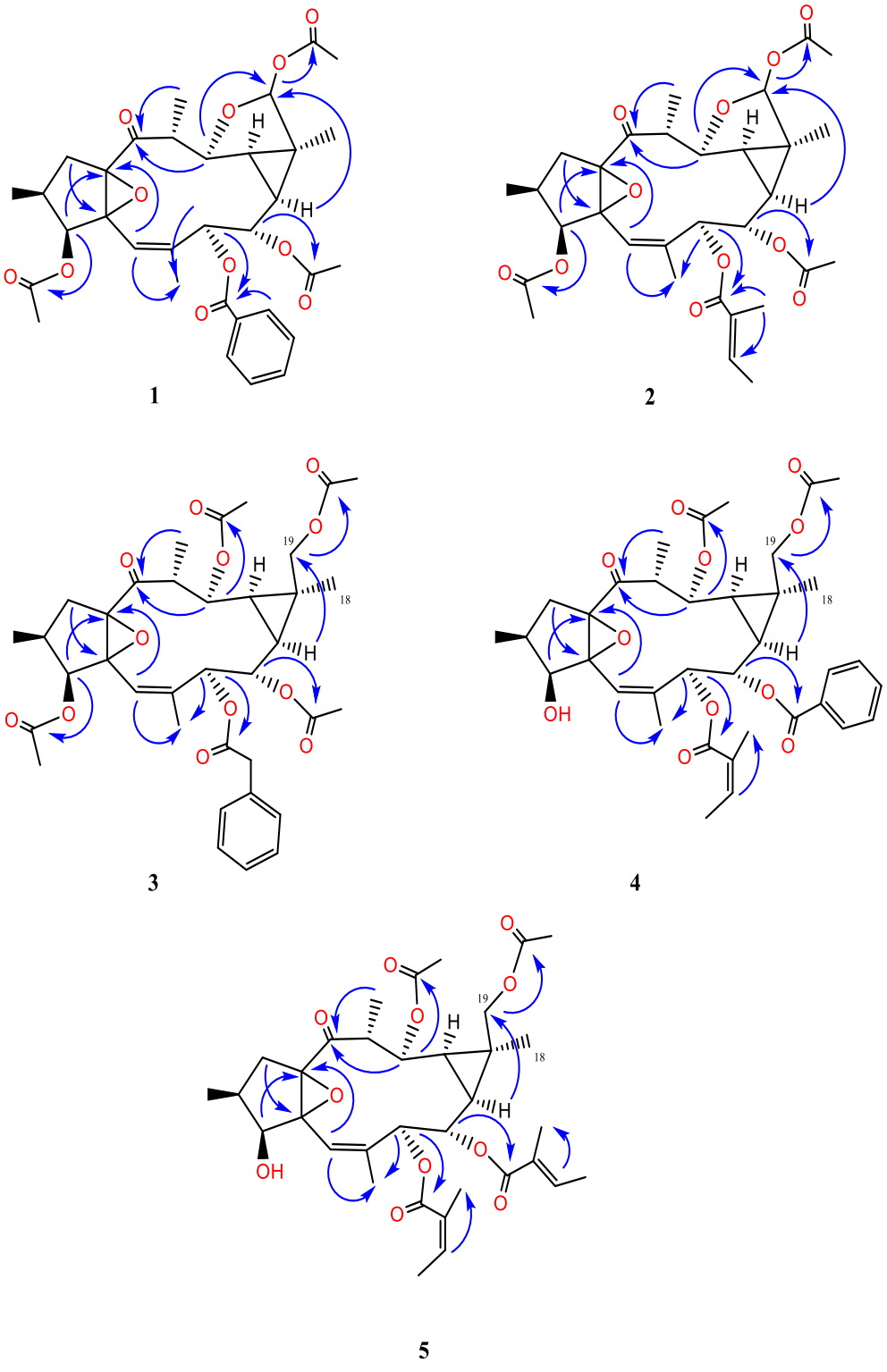

Figure S2. Key HMBC correlations of compounds (**1-5**)

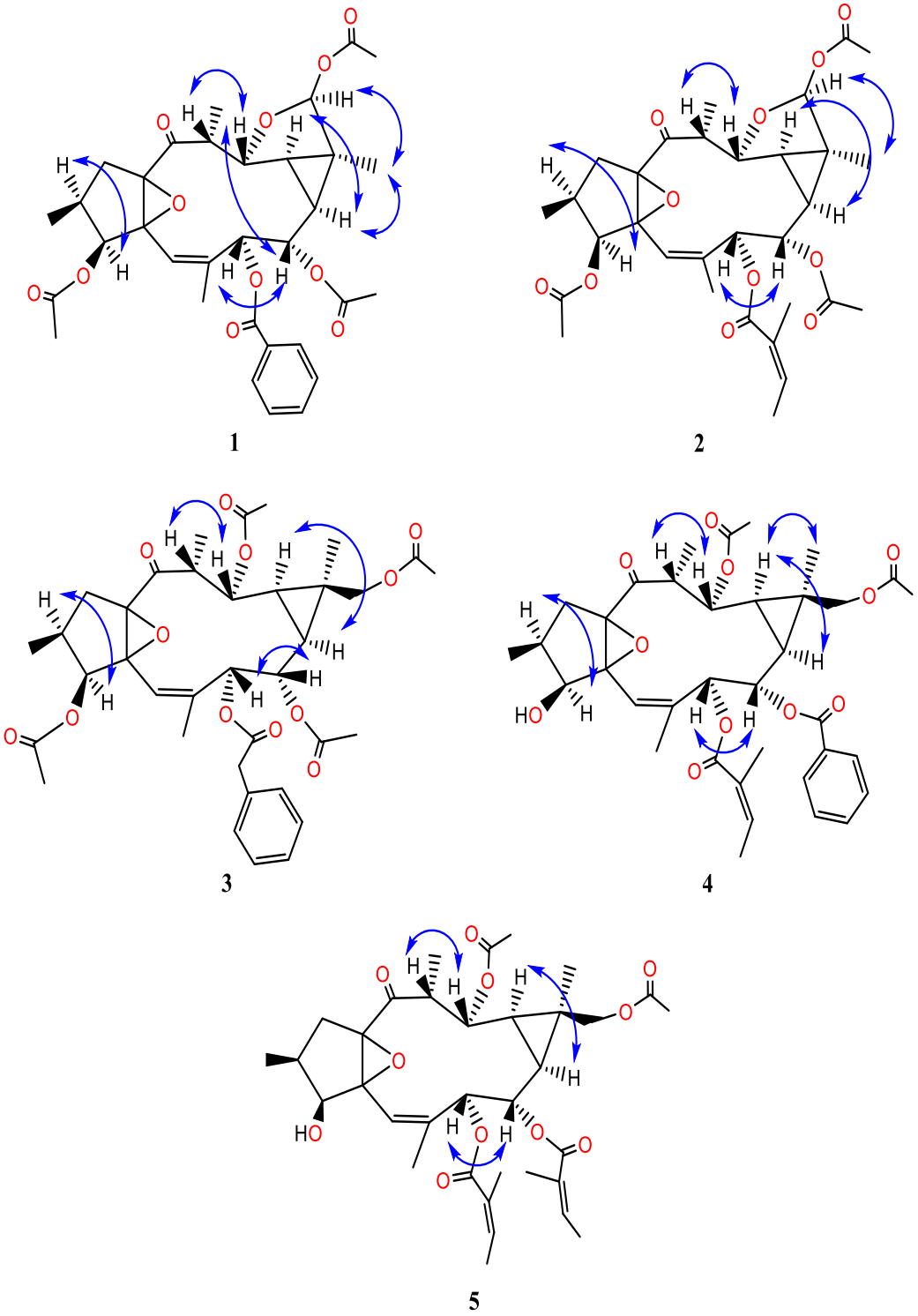

Figure S3. Key NOESY correlations of compounds (**1-5**)

no.	δH (*J* in Hz)	δC
1*α*	2.56 dd (15.0, 9.0)	34.1
1*β*	1.67 d (15.0)	
2	2.34 m	29.2
3	5.03 d (8.4)	77.1
4		73.3
5	5.70 s	116.7
6		142.1
7	5.45 brs	77.2
8	5.02 dd (11.2, 1.2)	70.2
9	1.61 dd (10.8, 9.0)	27.2
10		33.0
11	1.34 dd (8.7, 1.5)	31.0
12	4.65 dd (4.5, 1.5)	78.1
13	3.34 qd (6.6, 4.5)	48.7
14		206.4
15		72.9
16	0.84 d (7.2)	16.0
17	2.08 s	16.6
18	1.25 s	17.0
19	6.13 s	103.1
20	0.96 d (6.6)	6.8
3-OAc		170.5
	1.99 s	19.1
8-OAc		170.6
	1.87 s	19.5
12-OAc		
19-OAc		170.8
	2.01 s	19.9
7-R		**O-Bz**
C=O		170.5
1'		129.5
2'	7.99 m	129.3
3'	7.42 ddd (7.2, 7.2, 1)	128.5
4'	7.55 dddd (7.5, 7.5, 1.5, 1.5)	133.3
5'	7.42 ddd (7.2, 7.2, 1.5)	128.5
6'	7.99 m	129.3
7'	-	-

Table S1. ^{1}H and ^{13}C NMR Spectroscopic Data of compound **1**

no.	δH (*J* in Hz)	δC
1*α*	2.59 dd (14.7, 9.0)	34.1
1*β*	1.72 d (15.0)	
2	2.36 m	29.3
3	5.06 d (8.4)	77.1
4		73.3
5	5.53 s	116.4
6		142.4
7	5.22 brs	77.1
8	4.92 d (11.1)	70.2
9	1.46 dd (10.8, 9.0)	27.2
10		32.7
11	1.25 m	30.9
12	4.58 d (4.8)	78.0
13	3.30 qd (6.9, 5.1)	48.7
14		206.4
15		72.9
16	0.84 d (7.5)	16.0
17	1.97 d (1.8)	16.5
18	1.20 s	17.0
19	6.03 s	103.0
20	0.93 d 6.6	6.8
3-OAc		170.5
	1.97 s	19.0
8-OAc		170.7
	1.98 s	19.9
12-OAc		
19-OAc		170.6
	1.84 s	19.5
7-R		**O-Ang**
C=O		166.5
1'		
2'		128.0
3'	6.86 q (6.6)	138.4
4'	1.74 d (6.6)	13.2
5'	1.76 s	10.8
6'	-	-
7'	-	-

Table S2. ^{1}H and ^{13}C NMR Spectroscopic Data of compound **2**

no.	δH (*J* in Hz)	δC
1*α*	2.70 dd (14.7, 9.0)	31.1
1*β*	1.60 d (14.7)	
2	2.41 m	29.3
3	5.13 d (8.7)	76.8
4		71.0
5	5.43 m	117.6
6		138.7
7	5.04 d (1.8)	76.4
8	4.54 dd (10.8, 1.8)	70.7
9	1.30 dd (10.8, 9.0)	25.0
10		21.6
11	1.15 dd (11.1, 9.0)	30.9
12	4.84 dd (11.1, 7.8)	69.4
13	2.82 dq (7.5, 7.2)	43.0
14		207.0
15		73.4
16	0.84 d (7.5)	15.9
17	1.96 d (1.5)	16.2
18	1.00 s	23.2
19	19*α*: 4.01 d (12.0)	64.7
	19*β*: 3.46 d (12.0)	
20	0.92 d (7.2)	12.4
3-OAc		170.6
	2.00 s	19.7
8-OAc		170.4
	1.94 s	19.0
12-OAc		170.8
	1.89 s	19.33
19-OAc		171.3
	1.88 s	19.5
7-R		**O-Bzl**
C=O		170.5
1'		134.1
2'		129.1
3'	7.20 5H m	126.8
4'		128.2
5'		126.8
6'		129.1
7'	3.65 s	40.7

Table S3. ^{1}H and ^{13}C NMR Spectroscopic Data of compound **3**

no.	δH (*J* in Hz)	δC
1*α*	2.03 dd (13.5, 10.5)	32.6
1*β*	1.85 d (14.0)	
2	1.84 m	33.2
3	3.83 dd (6.5, 5.5)	75.2
4		73.3
5	6.11 q (1.5)	118.4
6		136.2
7	5.43 d (1.5)	75.9
8	5.14 dd (11.0, 2.0)	72.5
9	1.65 m	25.5
10		21.7
11	1.37 dd (11.5, 9.0)	31.6
12	5.08 dd (11.5, 3.5)	69.5
13	2.94 qd (7.0, 3.5)	43.4
14		207.8
15		73.2
16	0.88 d (7.0)	13.0
17	2.11 d (1.5)	17.7
18	1.16 s	24.4
19*α*	3.88 d (12.0)	64.9
19*β*	3.62 d (12.0)	
20	0.95 d (7.0)	13.4
3-OAc	3-OH: 5.32 d (6.5)	
12-OAc		170.3
	2.03 s	21.3
19- OAc		170.5
	1.64 s	20.5
7-R		**O-Ang**
C=O		166.3
1'		
2'		128.2
3'	6.89 q (7.0)	139.0
4'	1.79 d (7.0)	14.8
5'	1.78 s	12.5
6'	-	-
8-R		**O-Bz**
C=O		165.2
1''		129.8
2''	7.87 dd (7.5, 1.5)	129.6
3''	7.53 dd (7.5, 7.5)	129.4
4''	7.66 m	134.0
5''	7.53 dd (7.5, 7.5)	129.4
6''	7.87 dd (7.5, 1.5)	125.6

Table S4. ^{1}H and ^{13}C NMR Spectroscopic Data of compound **4**

no.	δH (*J* in Hz)	δC
1*α*	2.19, m	31.8
1*β*	1.90, m	
2	1.90 m	33.0
3	3.90 d (5.0)	75.7
4		73.2
5	6.16 s	117.8
6		136.8
7	5.29 d (1.5)	76.2
8	4.82 dd (11.0, 1.5)	70.9
9	1.64 dd (11.0, 9.0)	25.6
10		21.6
11	1.42 dd (11.0, 9.0)	31.3
12	5.01 dd (11.5, 3.5)	69.5
13	3.04 qd (7.0, 3.5)	43.2
14		207.8
15		73.0
16	0.99 d (6.5)	11.0
17	2.13 s	16.4
18	1.16 s	23.2
19*α*	4.08 d (12.0)	64.8
19*β*	3.60 d (12.0)	
20	1.04 d (7.0)	12.3
3-OAc		
12-OAc		170.8
	2.10 s	19.7
19- OAc		171.2
	1.93 s	19.3
7-R		**O-Ang**
C=O		166.6
1'		
2'		128.1
3'	6.95 m	138.3
4'	1.84 d (7.0)	13.1
5'	1.87 s	10.8
6'	-	-
8-R		**O-Ang**
C=O		166.9
1''		
2''		128.0
3''	6.83 m	138.3
4''	1.81 d (7.5)	13.1
5''	1.80 s	10.6
6''	-	-

Table S5. ^{1}H and ^{13}C NMR Spectroscopic Data of compound **5**

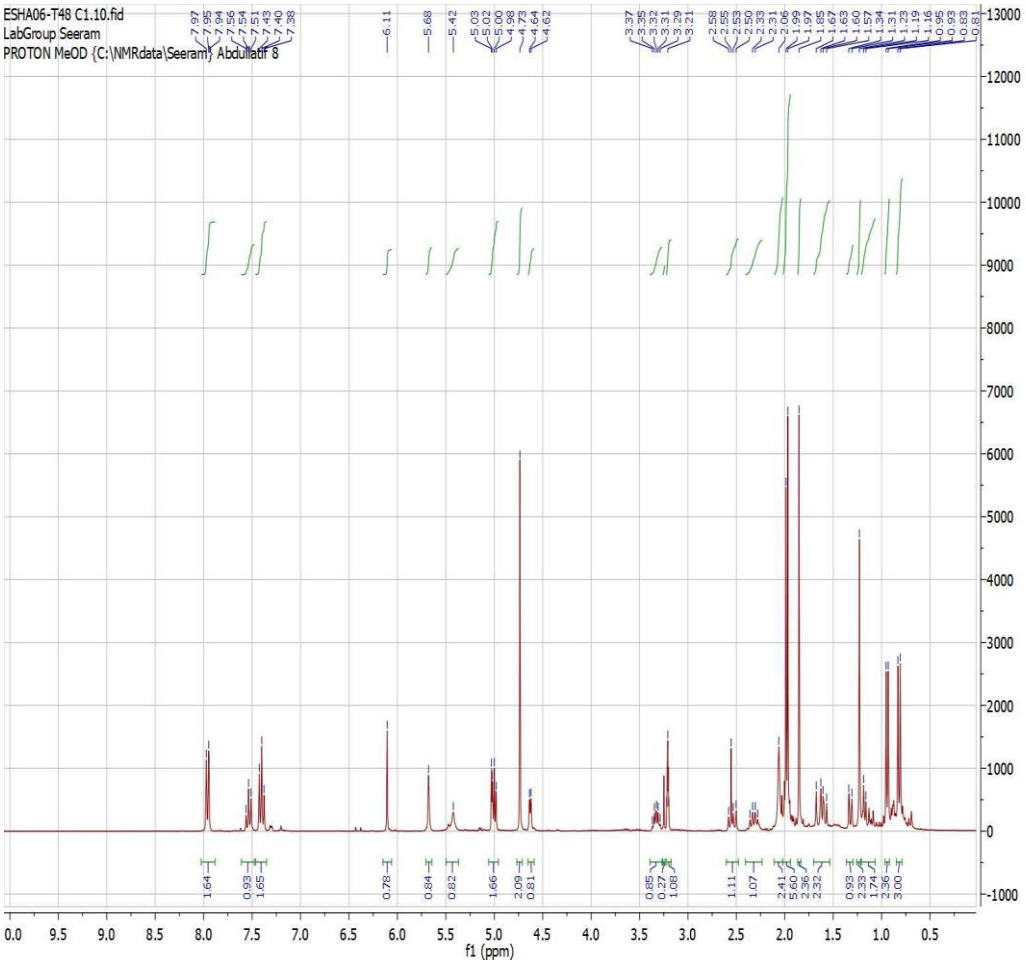

Figure S4. 1H NMR (300 and 75 MHz, CD_3OD) spectra of **1**

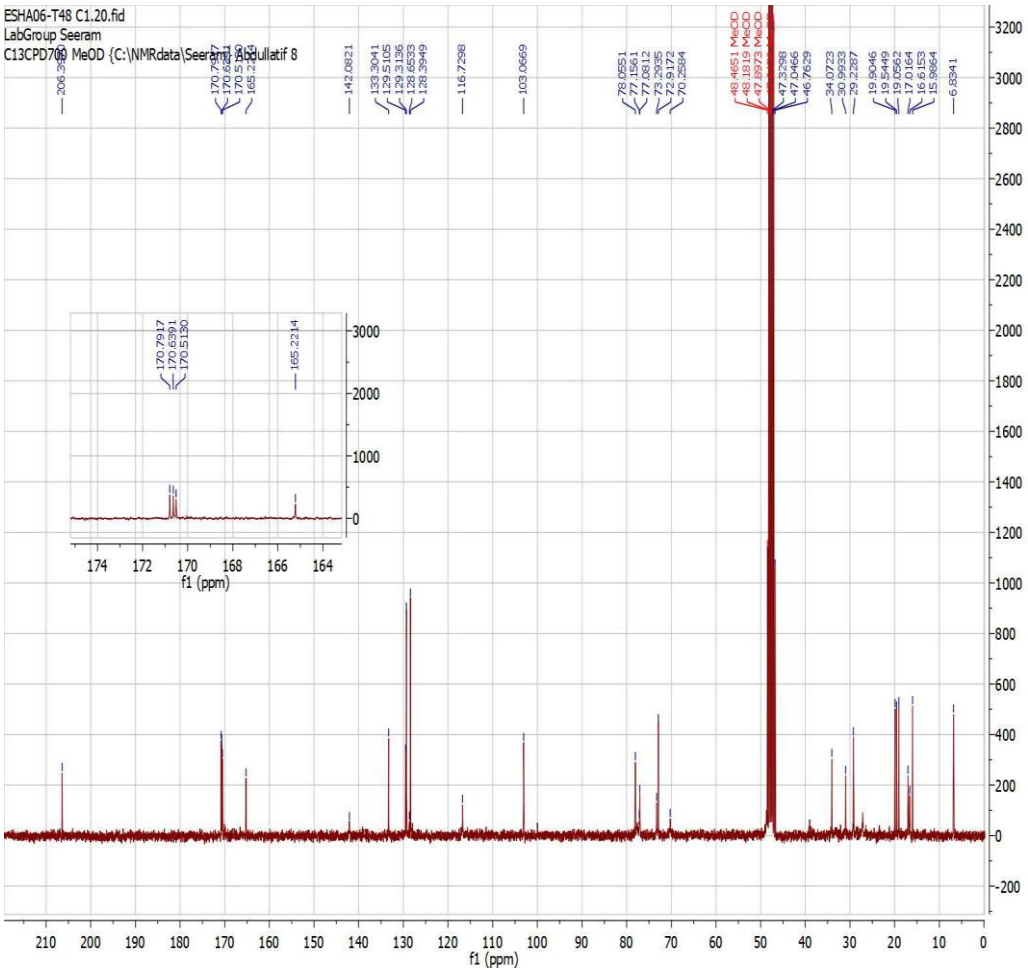

Figure S5. 13C NMR (300 and 75 MHz, CD_3OD) spectra of **1**

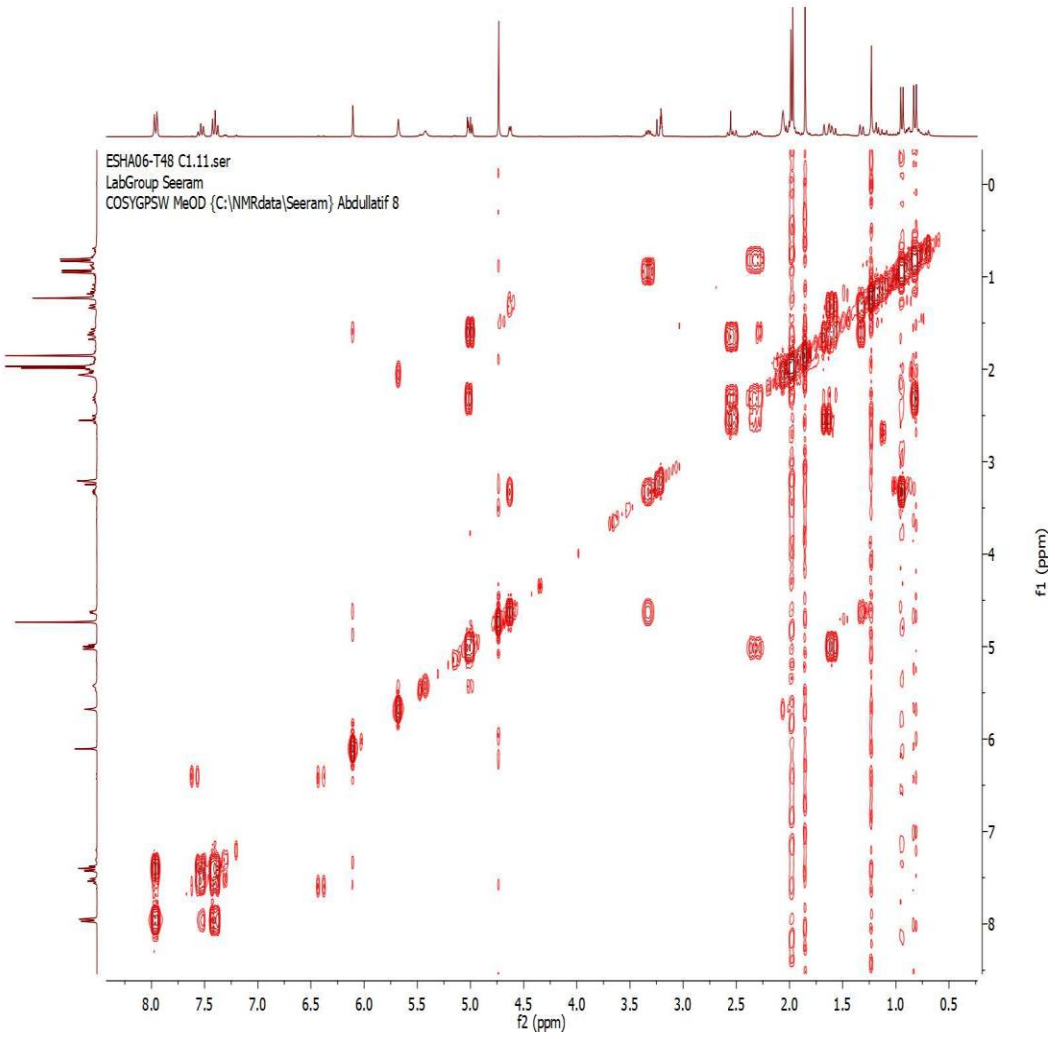

Figure S6. 1H-1H COSY (300 and 75 MHz, CD_3OD) spectra of **1**

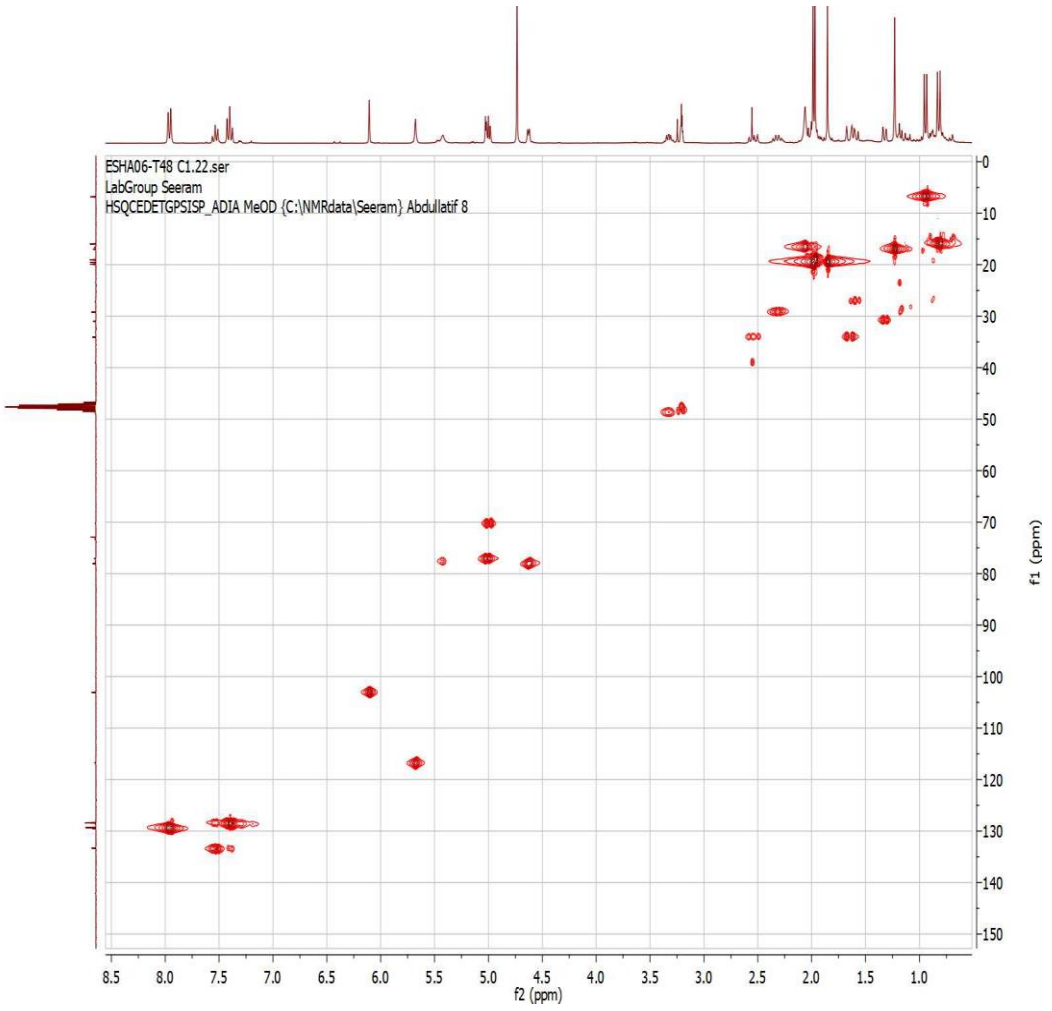

Figure S7. HSQC (300 and 75 MHz, CD_3OD) spectra of **1**

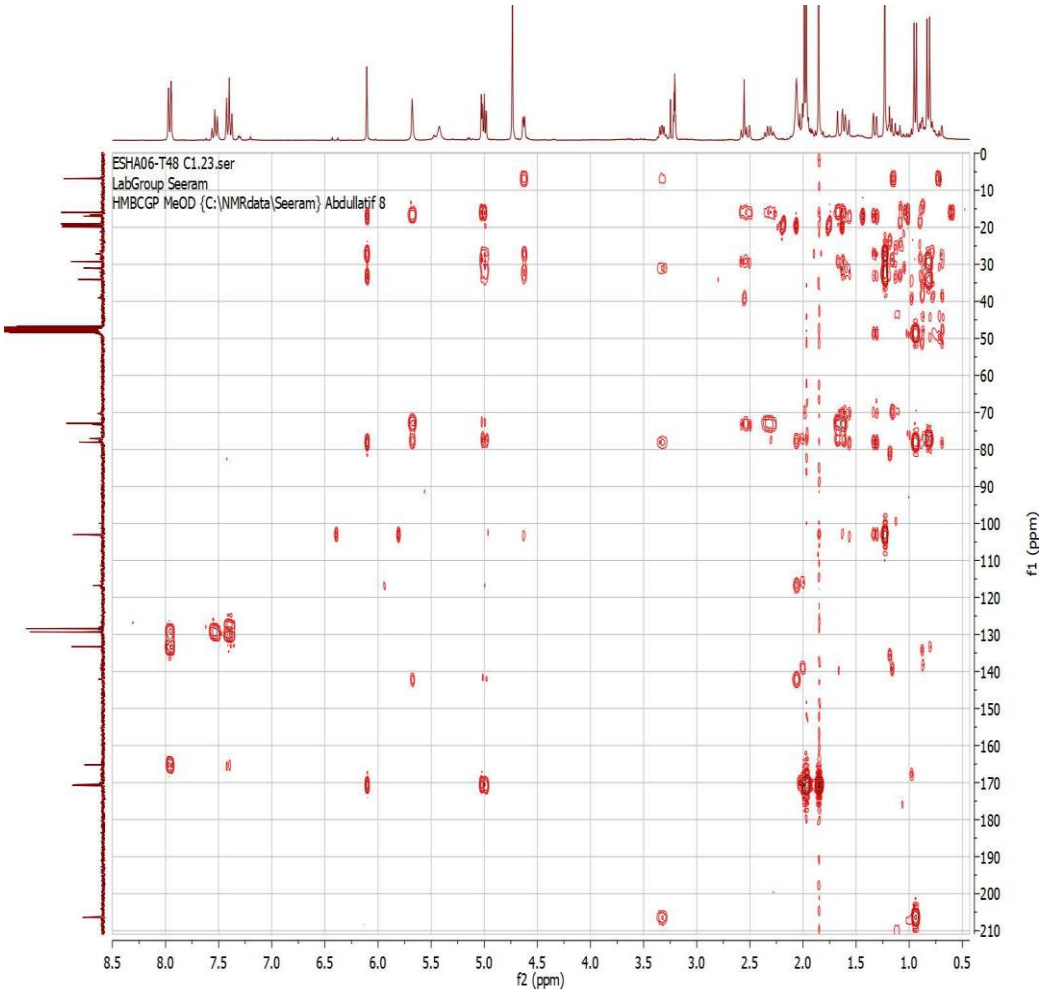

Figure S8. HMBC (300 and 75 MHz, CD_3OD) spectra of **1**

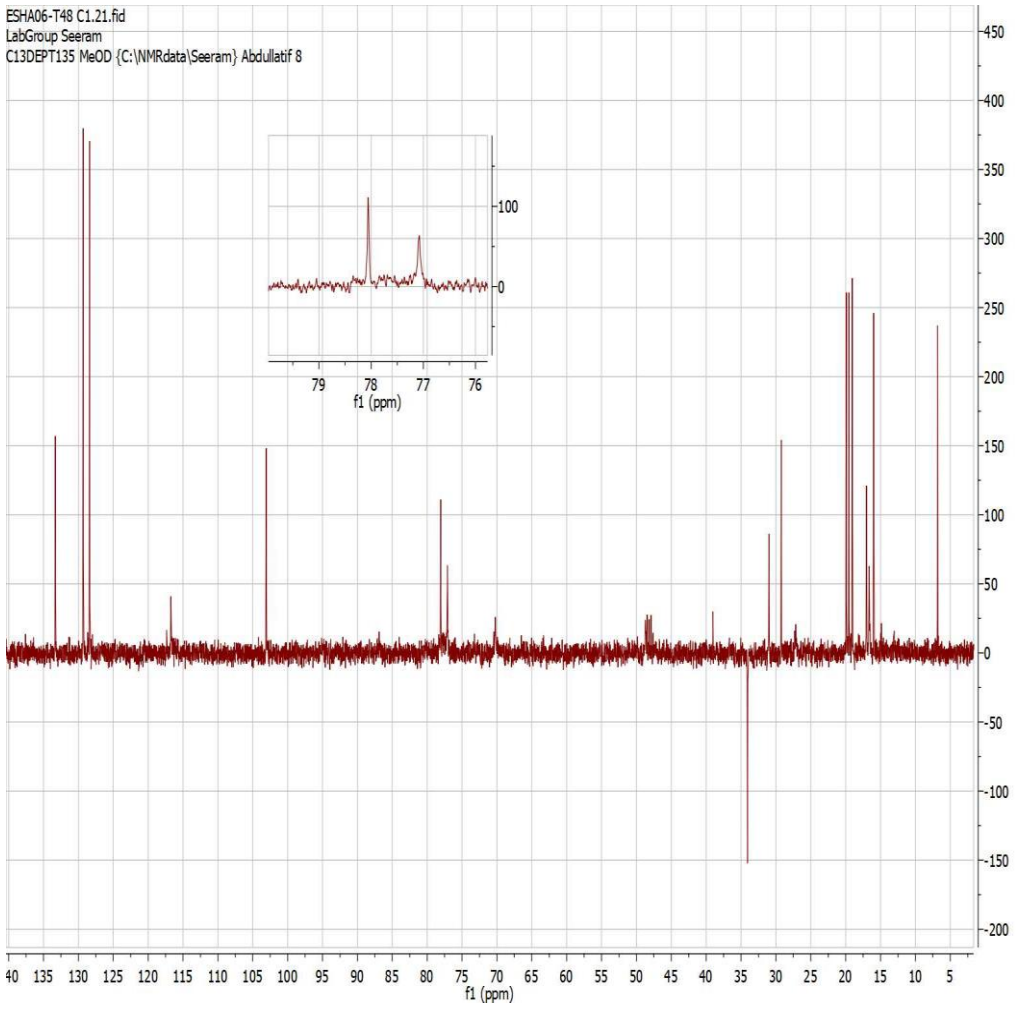

Figure S9. ^{13}C DEPT (300 and 75 MHz, CD_3OD) spectra of **1**

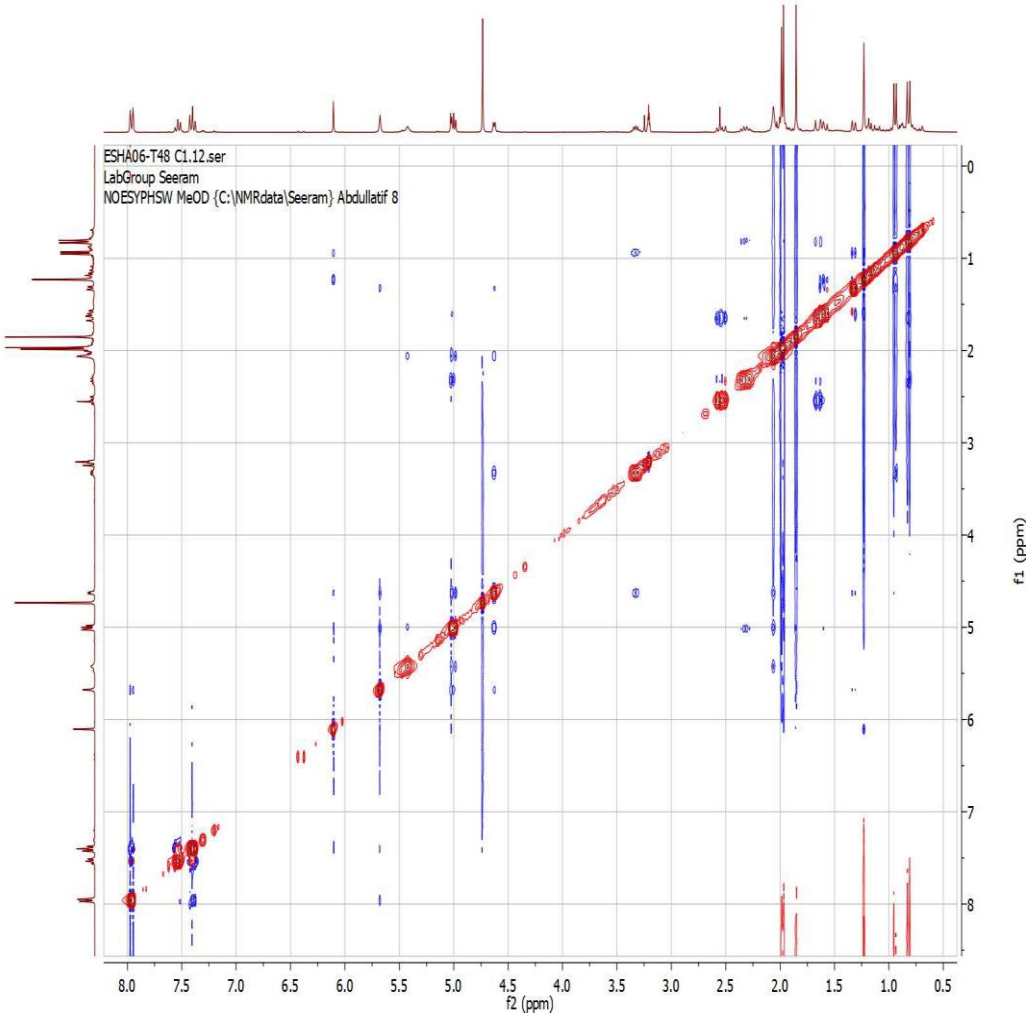

Figure S10. NOESY (300 and 75 MHz, CD_3OD) spectra of **1**

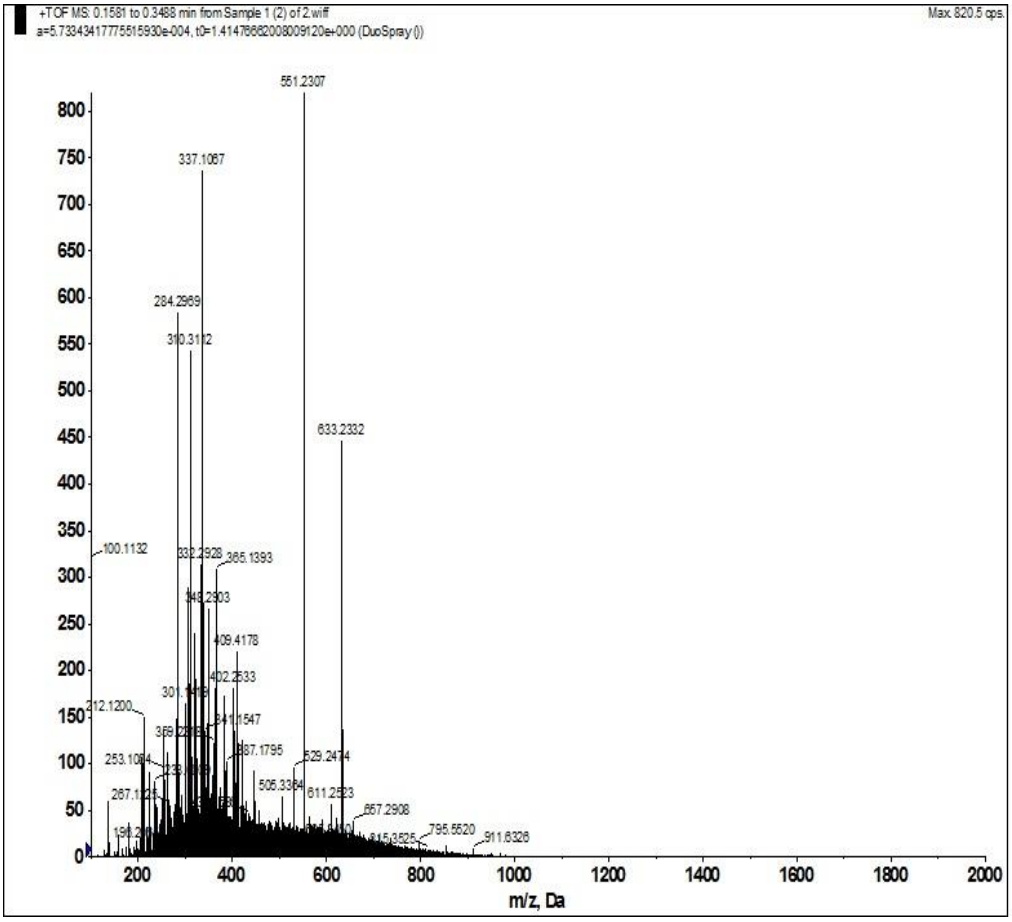

(+)-HRESIMS *m/z* **633.2332** $[M + Na]^+$ (calcd for $C_{33}H_{38}O_{11}Na$, **633.2312**).

Figure S11. HRESI (+) MS spectra of **1**

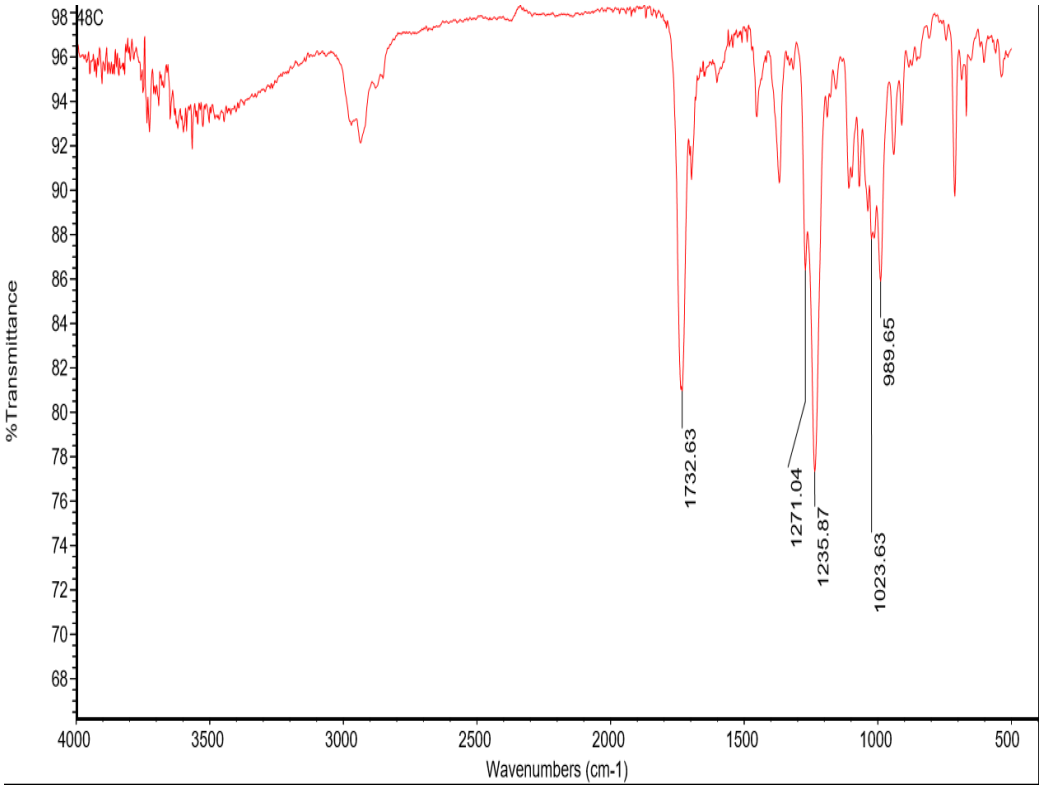

IR (KBr) ν_{max} 2965, 1732, 1271, 1235, 1023, 989 cm^{-1}

Figure S12. IR spectra of **1**

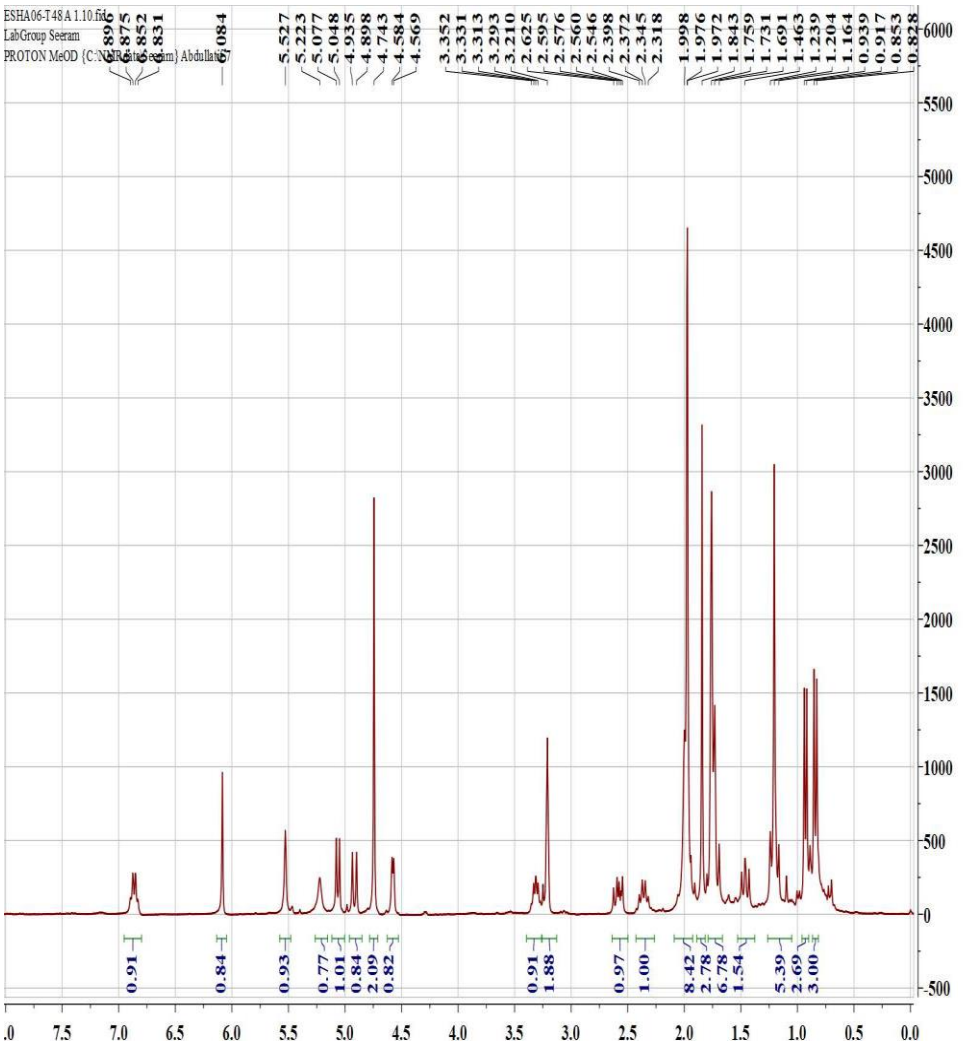

Figure S13. ^{1}H NMR (300 and 75 MHz, CD3OD) spectra of **2**

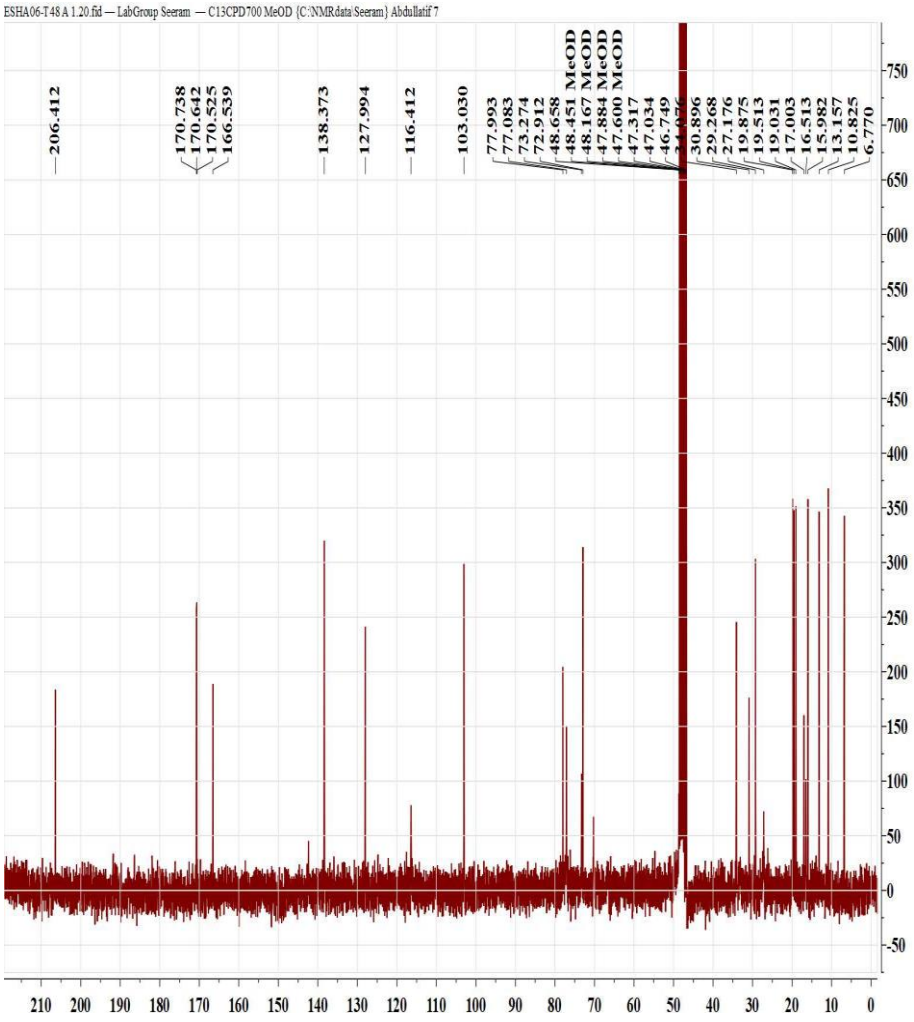

Figure S14. ^{13}C NMR (300 and 75 MHz, CD_3OD) spectra of **2**

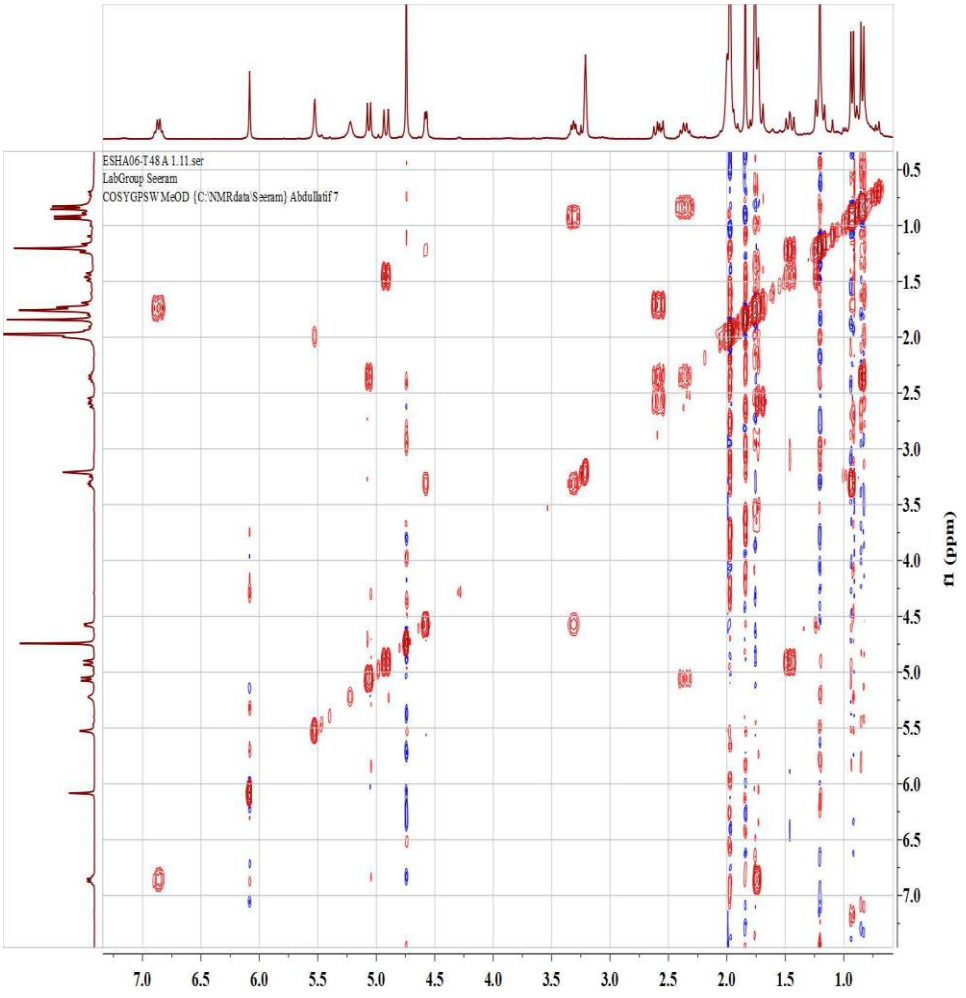

Figure S15. ^{1}H-^{1}H COSY (300 and 75 MHz, CD3OD) spectra of **2**

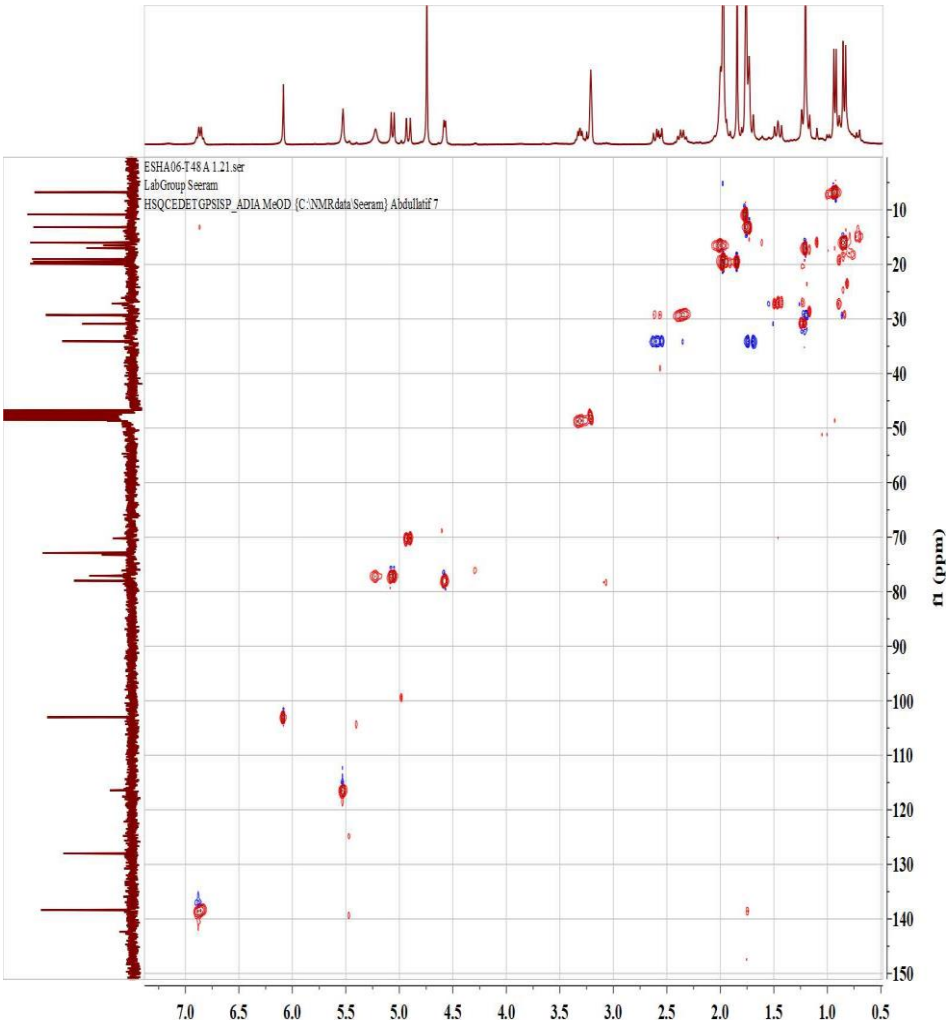

Figure S16. HSQC (300 and 75 MHz, CD_3OD) spectra of **2**

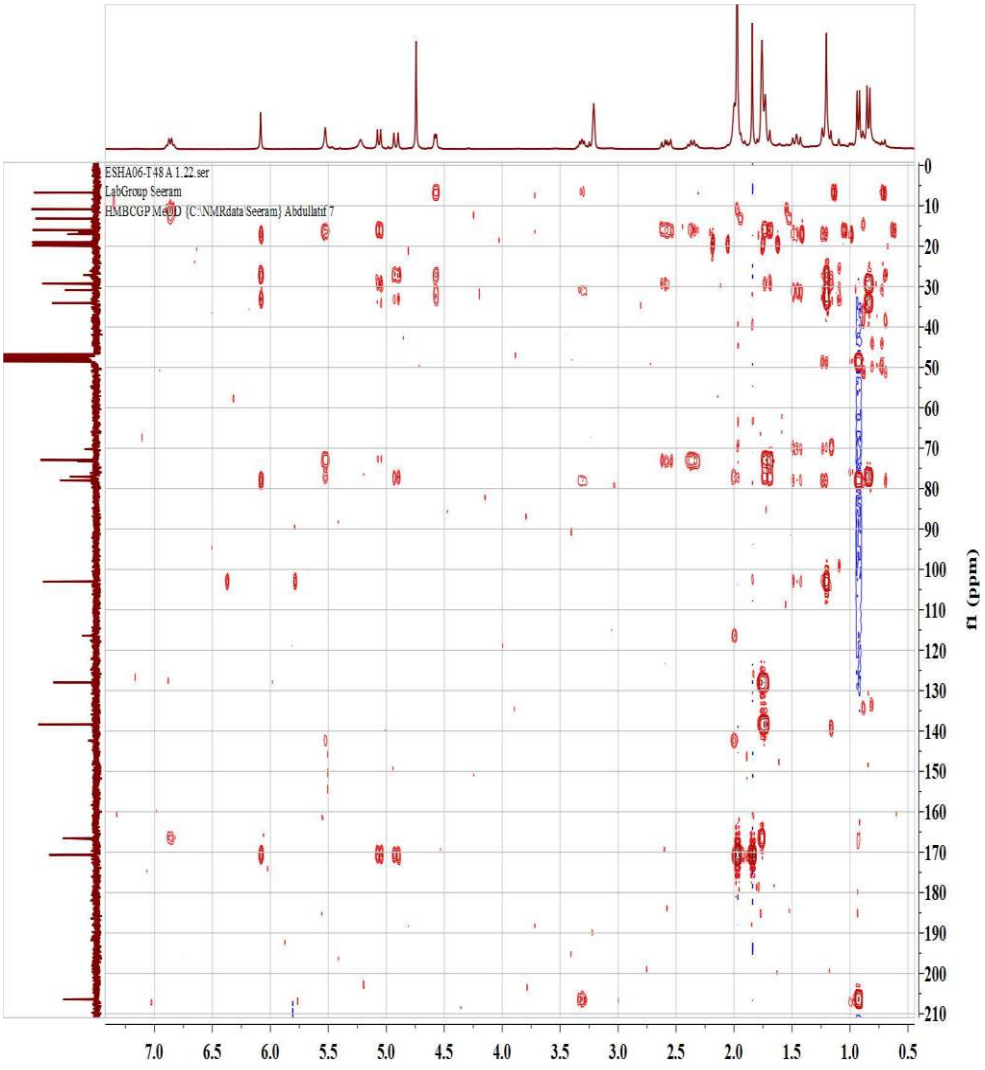

Figure S17. HMBC (300 and 75 MHz, CD_3OD) spectra of **2**

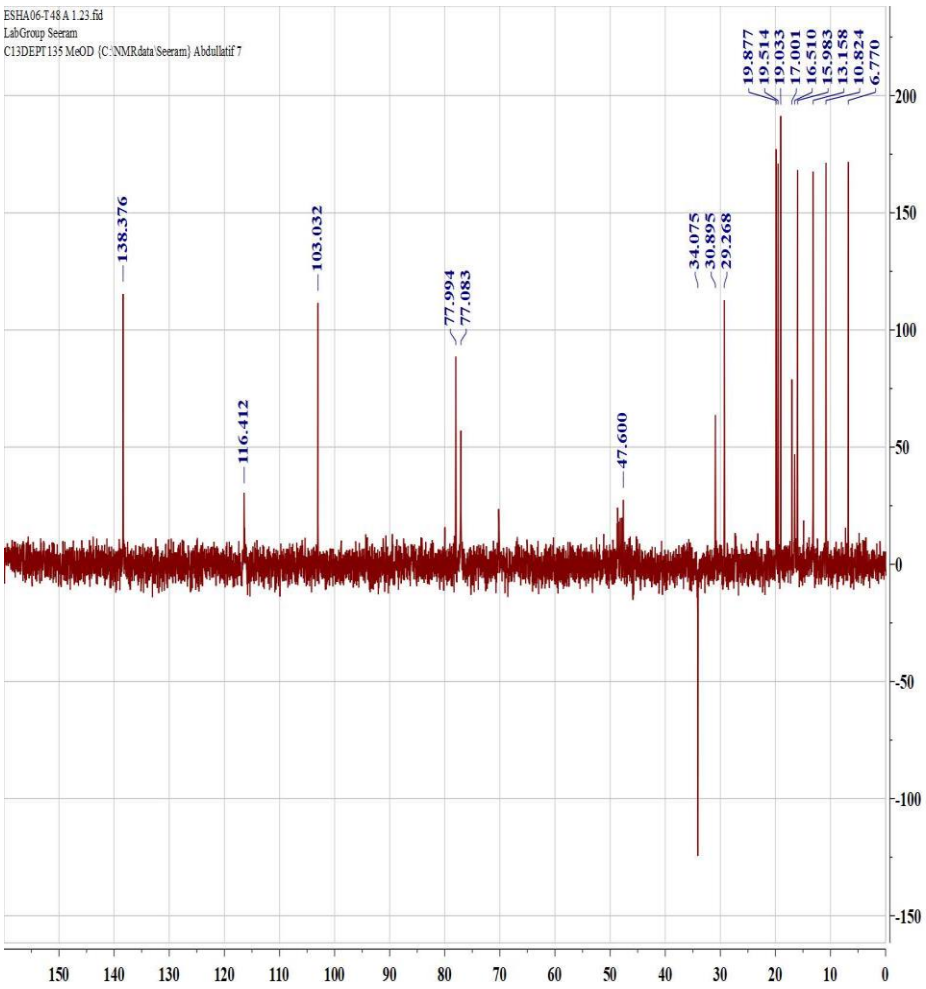

Figure S18. ^{13}C DEPT (300 and 75 MHz, CD_3OD) spectra of **2**

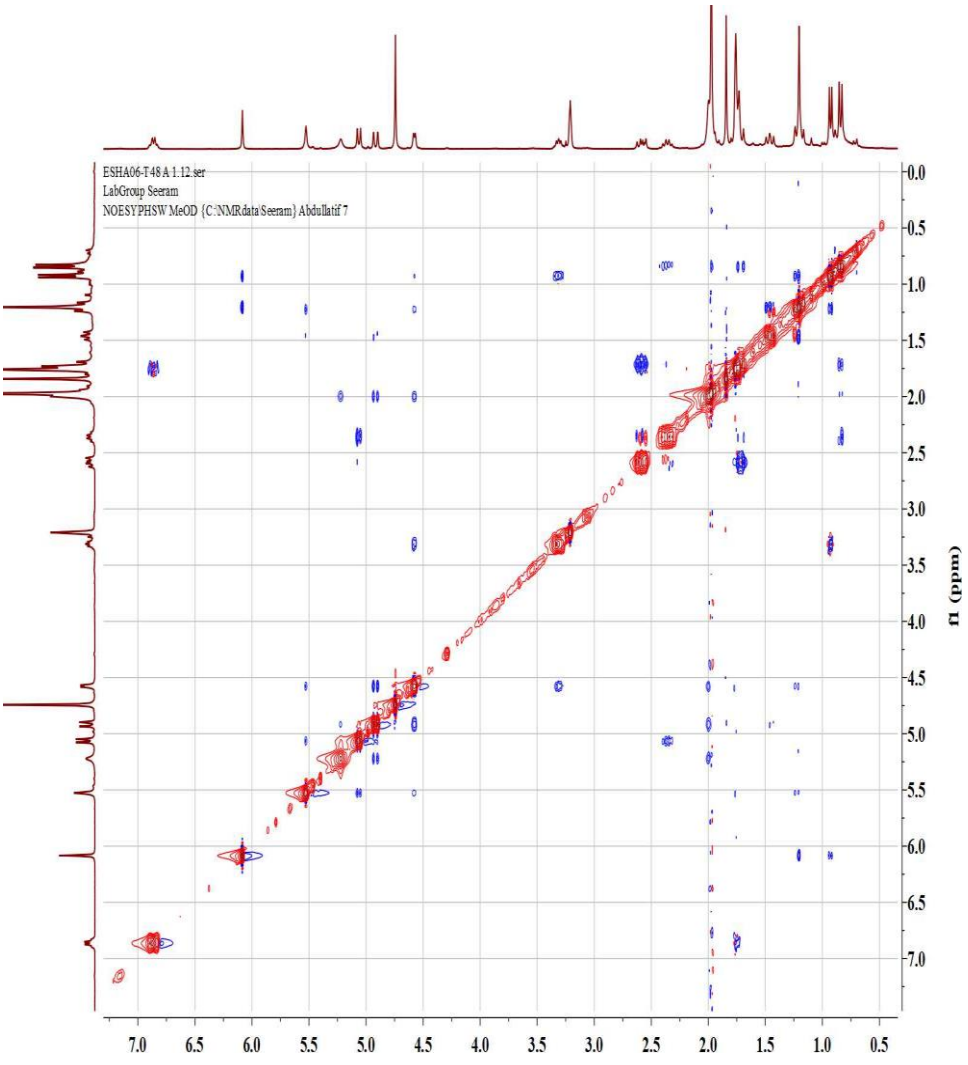

Figure S19. NOESY (300 and 75 MHz, CD_3OD) spectra of **2**

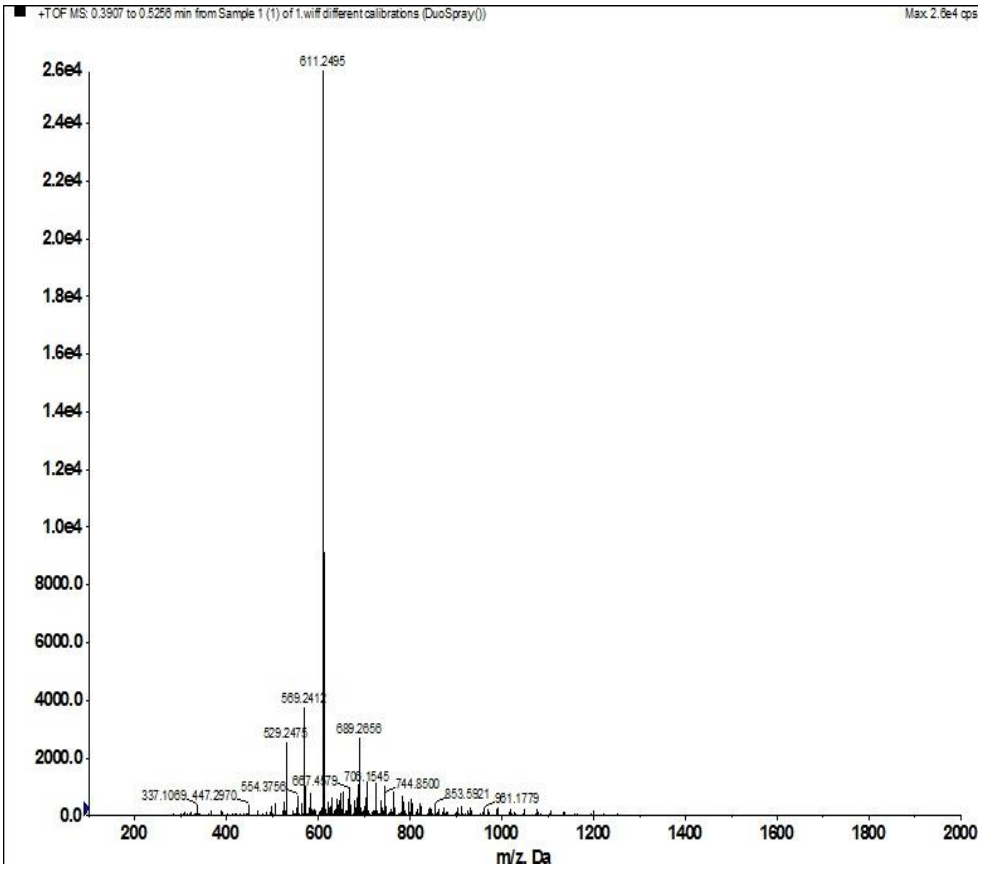

(+)-HRESIMS *m/z* **611.2495** $[M + Na]^+$ (calcd for $C_{31}H_{40}O_{11}Na$, **611.2468**).

Figure S20. HRESI (+) MS spectra of **2**

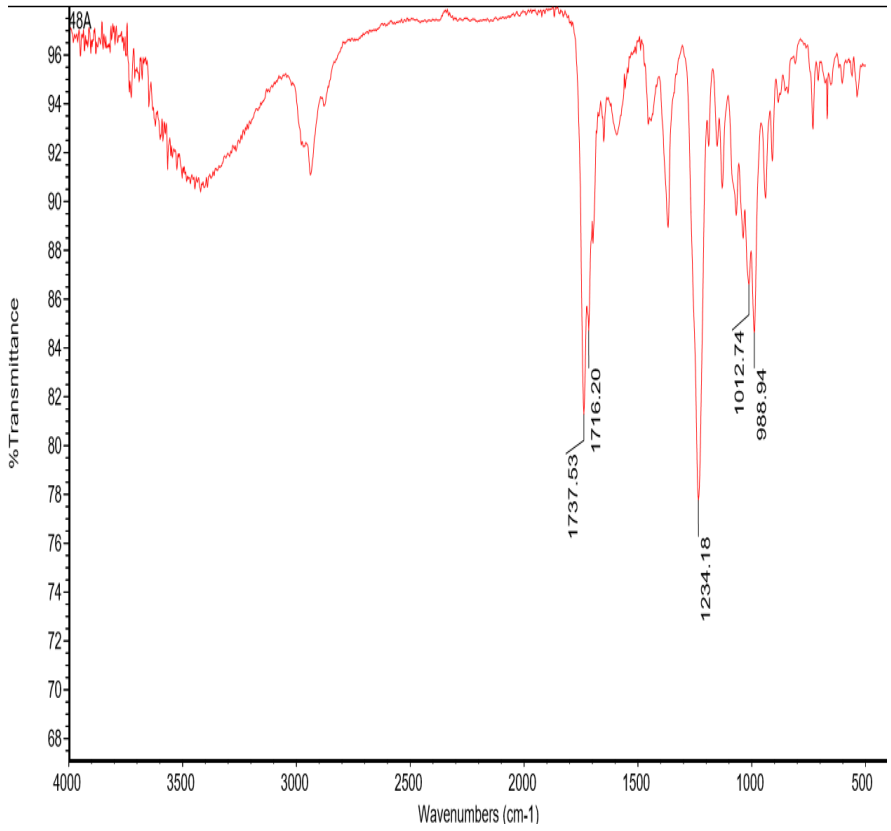

IR (KBr) ν_{max} 1737, 1716, 1234, 1012, 988 cm^{-1}

Figure S21. IR spectra of **2**

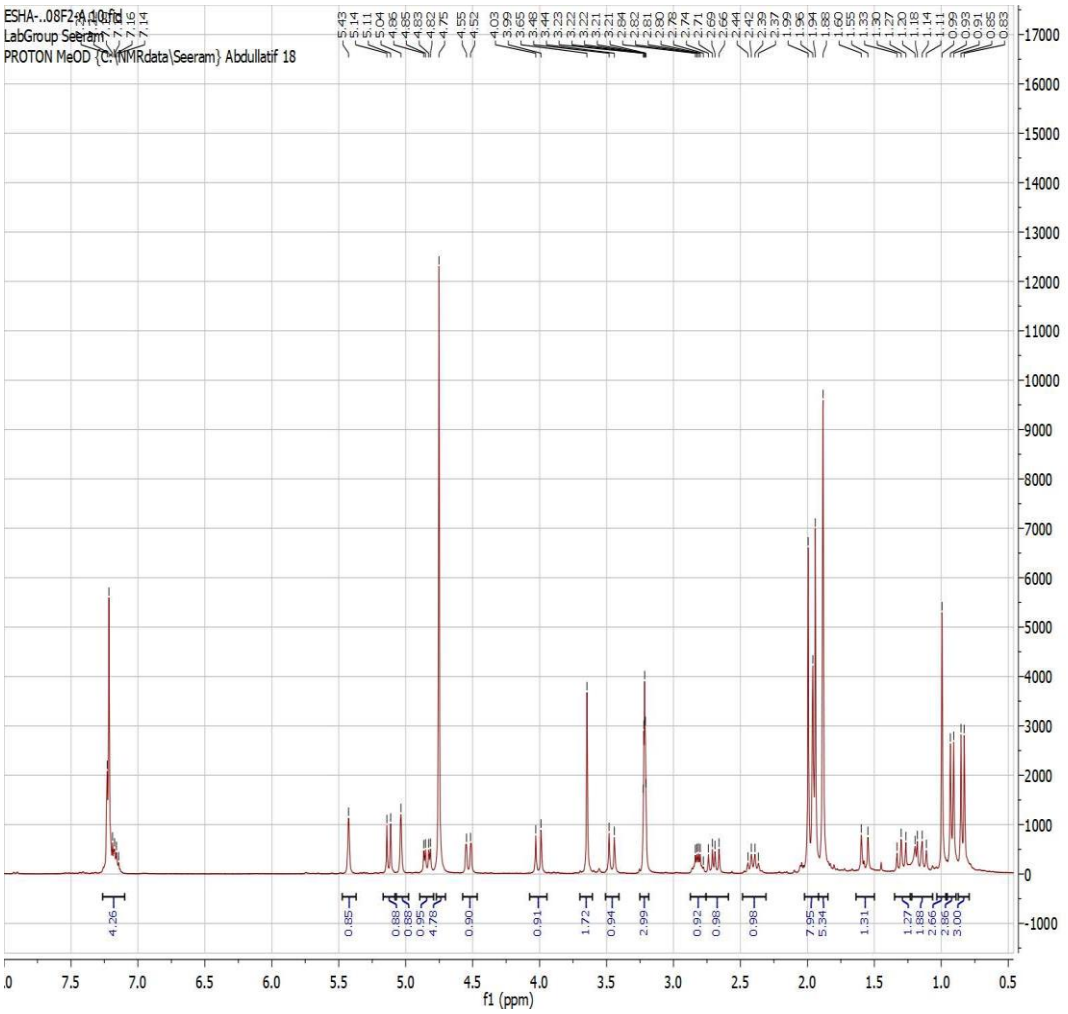

Figure S22. ^{1}H NMR (300 and 75 MHz, CD3OD) spectra of **3**

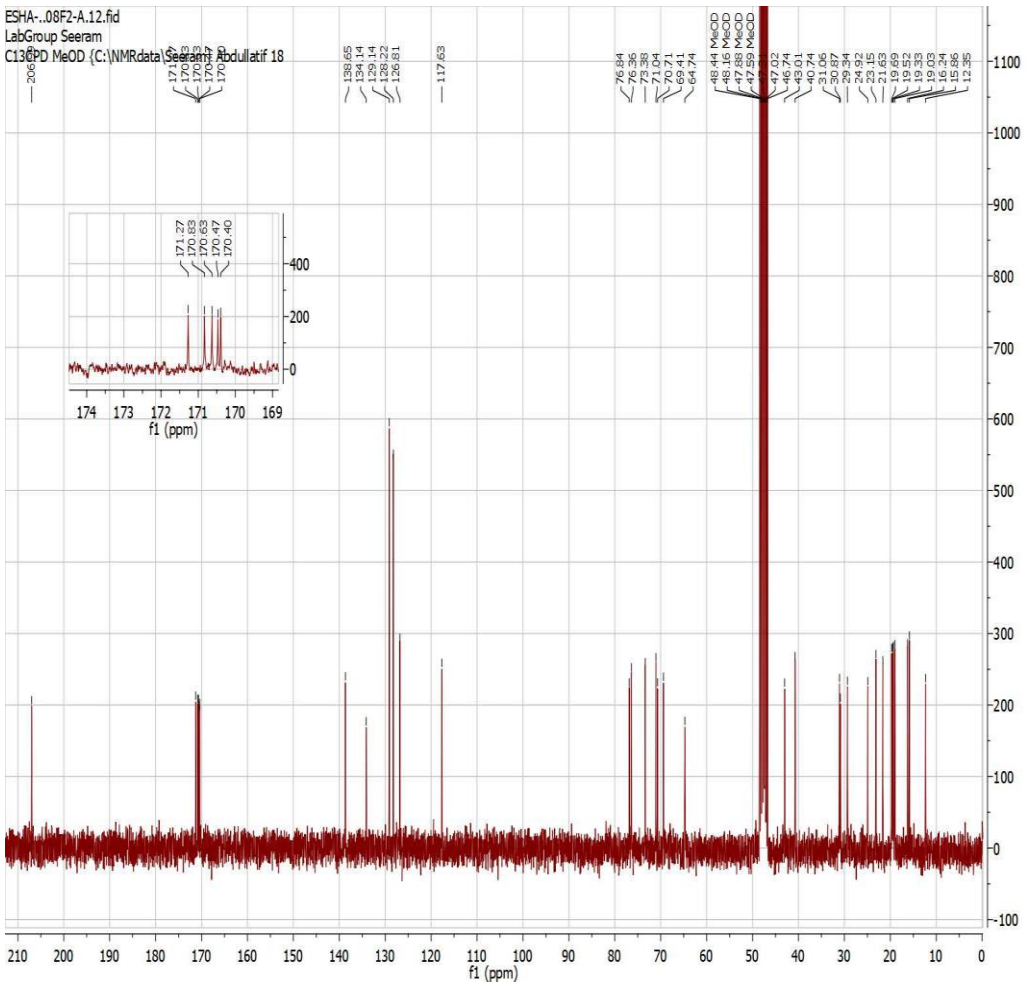

Figure S23.[13]C NMR (300 and 75 MHz, CD_3OD) spectra of **3**

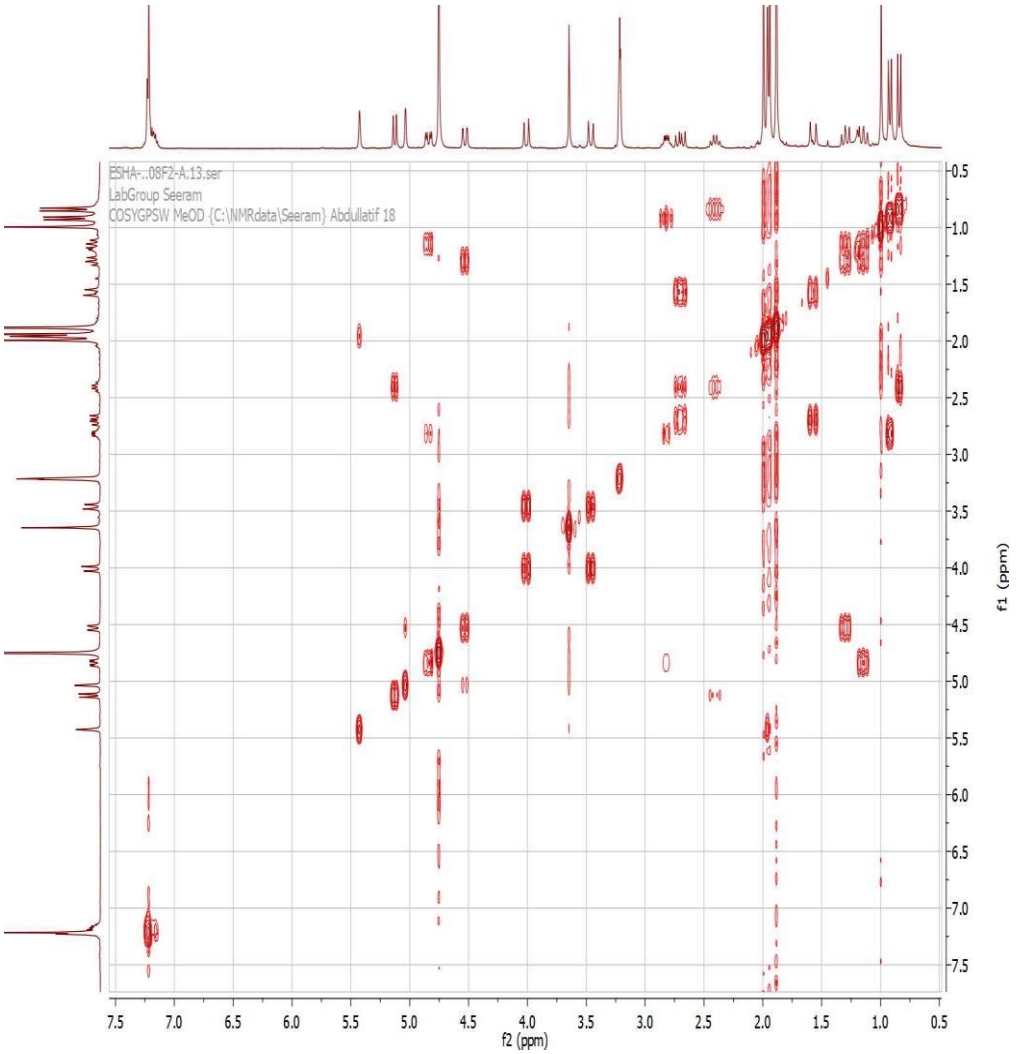

Figure S24. ^{1}H-^{1}H COSY (300 and 75 MHz, CD3OD) spectra of **3**

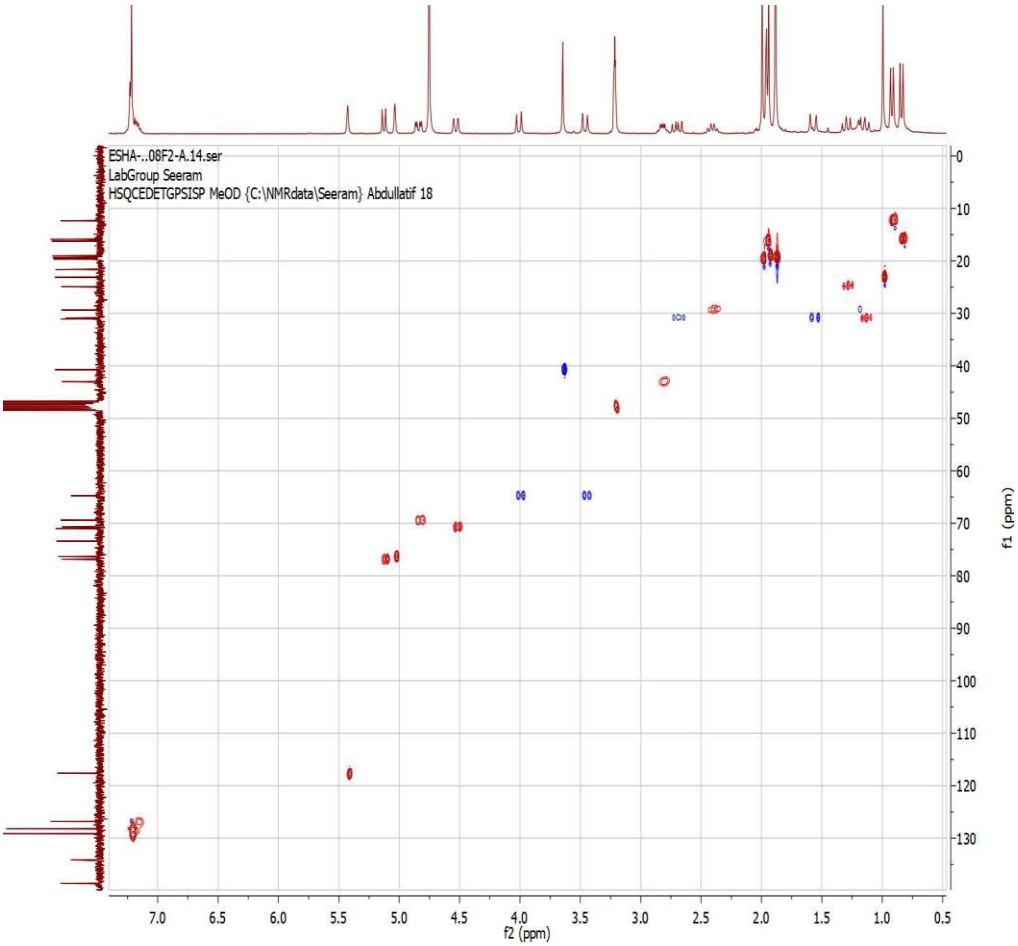

Figure S25. HSQC (300 and 75 MHz, CD_3OD) spectra of **3**

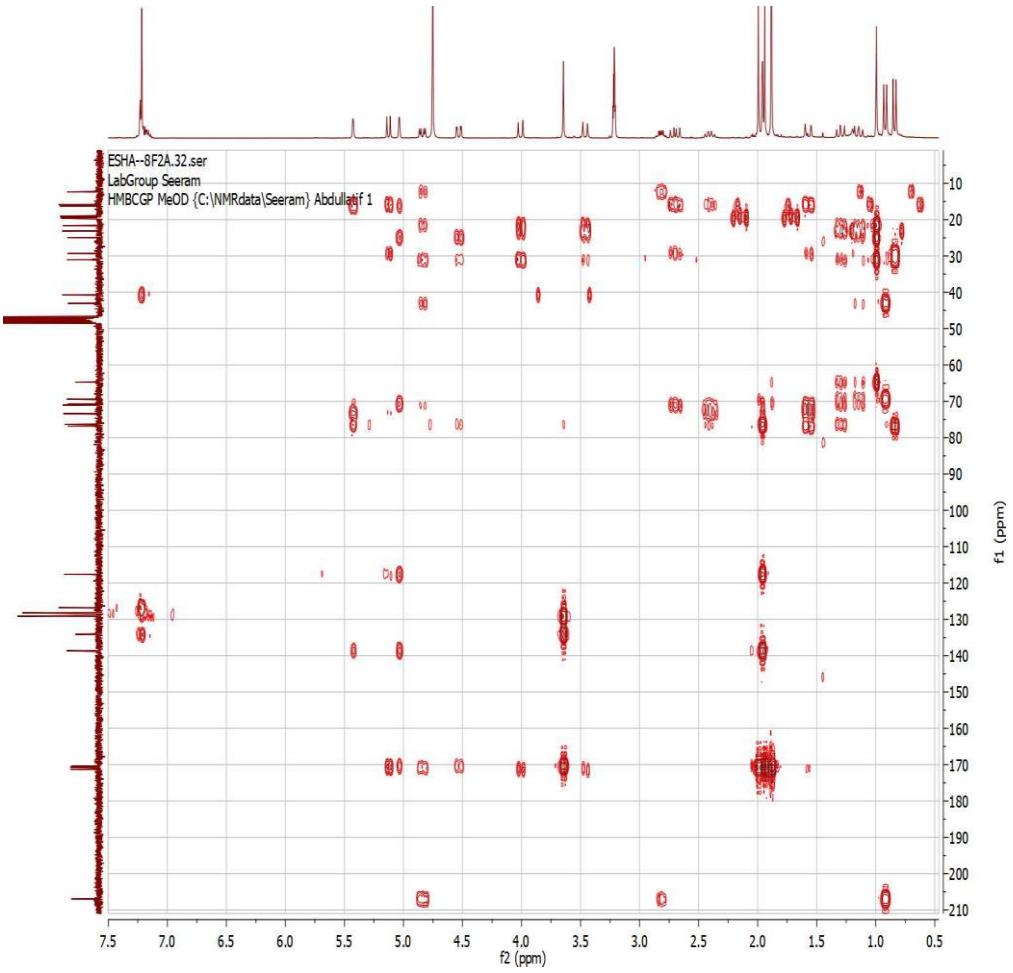

Figure S26. HMBC (300 and 75 MHz, CD_3OD) spectra of **3**

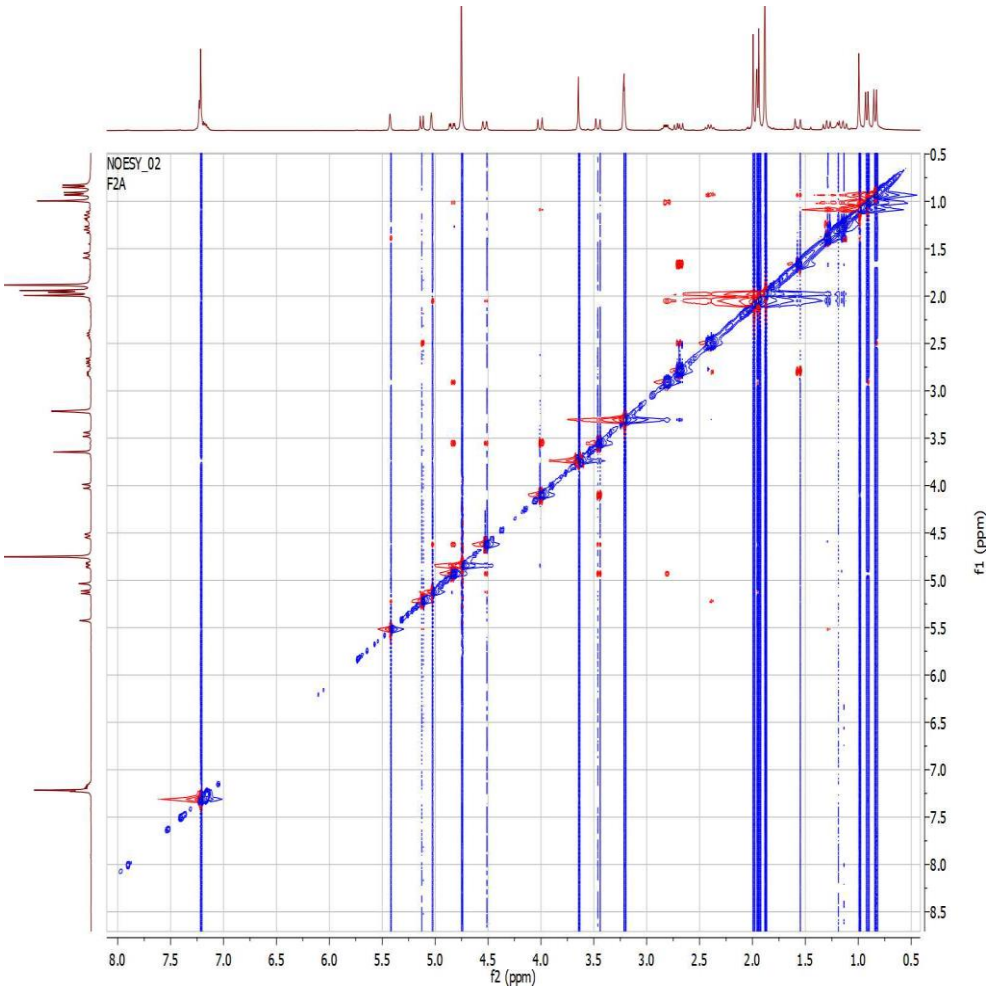

Figure S27. NOESY (300 and 75 MHz, CD_3OD) spectra of **3**

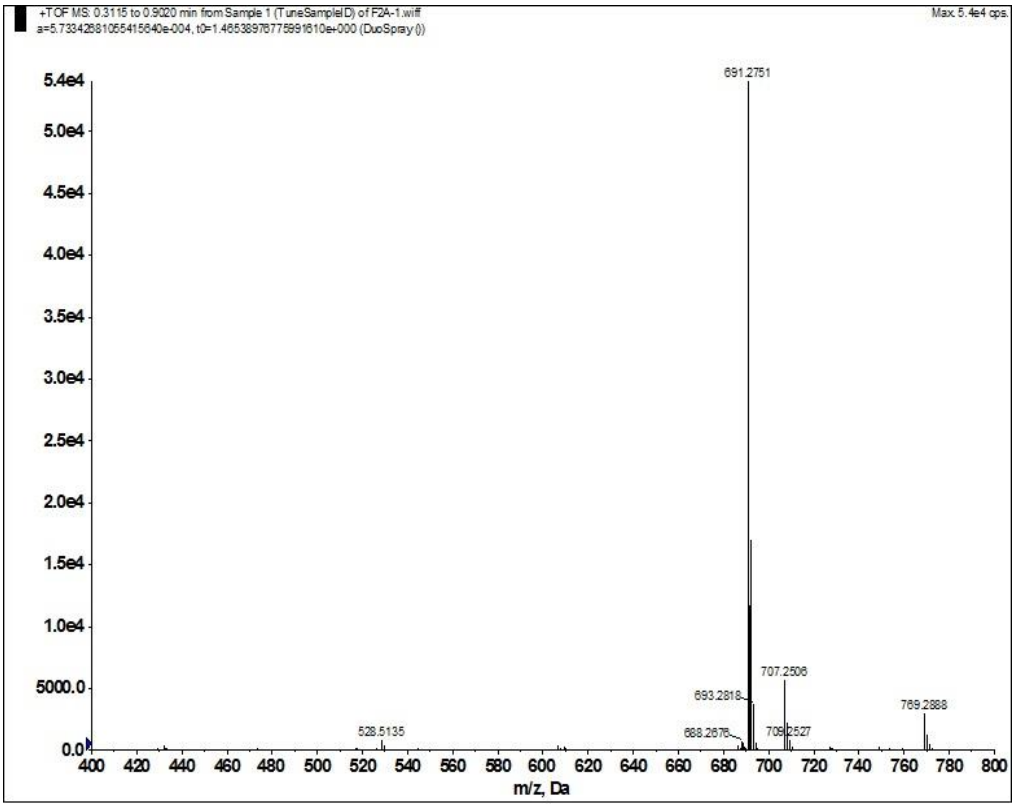

(+)-HRESIMS *m/z* **691.2751** $[M + Na]^+$ (calcd for $C_{36}H_{44}O_{12}Na$, **691.2730**).

Figure S28. HRESI (+) MS spectra of **3**

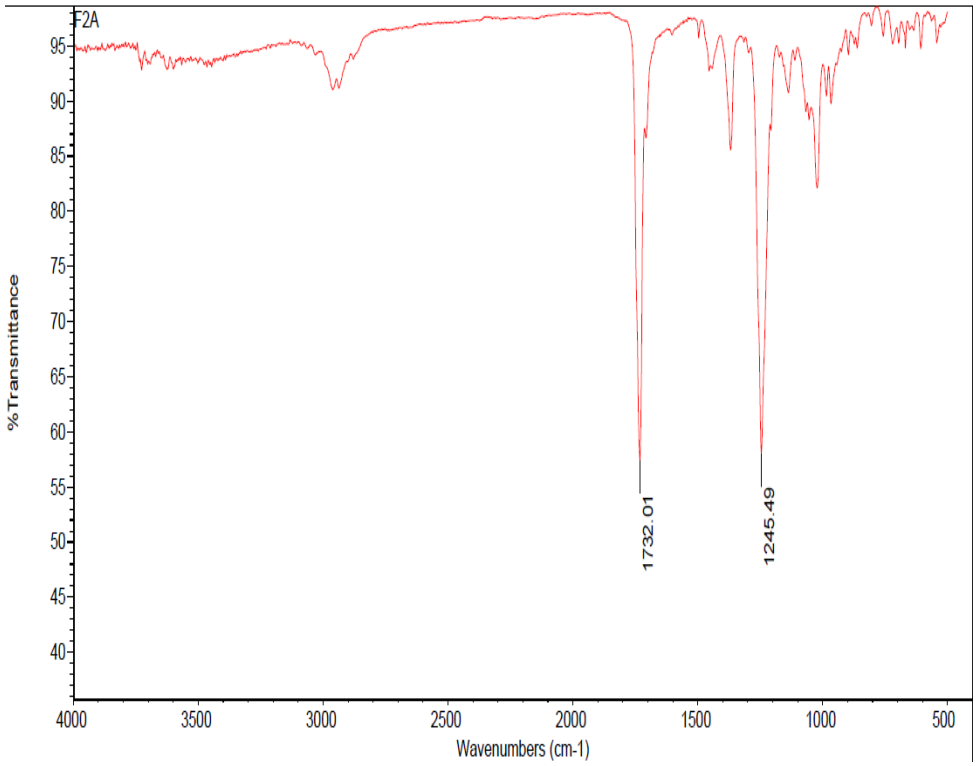

IR (KBr) ν_{max} 2965, 1732, 1245 cm^{-1}

Figure S29. IR spectra of **3**

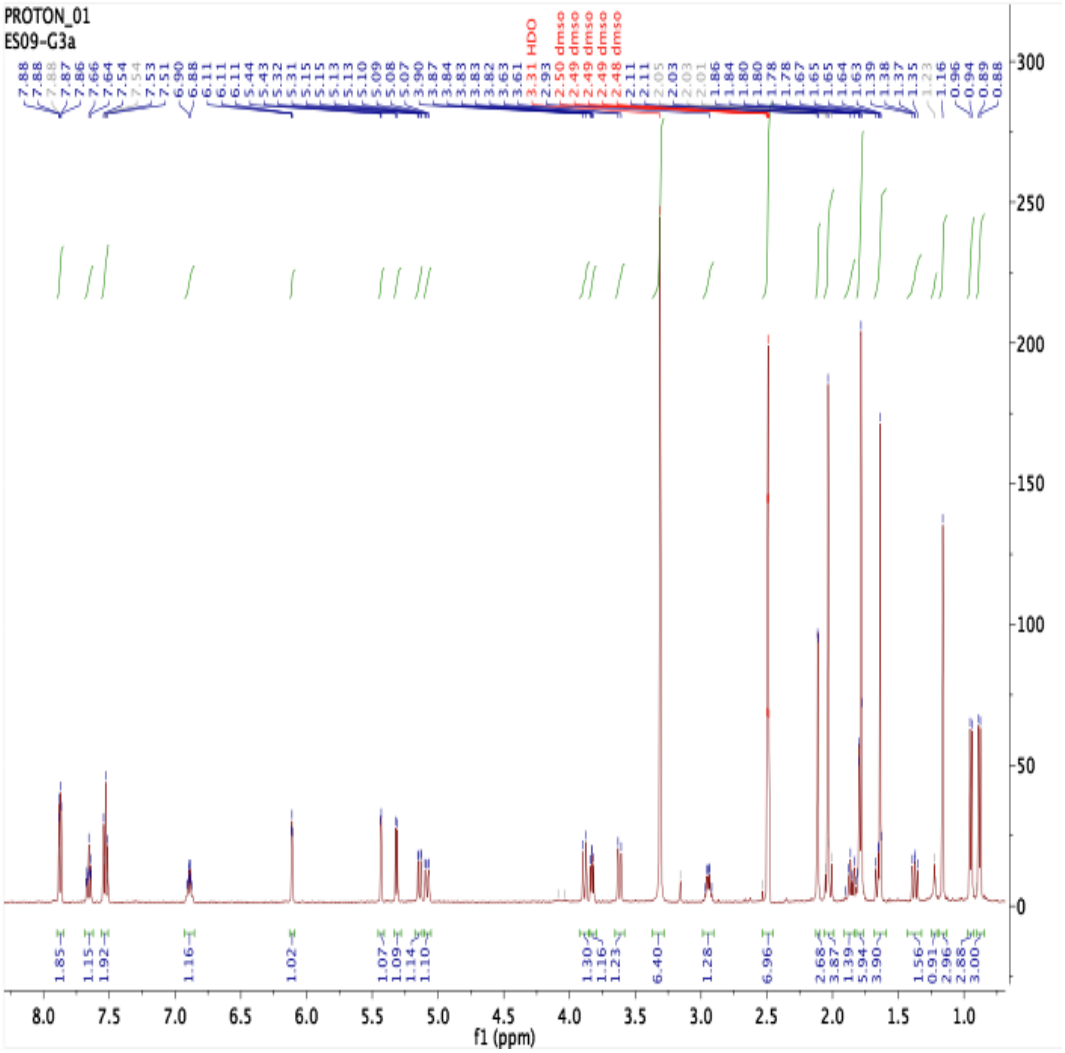

Figure S30. ^{1}H NMR (500 and 125 MHz, DMSO-d_6) spectra of **4**

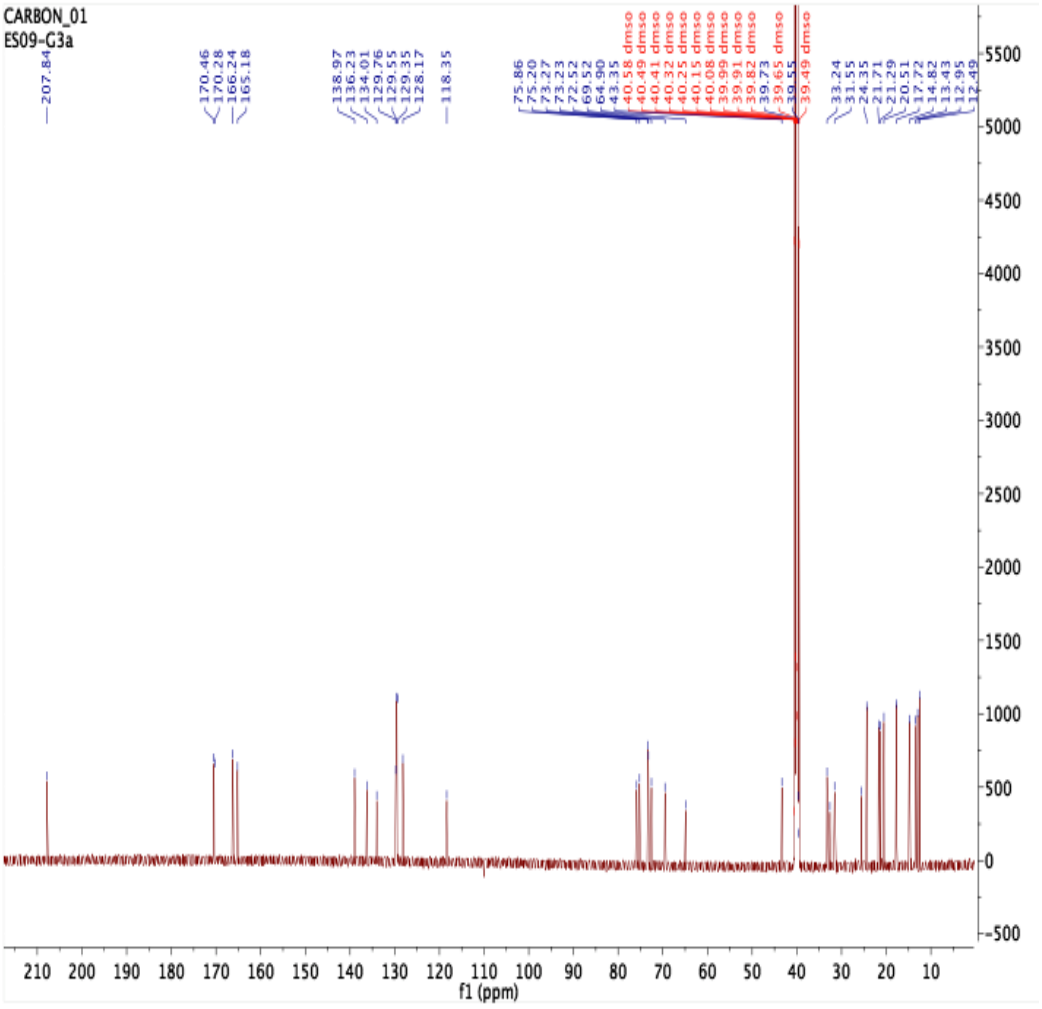

Figure S31. ^{13}C NMR (500 and 125 MHz, DMSO-d_6) spectra of **4**

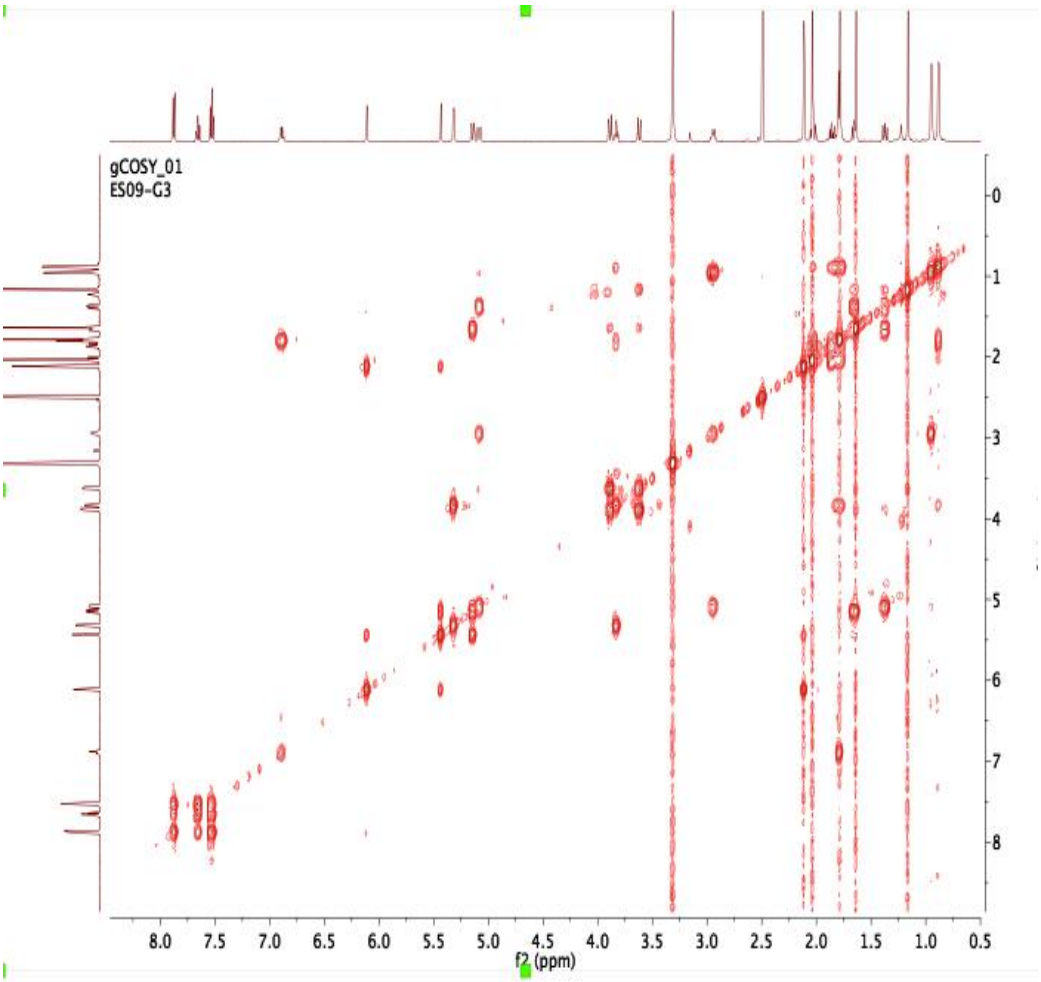

Figure S32. ^{1}H-^{1}H COSY (500 and 125 MHz, DMSO-d_6) spectra of **4**

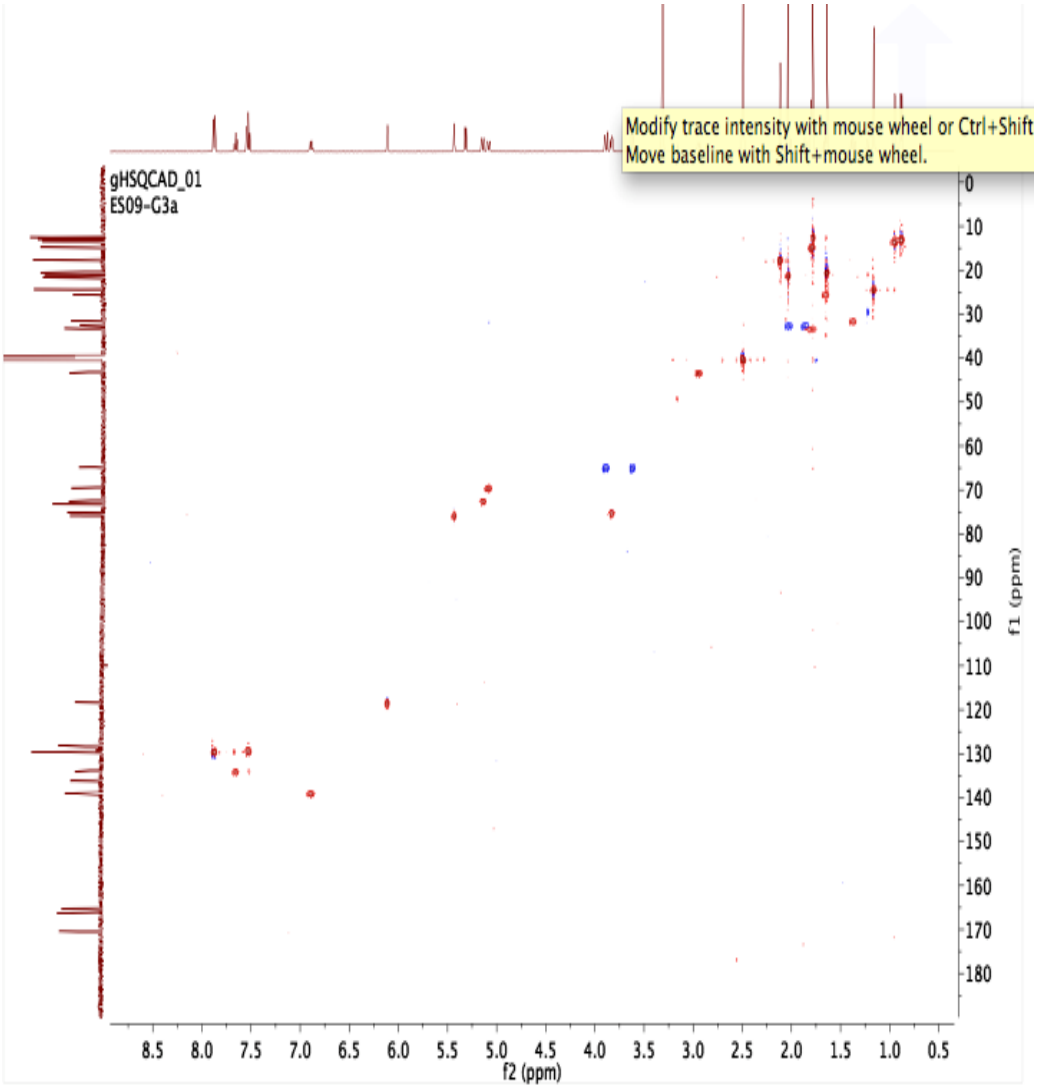

Figure S33. HSQC (500 and 125 MHz, DMSO-d_6) spectra of **4**

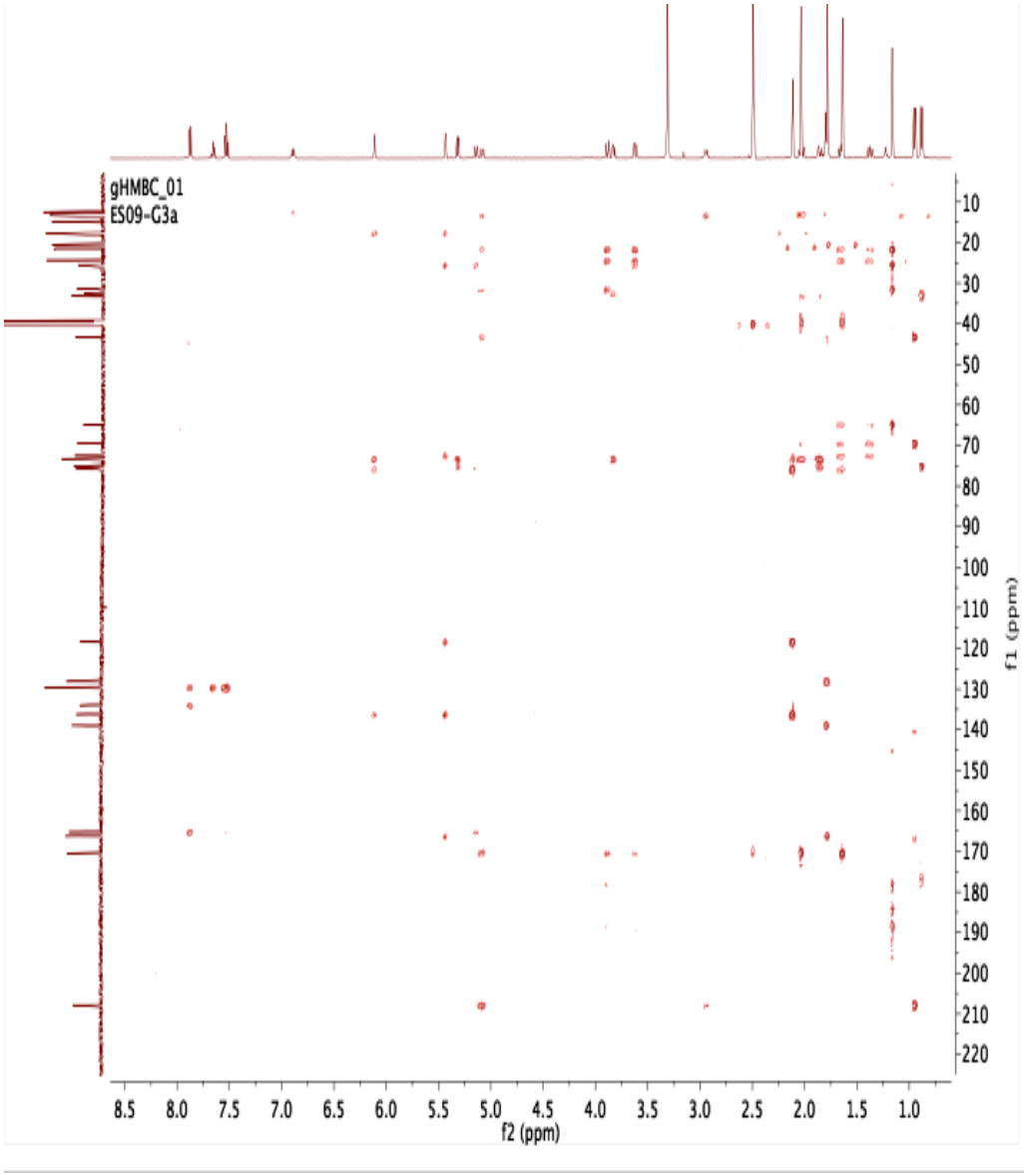

Figure S34. HMBC (500 and 125 MHz, DMSO-d_6) spectra of **4**

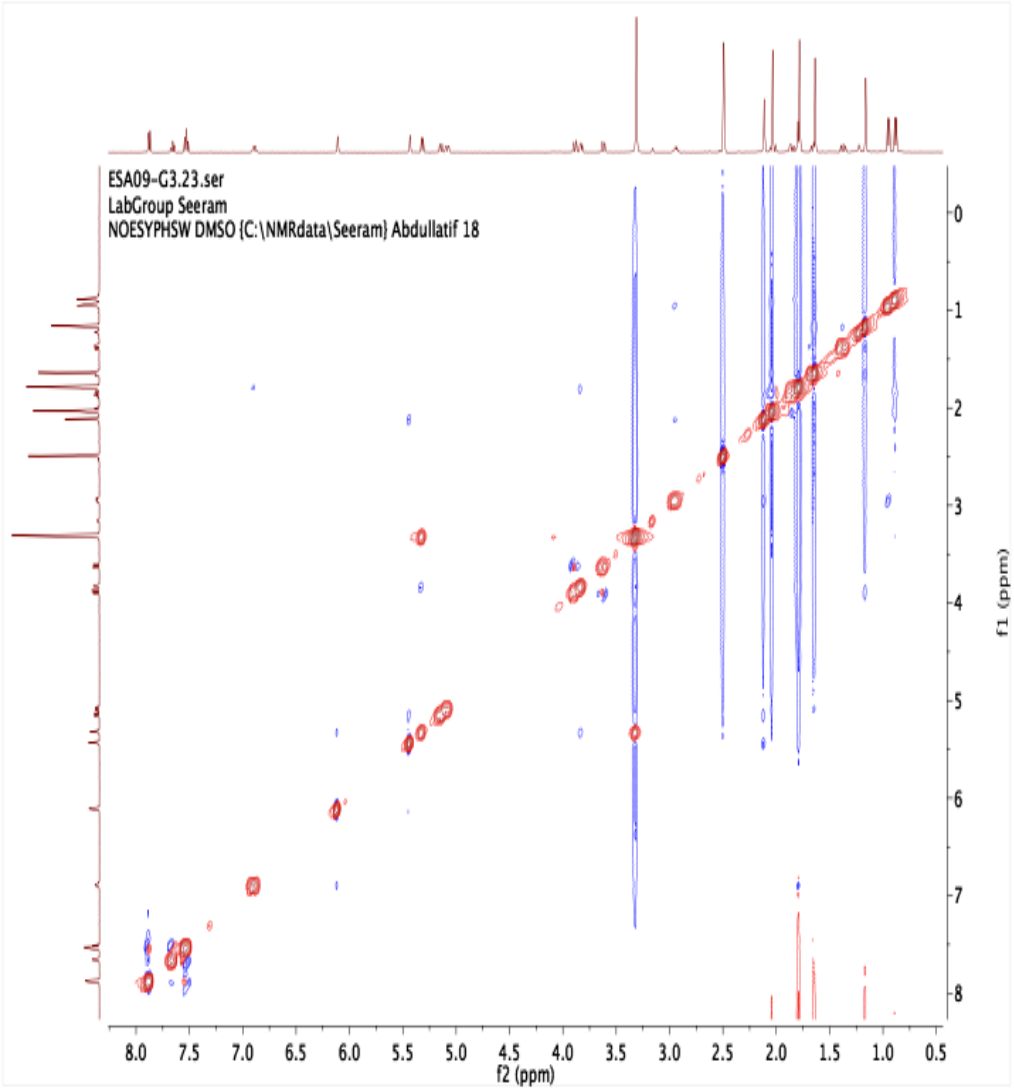

Figure S35. NOESY (500 and 125 MHz, DMSO-d_6) spectra of **4**

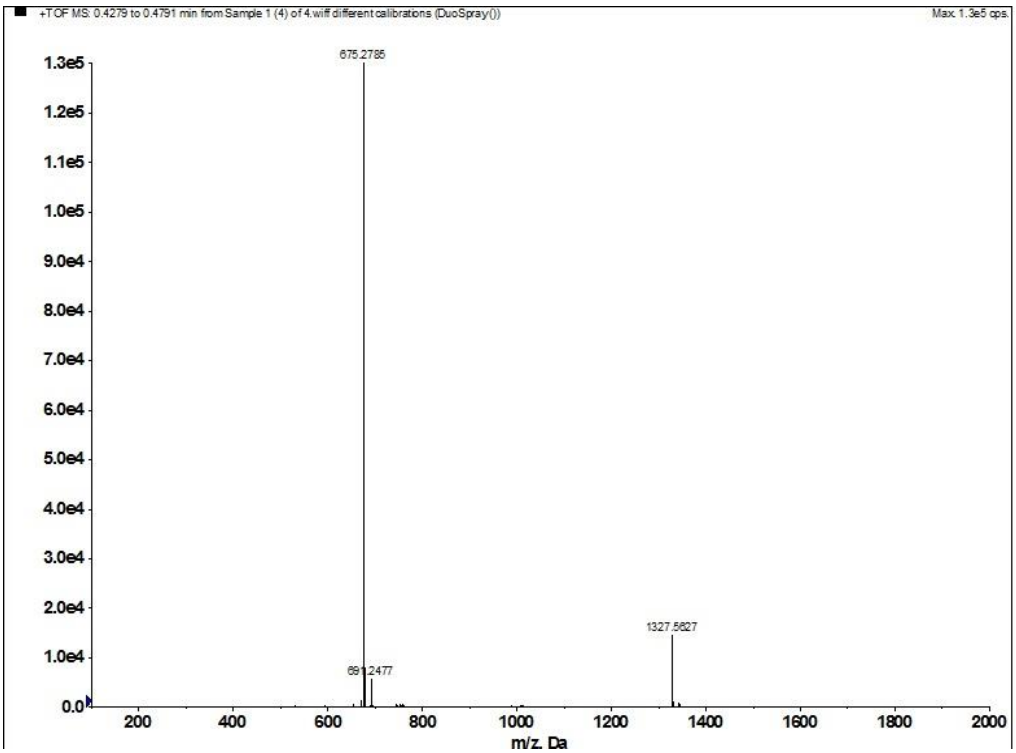

(+)-HRESIMS *m/z* **675.2785** $[M + Na]^+$ (calcd for $C_{36}H_{44}O_{11}Na$, **675.2781**).

Figure S36. HRESI (+) MS spectra of **4**

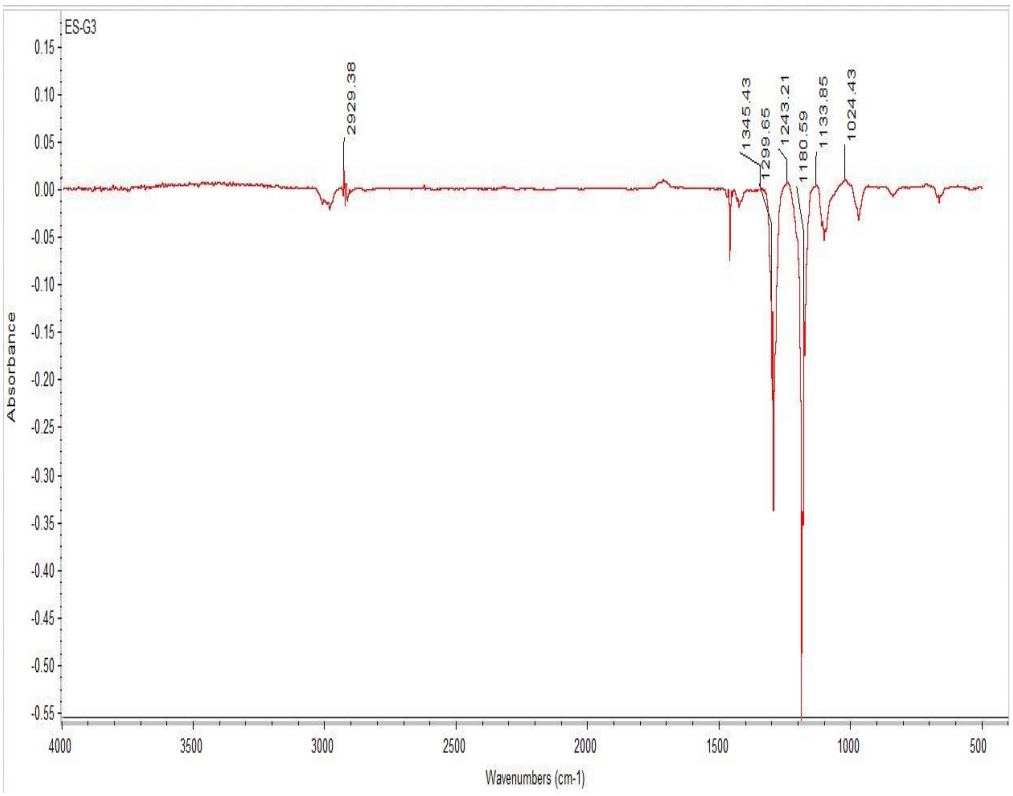

IR (KBr) ν_{max} 1716, 1299, 1243, 1180 cm^{-1}

Figure S37. IR spectra of **4**

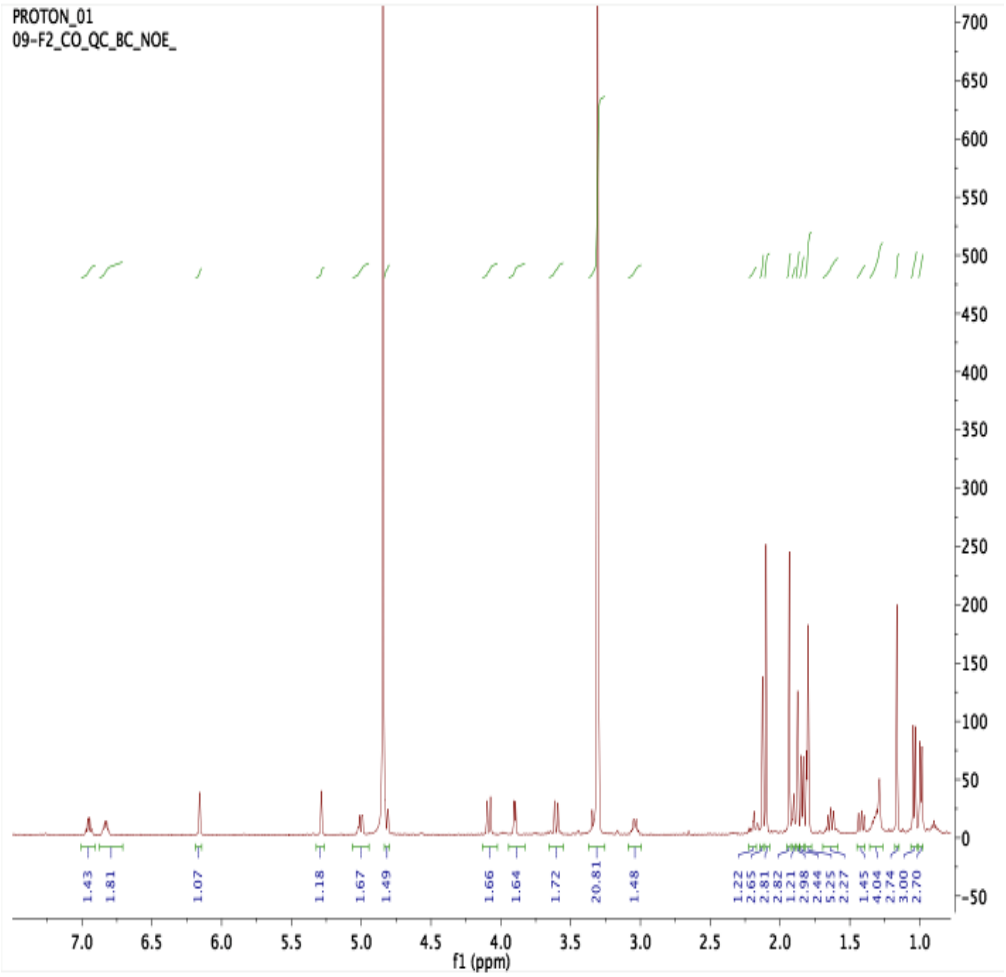

Figure S38. ^{1}H NMR (500 and 125 MHz, CD_3OD) spectra of **5**

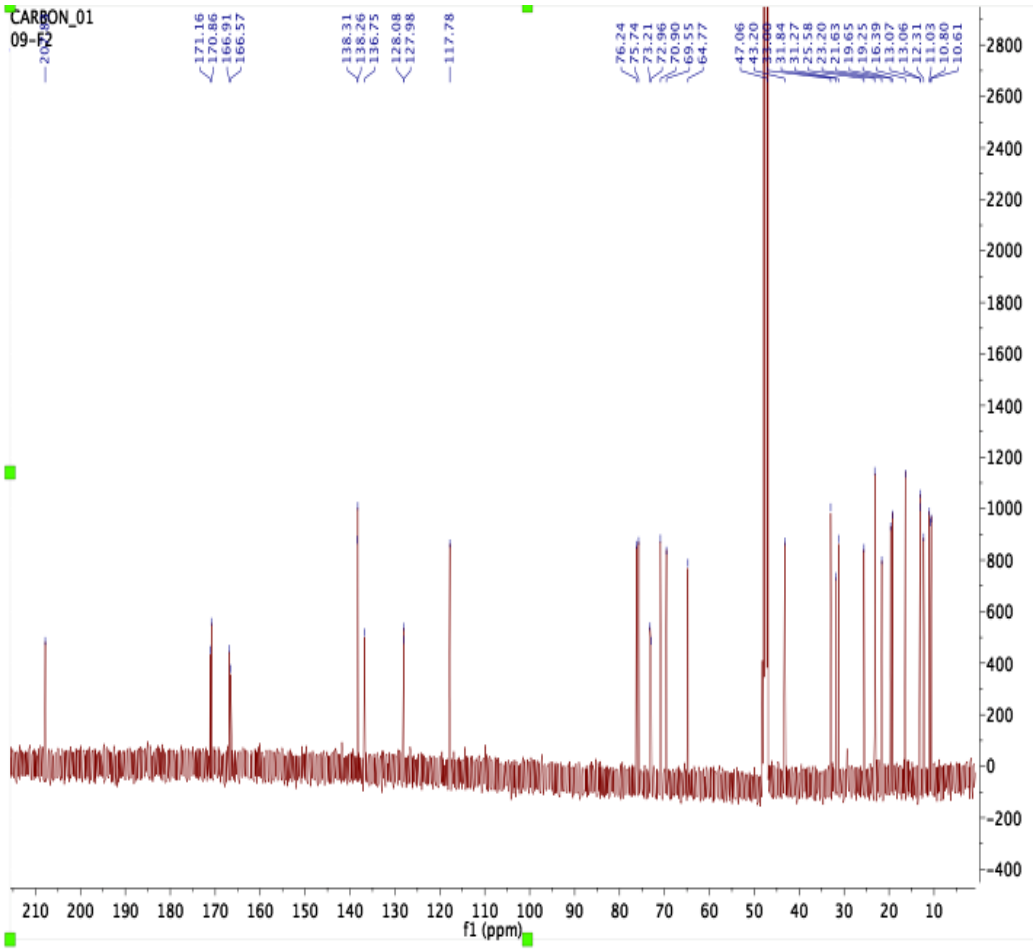

Figure S39. ^{13}C NMR (500 and 125 MHz, CD_3OD) spectra of **5**

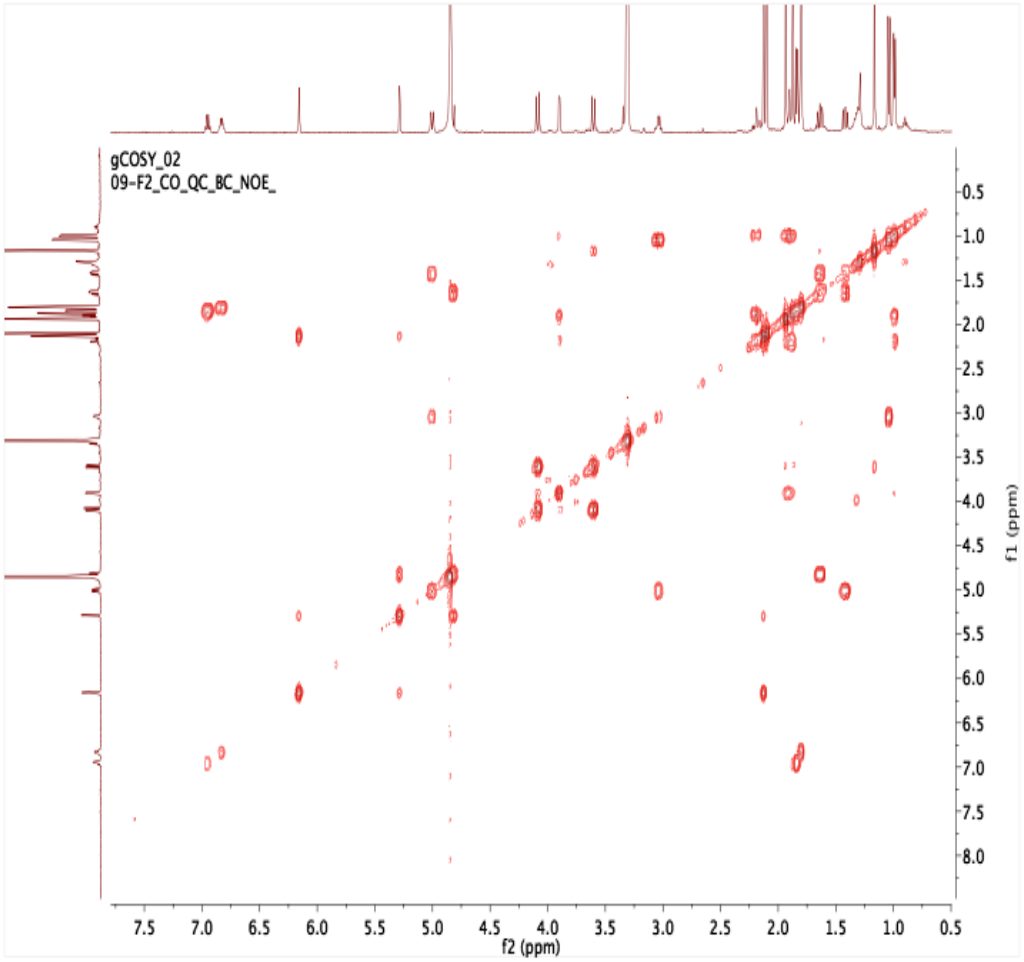

Figure S40. ^{1}H-^{1}H COSY (500 and 125 MHz, CD_3OD) spectra of **5**

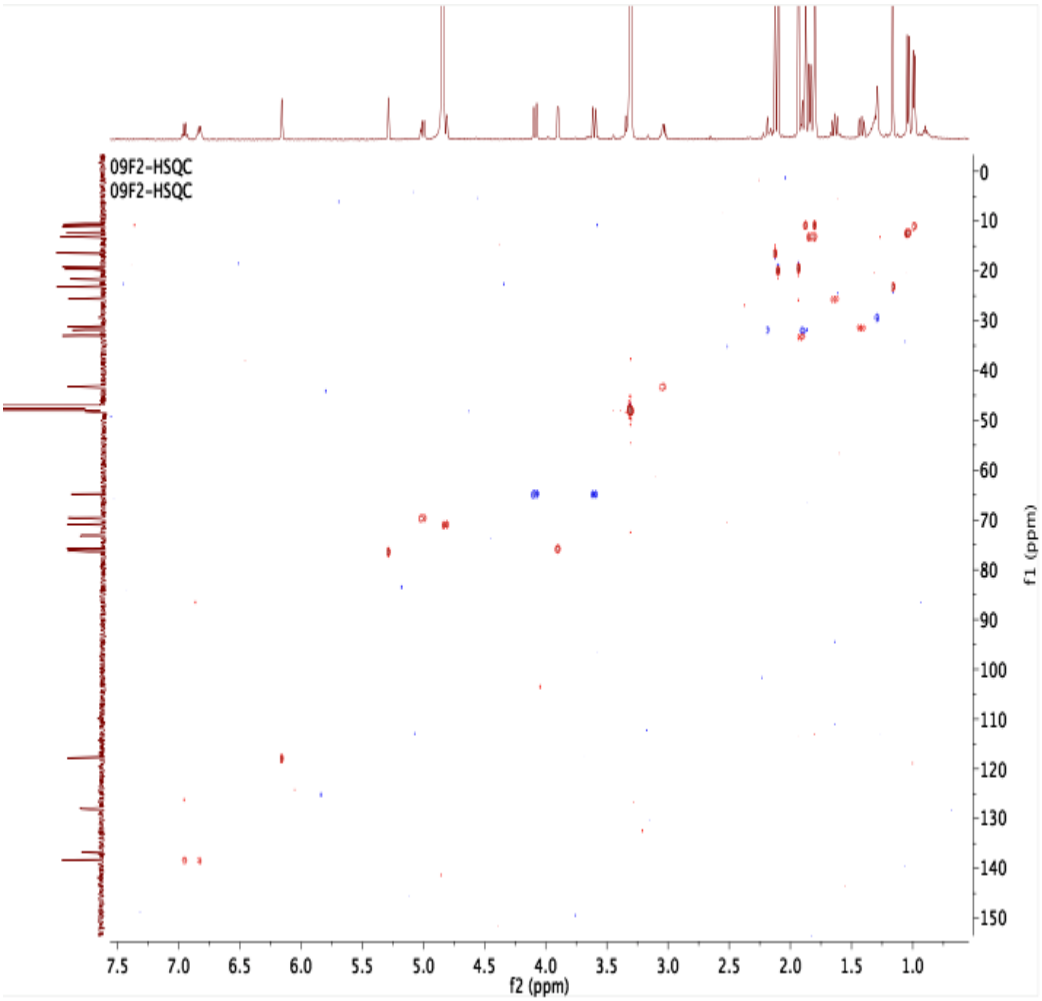

Figure S41. HSQC (500 and 125 MHz, CD_3OD) spectra of **5**

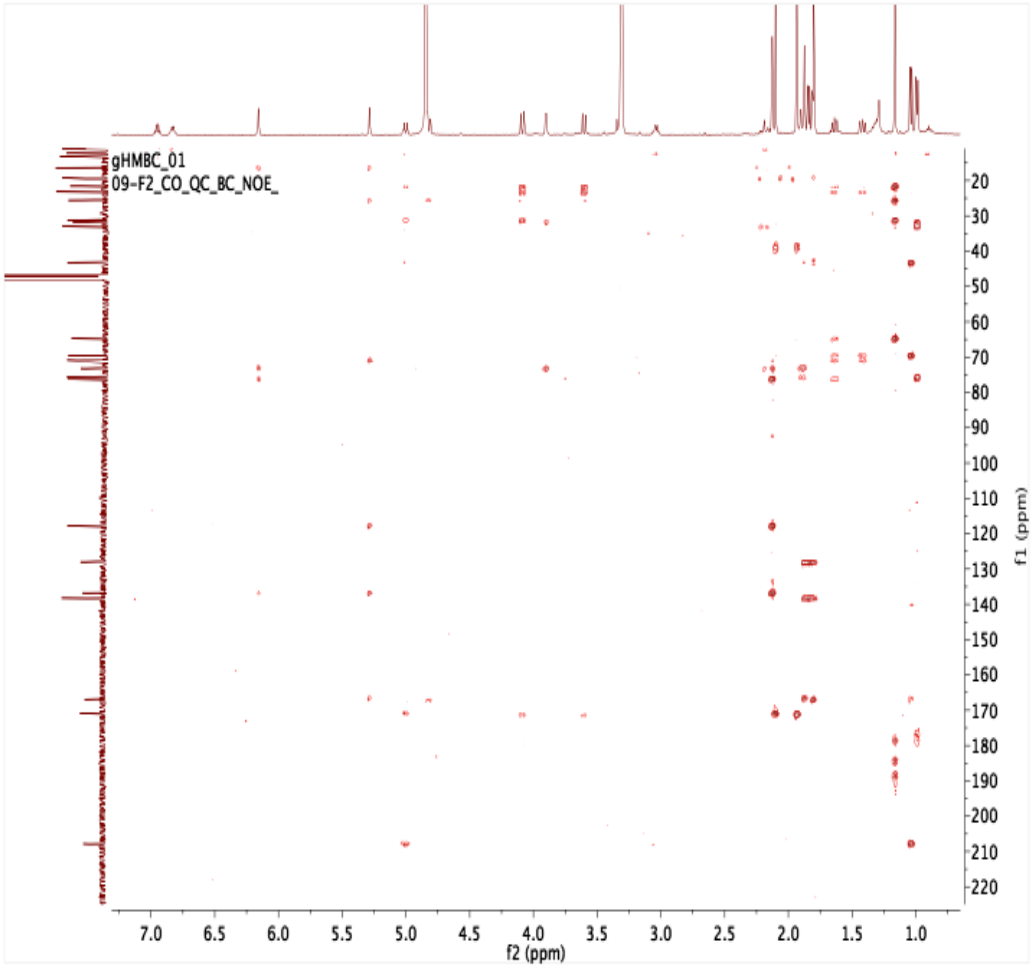

Figure S42. HMBC (500 and 125 MHz, CD_3OD) spectra of **5**

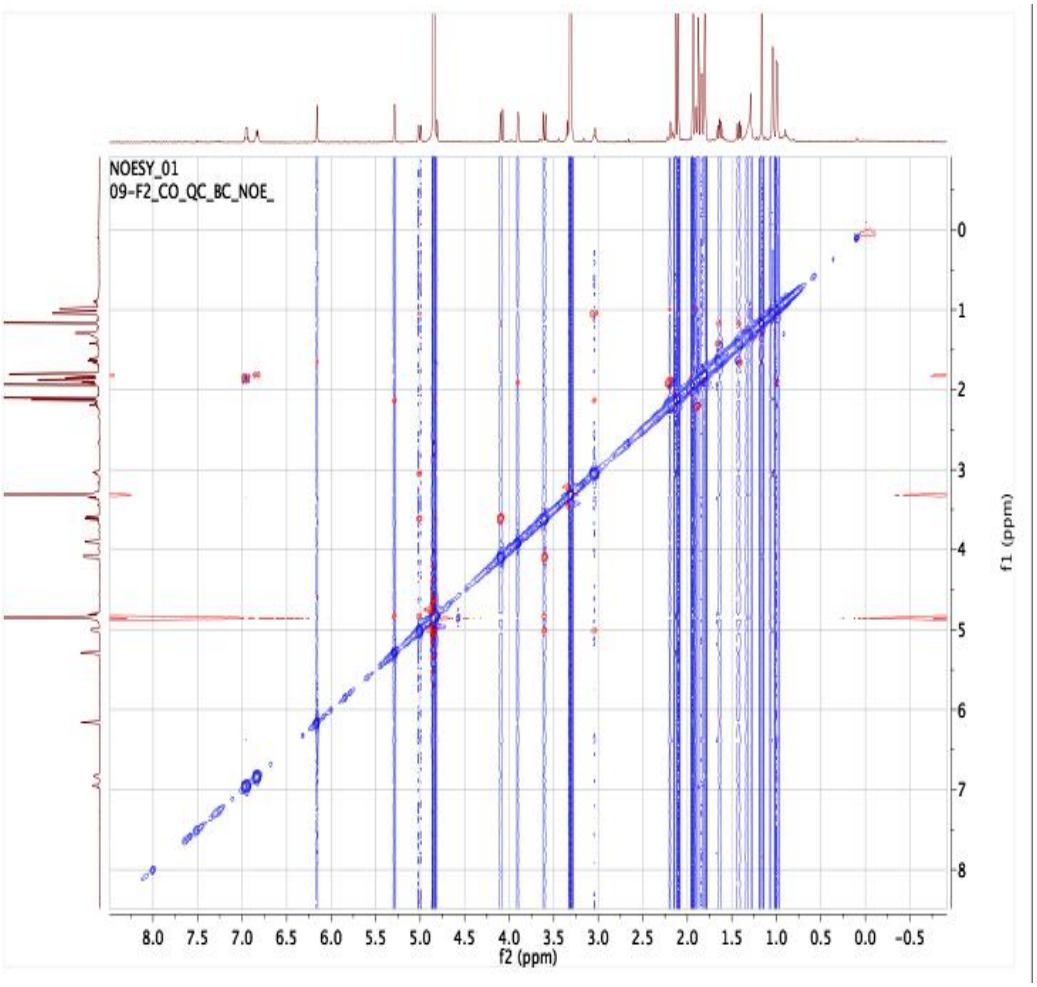

Figure S43. NOESY (500 and 125 MHz, CD_3OD) spectra of **5**

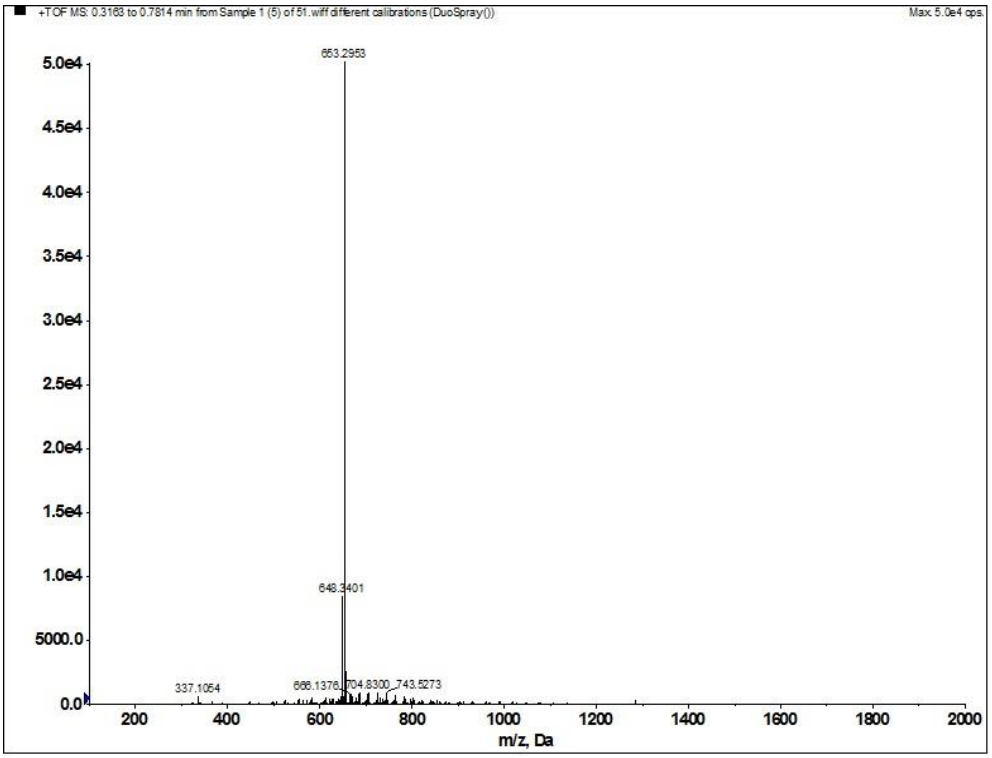

(+)-HRESIMS *m/z* **653.2953** $[M + Na]^+$ (calcd for $C_{34}H_{46}O_{11}Na$, **653.2938**).

Figure S44. HRESI (+) MS spectra of **5**

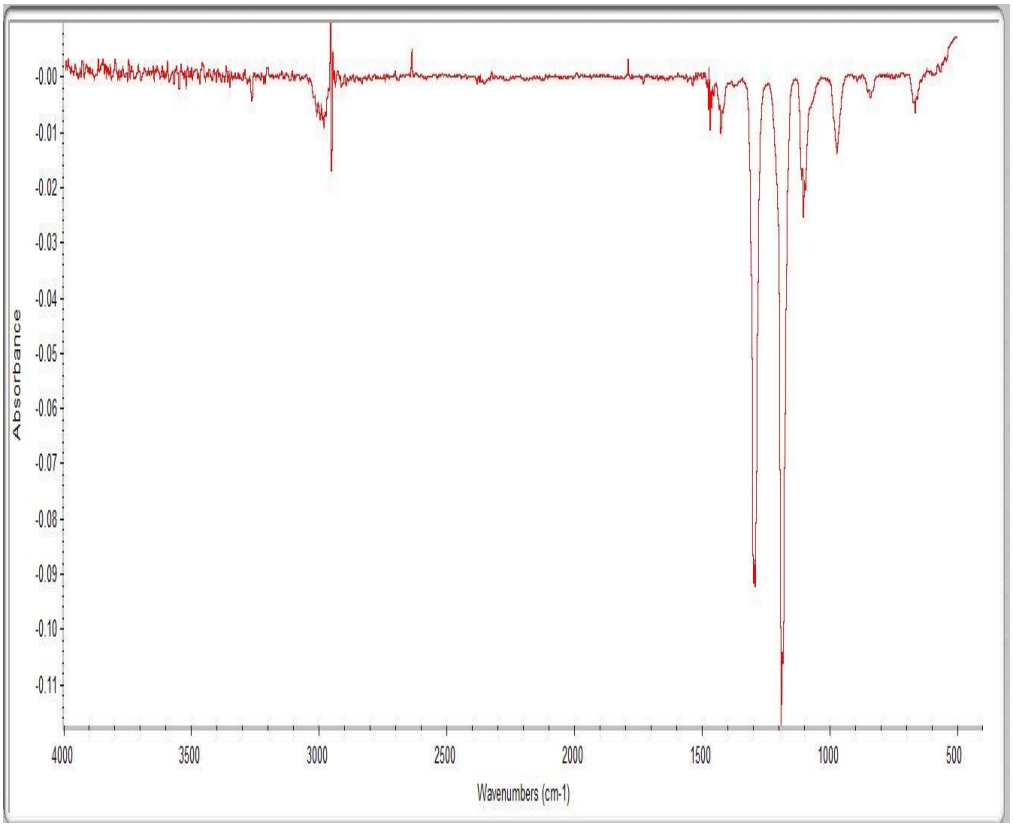

IR (KBr) ν_{max} 2958, 1344, 1241,1135 cm^{-}

Figure S45. IR spectra of **5**

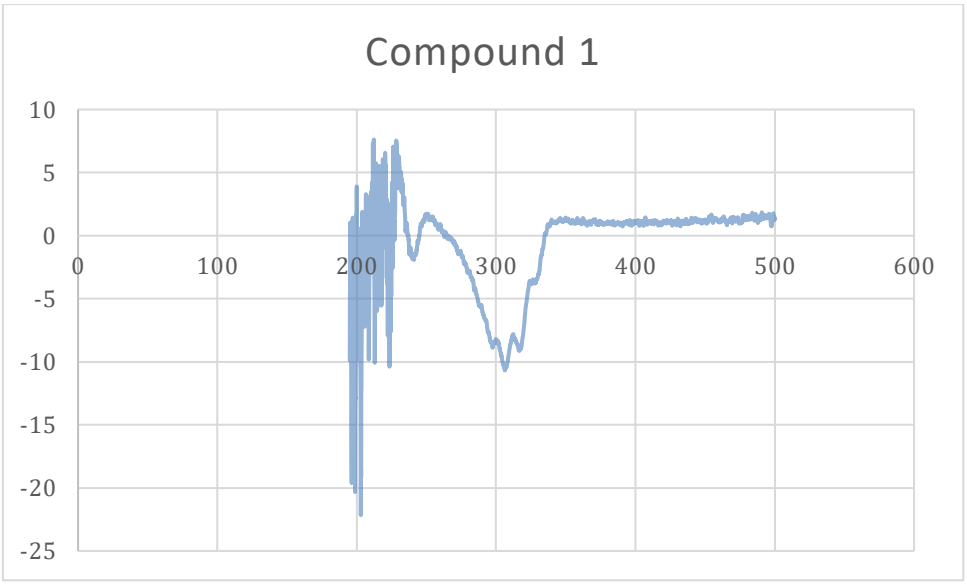

Figure S46. The experimental ECD spectrum of **1**

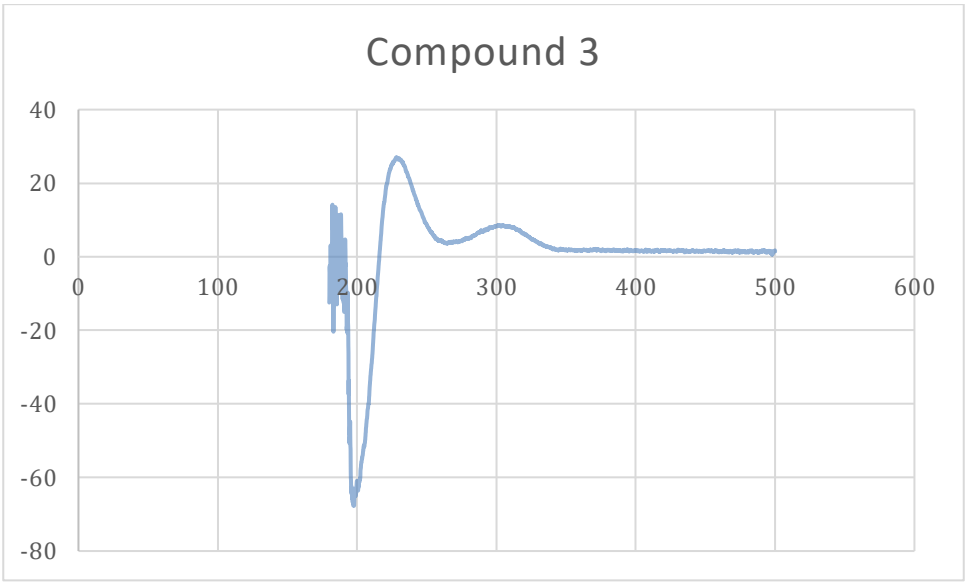

Figure S47. The experimental ECD spectrum of **3**

Appendix II

Manuscript I

Tables

Figures

Manuscript II

Tables

Figures

Label	Polyphenols %
Methanol Extraction	39.0
n-Hexanes Fraction	7.8
Ethyl Acetate Fraction	**58.8**
Butanol Fraction	32.7

Table S6. Polyphenol content assay of silver maple fractions.

Cmpds	Chemical name	UV (nm)
1	Ginnalin A	215, 276
2	Ginnalin B	217, 272
3	Ginnalin C	215, 276
4	Maplexin B	215, 276
5	Maplexin D	215, 278
6	Maplexin F	217, 278
7	methyl gallate	224, 275
8	methyl syringate	217 (s), 278
9	3-methoxy-4-hydroxyphenol 1-O-β-D-(6'-O-galloyl)-glucopyranoside	215, 277
10	pubinernoid A	220

Table S7. Compounds (**1-10**) retention time (R*t*).

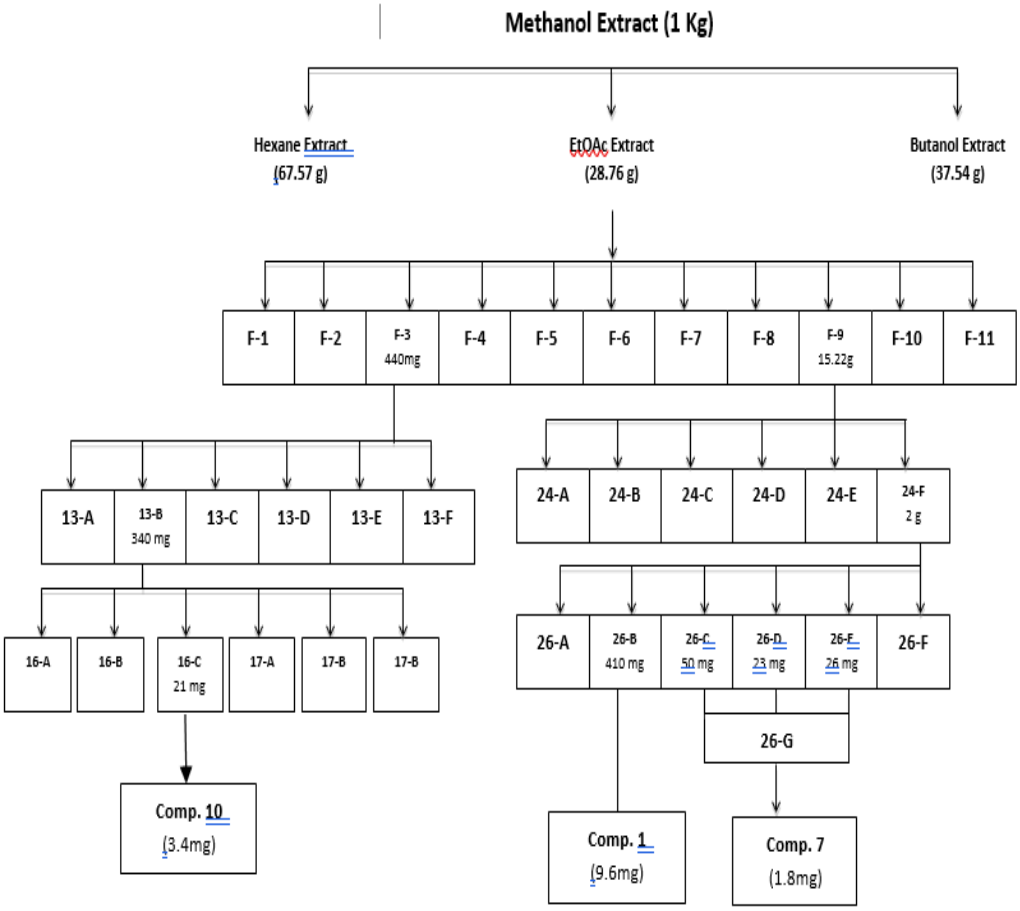

Figure S48. Extraction and isolation scheme of compounds **1, 7** and **10** from silver maple leaves (*Acer saccharinum).*

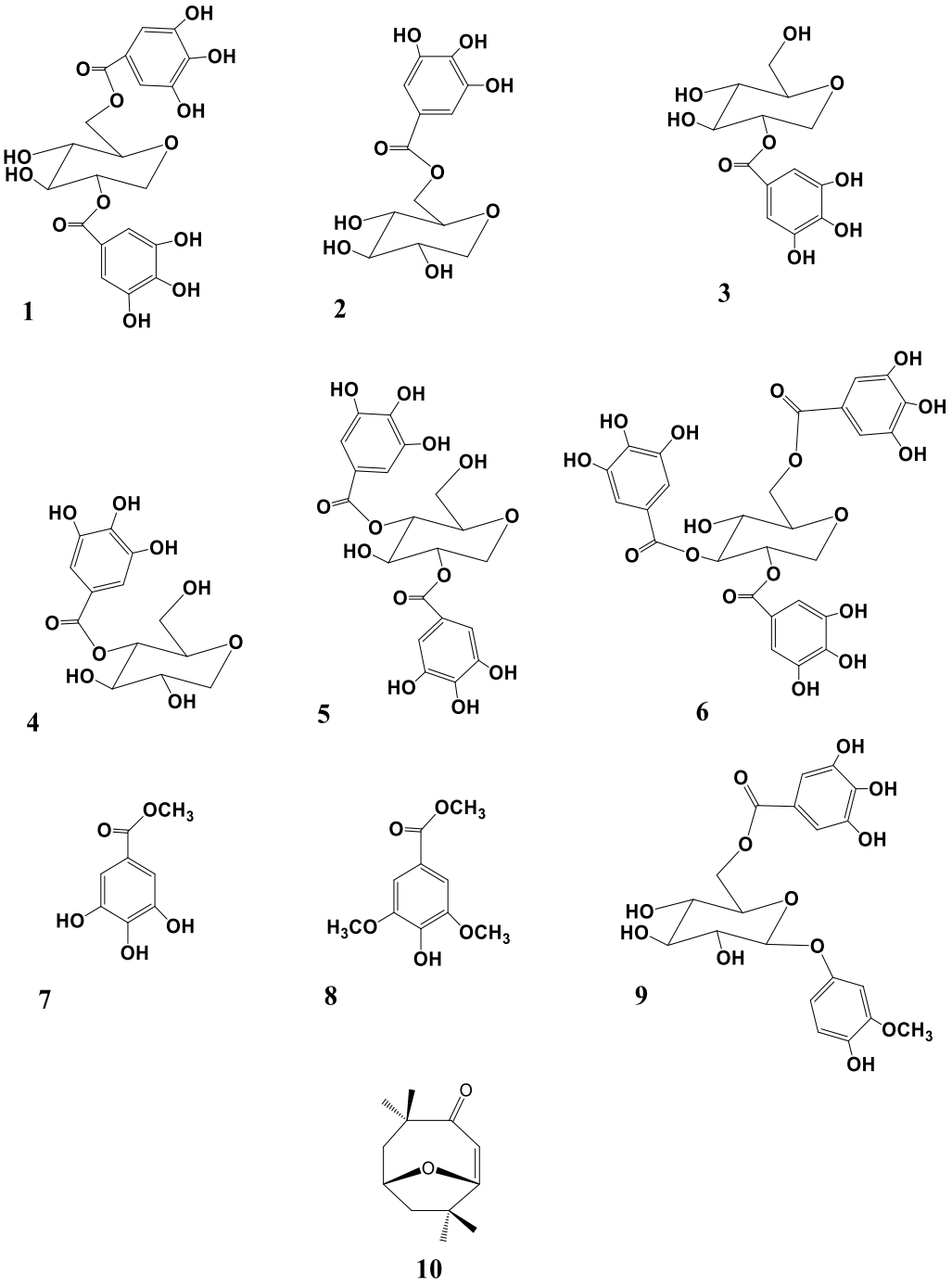

Figure S49. Chemical Structures of compounds **1-10** isolated from silver maple leaves.

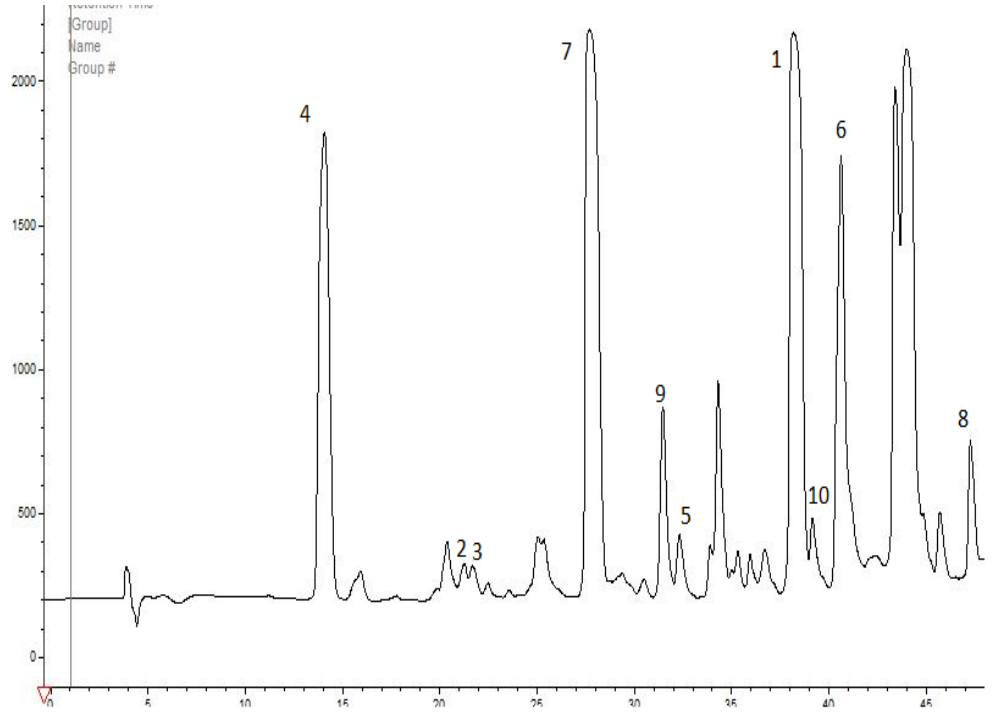

Figure S50. HPLC-DAD chromatogram of ethyl acetate extract of silver maple leaves showing the isolated compounds (**1-10**).

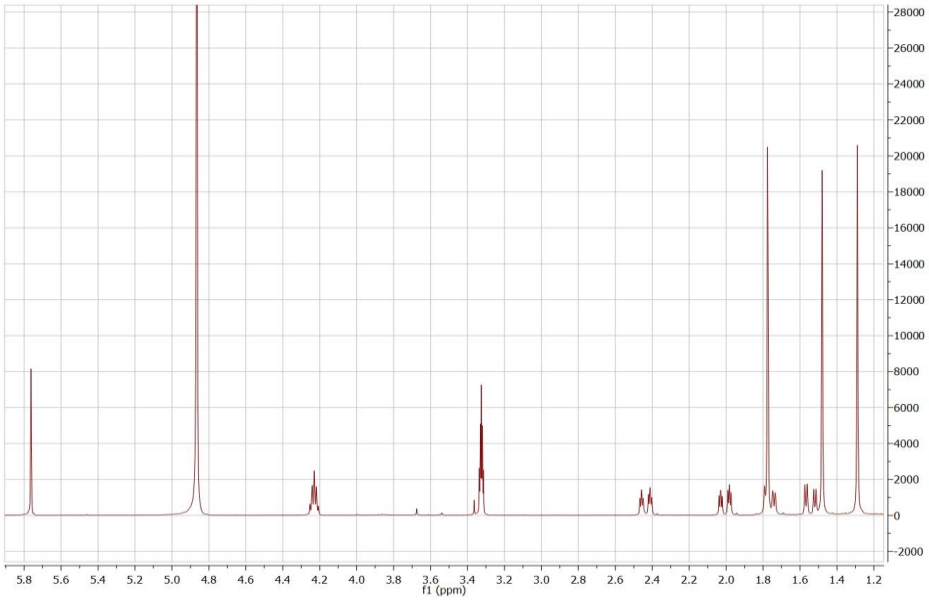

Figure S51. The ^{1}H NMR spectrum of compound **10**

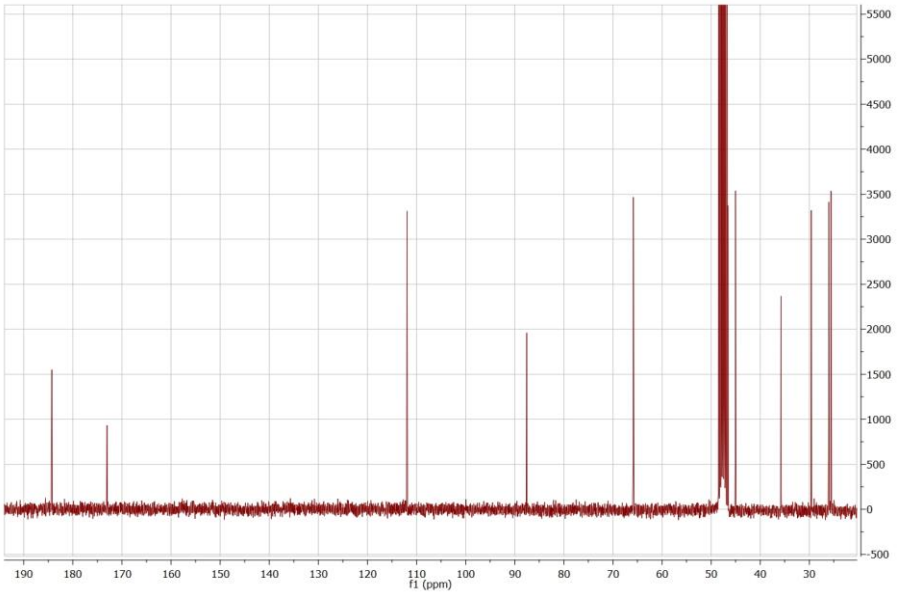

Figure S52. The ^{13}C NMR spectrum of compound **10**

Compound #	Absorption	Concentrsation (ug/mL)	MW	loge	Wavelengh
1	0.8053	1.2	610	5.61	208
	0.7422	8	610	4.75	272
2	0.5312	1.25	588	5.40	203
	0.5206	100	588	3.49	270
3	0.6443	5	668	4.93	210
	0.7734	100	668	3.71	270
4	0.5601	10	652	4.56	200
	0.2421	100	652	3.20	270
5	0.66	50	630	3.92	222
	0.2777	250	630	2.84	275

Table S8. The fixed wavelength of all compounds (**1-5**)

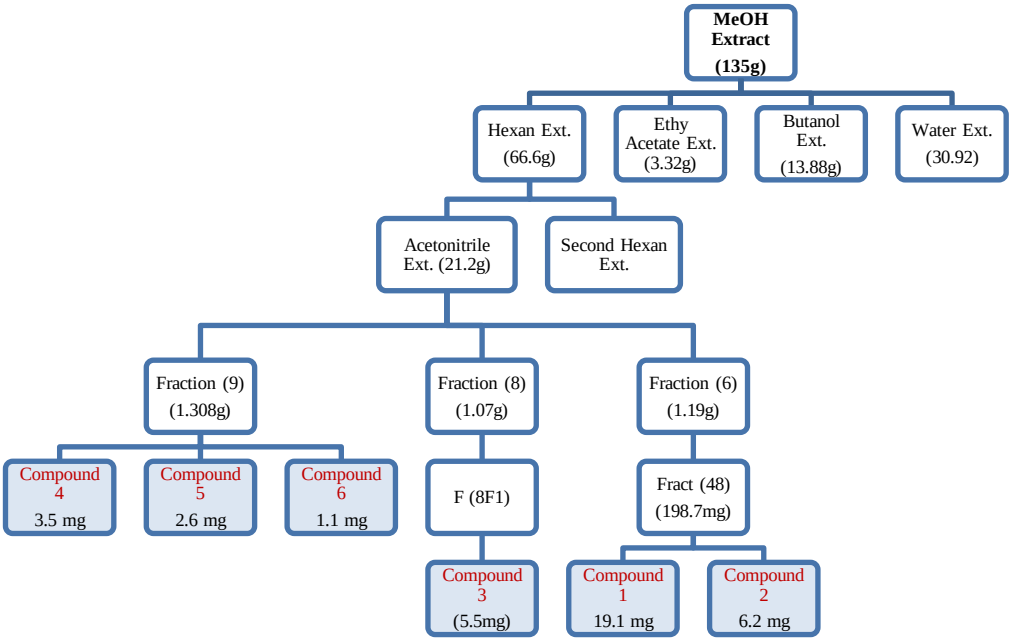

Figure S53. The isolation Scheme of compound **1-5**.

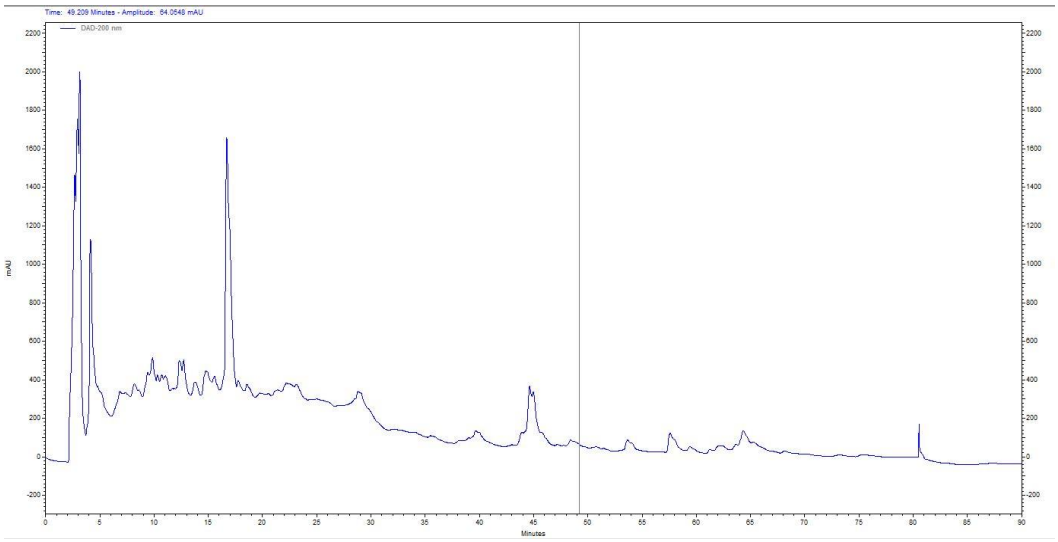

Figure S54. The HPLC-DAD profile for *Euphorbia saudiarabica* crude extract.

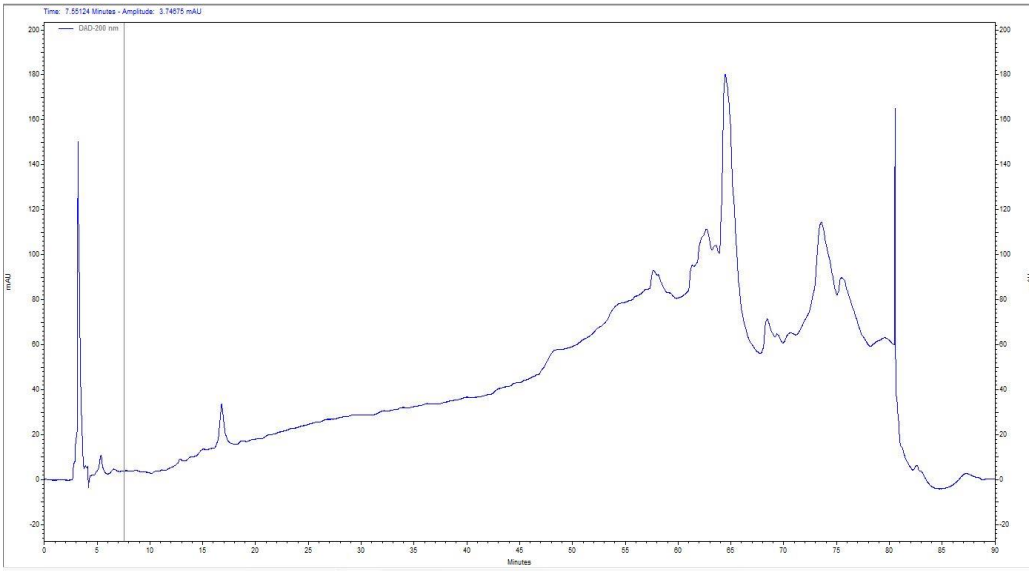

Figure S55. The HPLC-DAD profile for n-hexanes extract

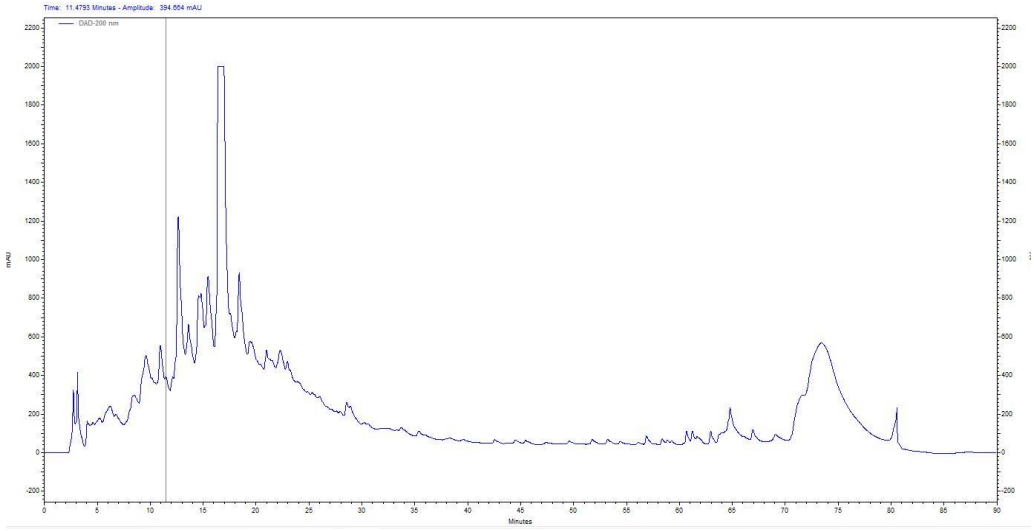

Figure S56. The HPLC-DAD profile for Ethyl Acetate extract

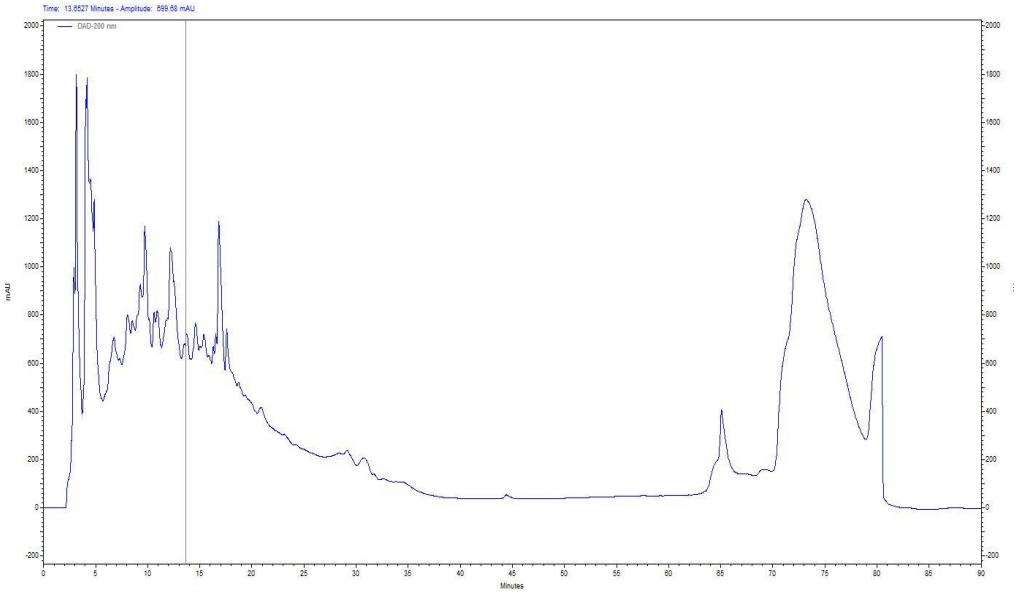

Figure S57. The HPLC-DAD profile for Butanol extract

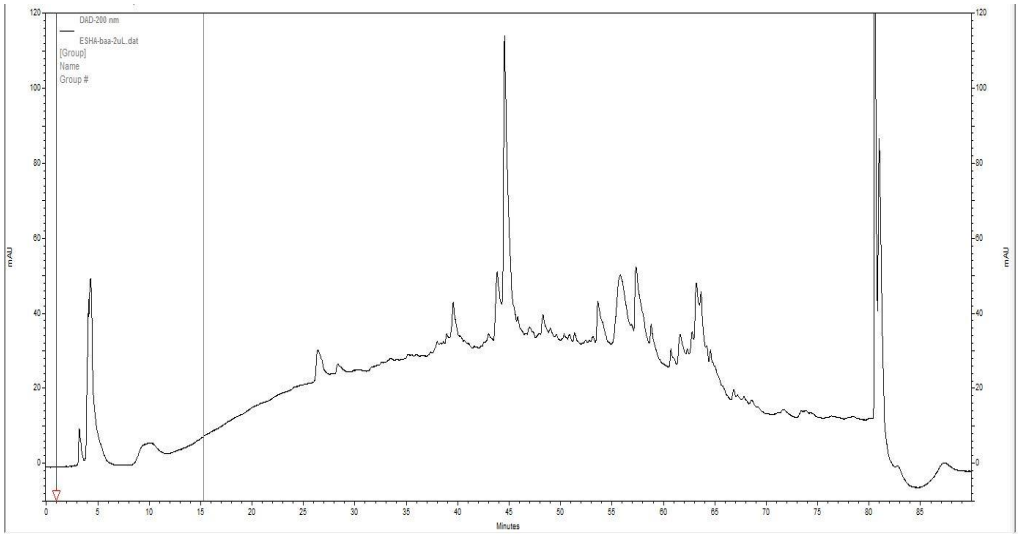

Figure S58. The HPLC-DAD profile for Acetonitrile extract

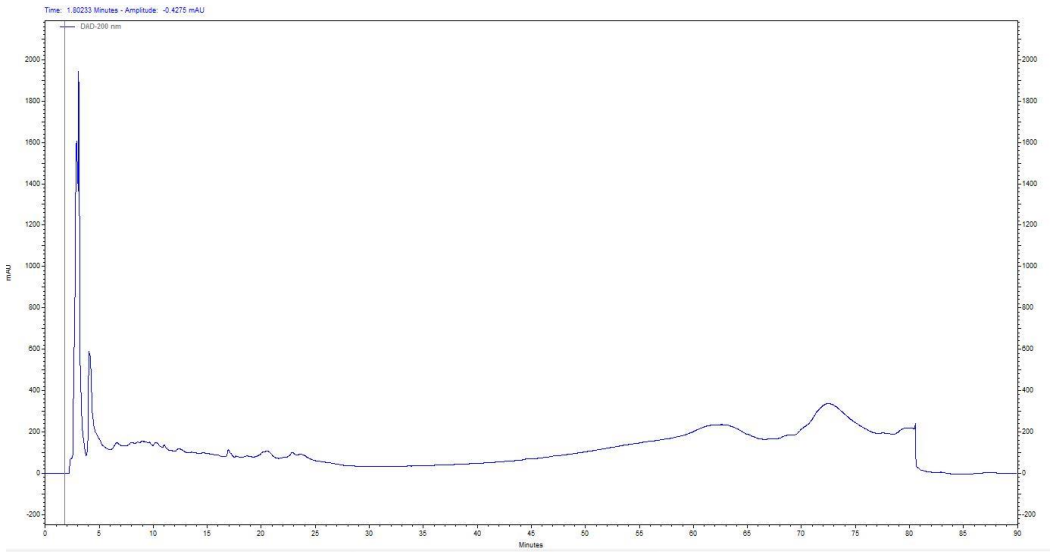

Figure S59. The HPLC-DAD profile for Water extract

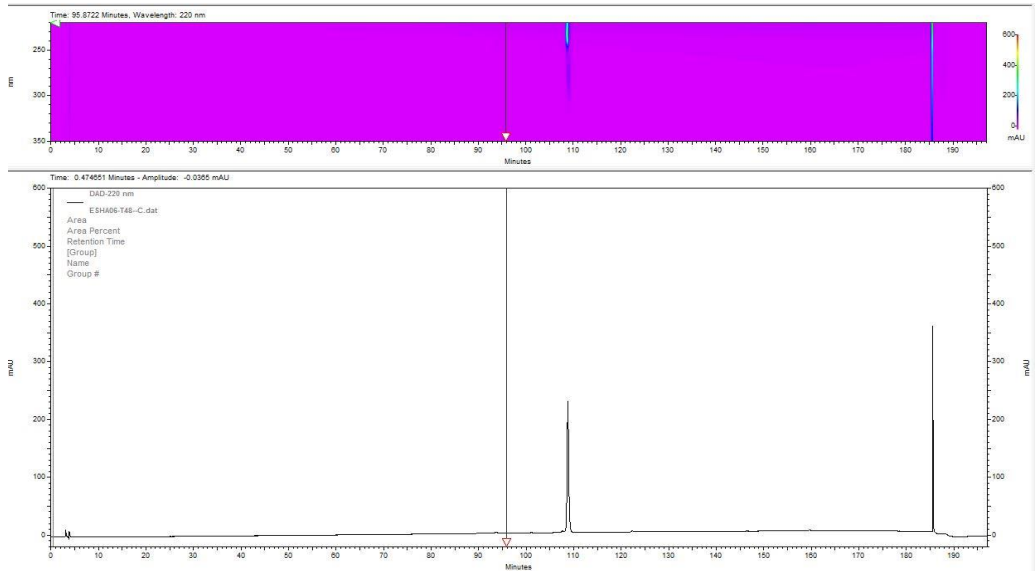

Figure S60. The HPLC-DAD profile for Pure compound **1**

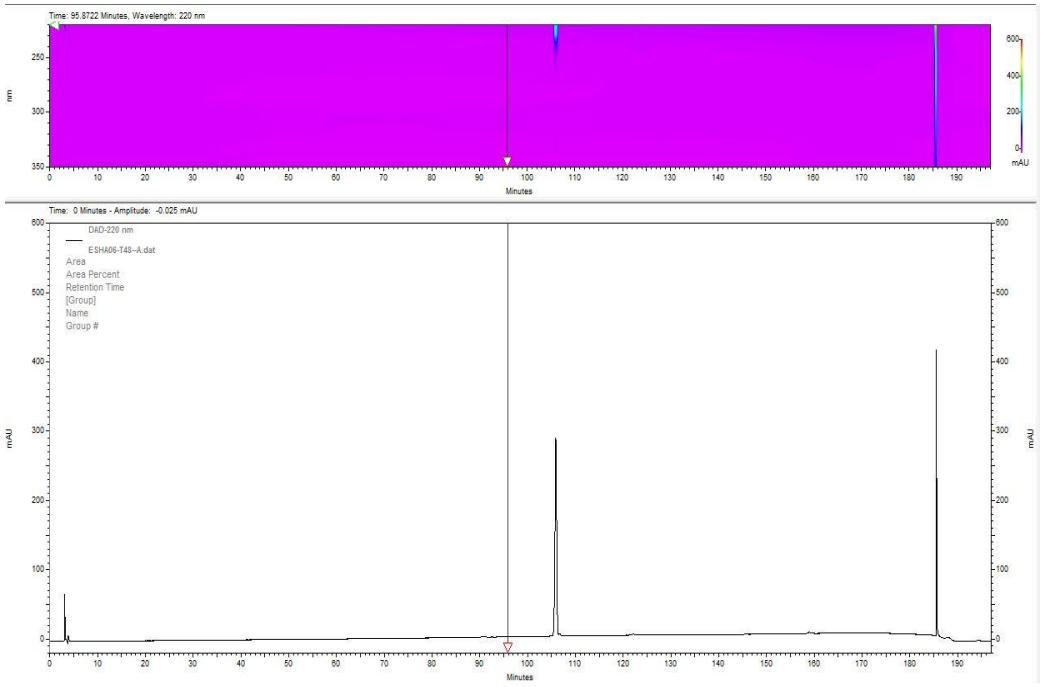

Figure S61. The HPLC-DAD profile for Pure compound **2**

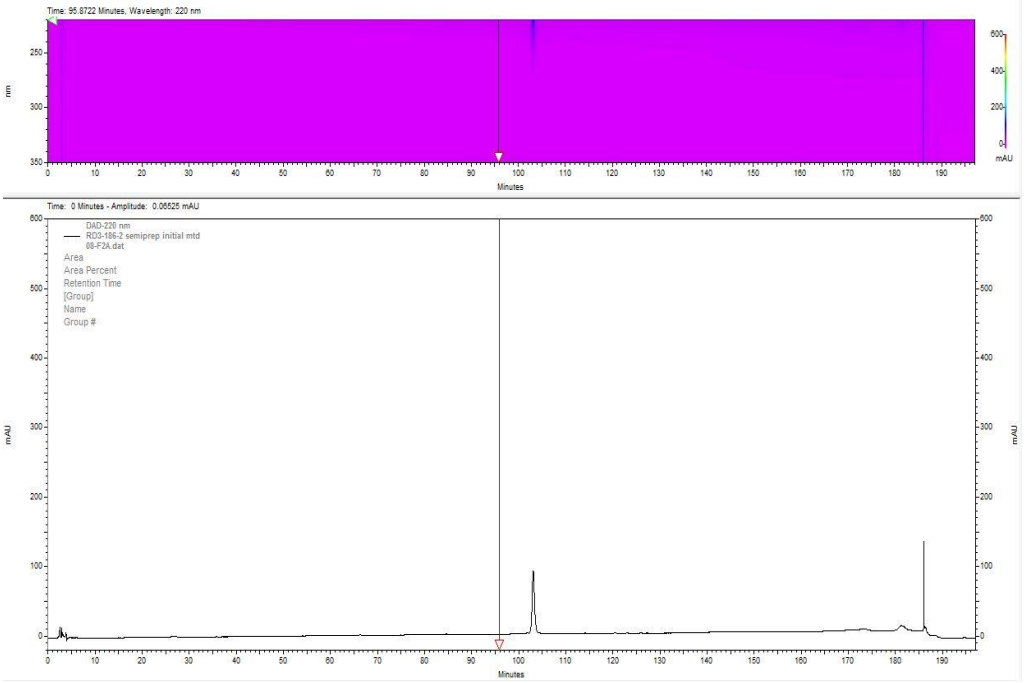

Figure S62. The HP-DAD profile for Pure compound **3**

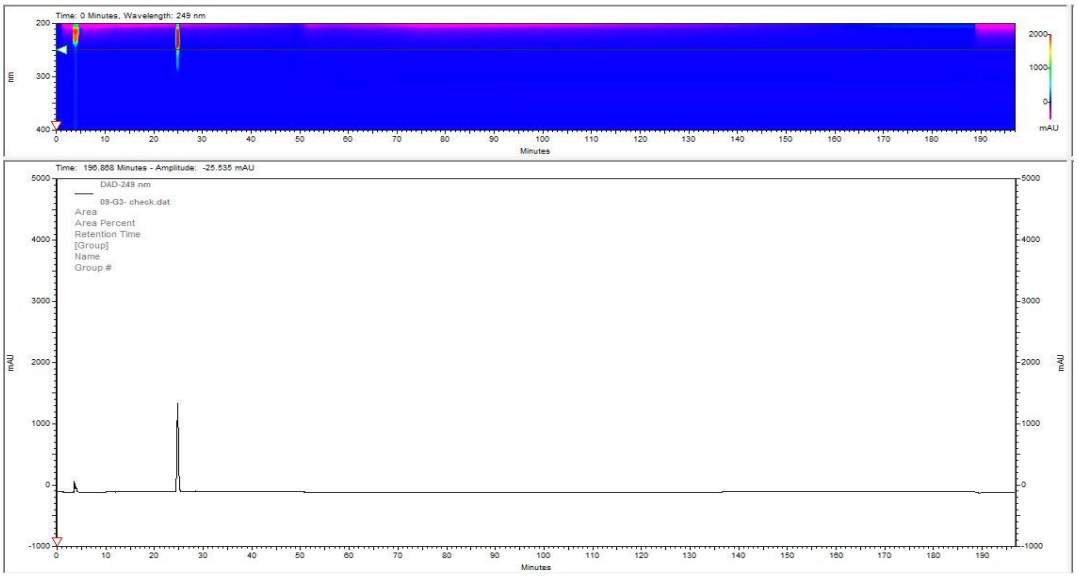

Figure S63. The HPLC-DAD profile for Pure compound **4**

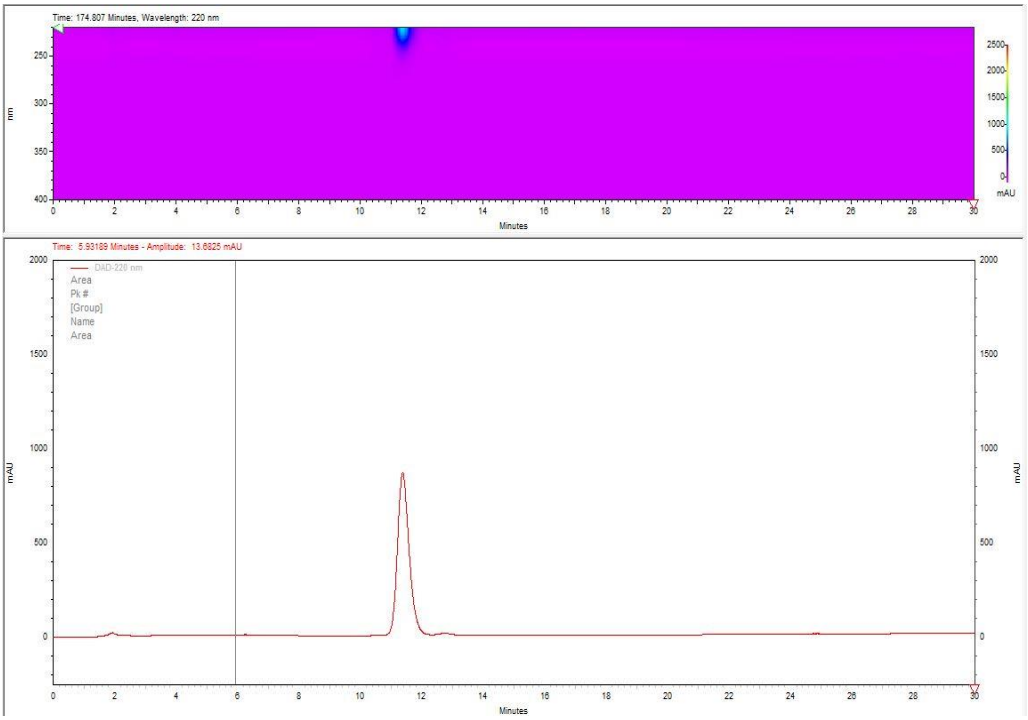

Figure S64. The HPLC-DAD profile for Pure compound **5**

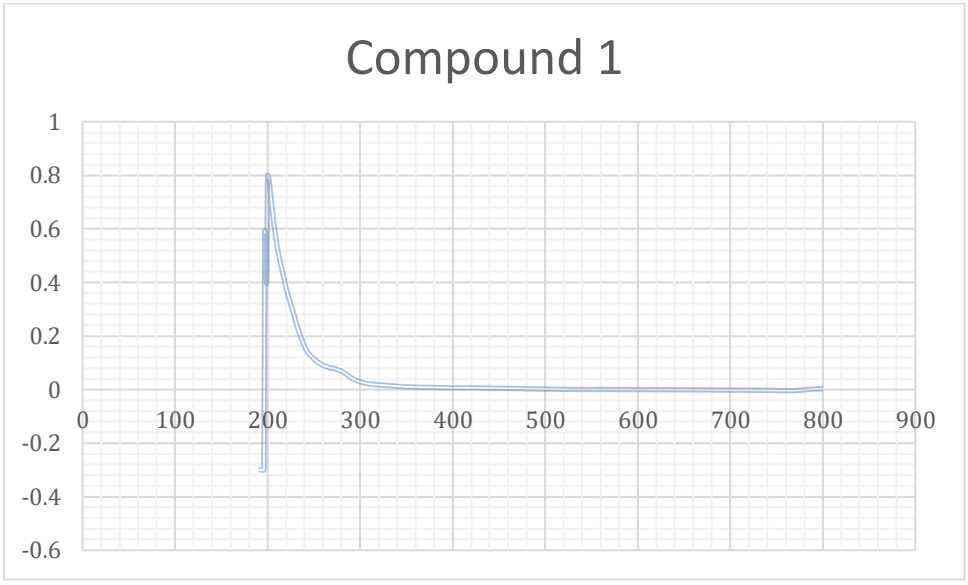

Figure S65. The UV-vis spectrum for compound **1**

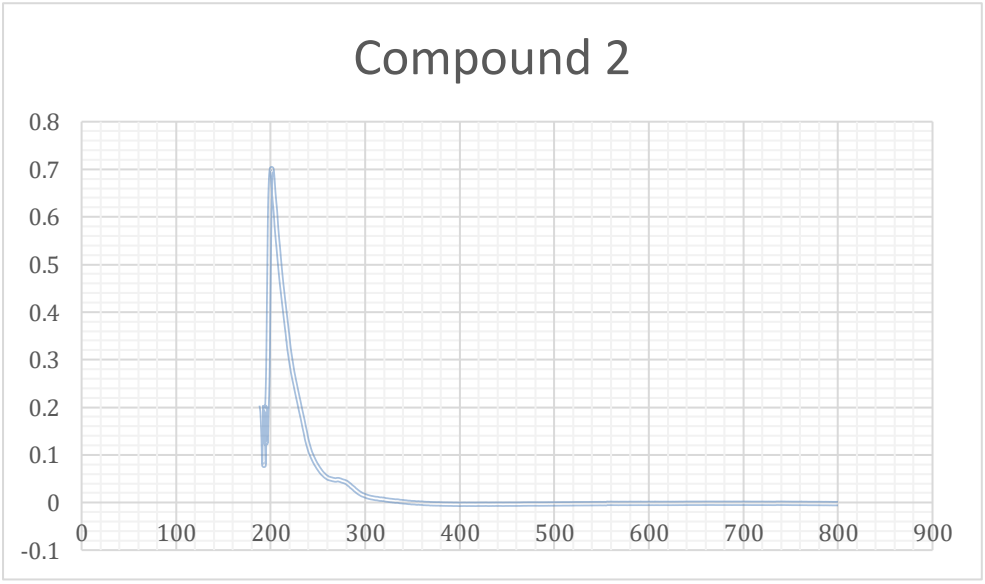

Figure S66. The UV-vis spectrum for compound **2**

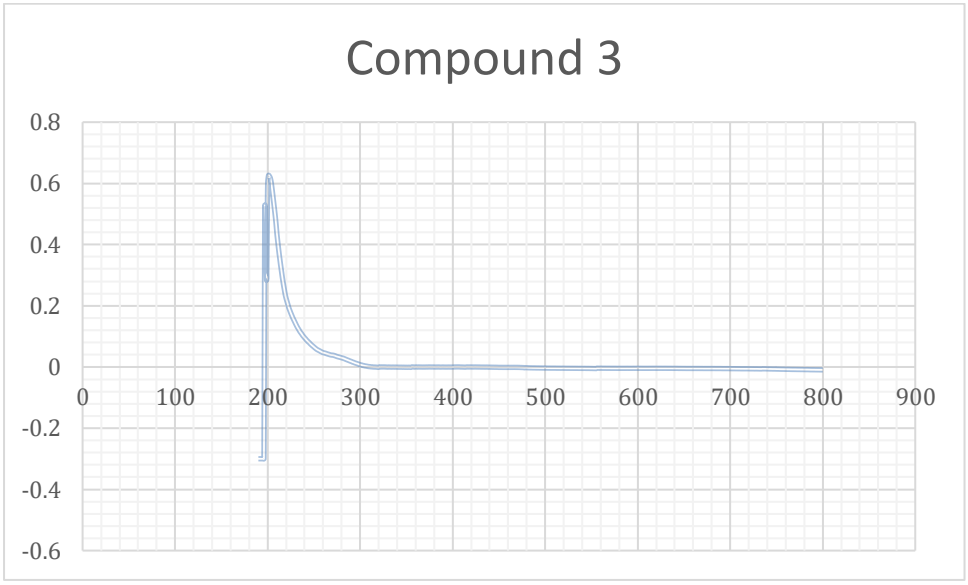

Figure S67. The UV-vis spectrum for compound **3**

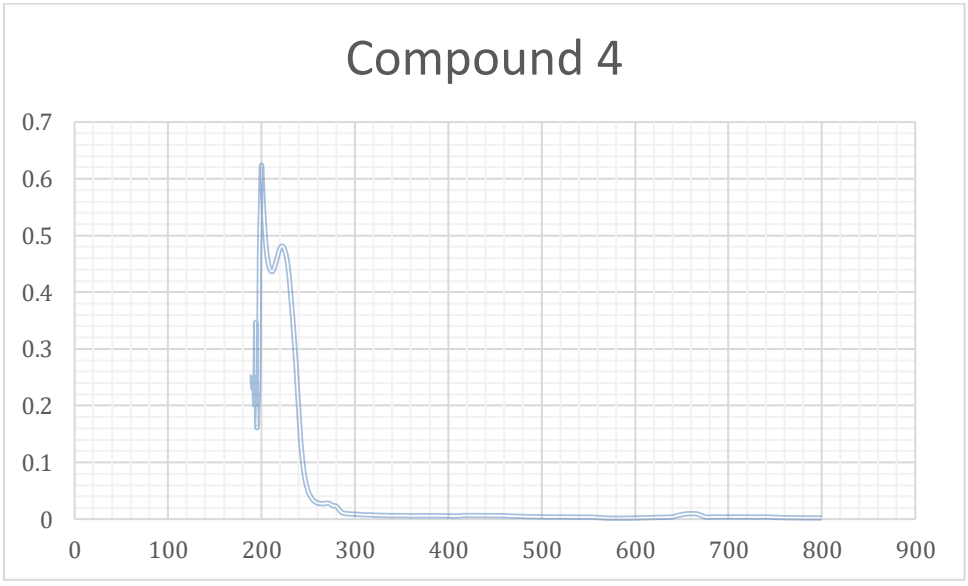

Figure S68. The UV-vis spectrum for compound **4**

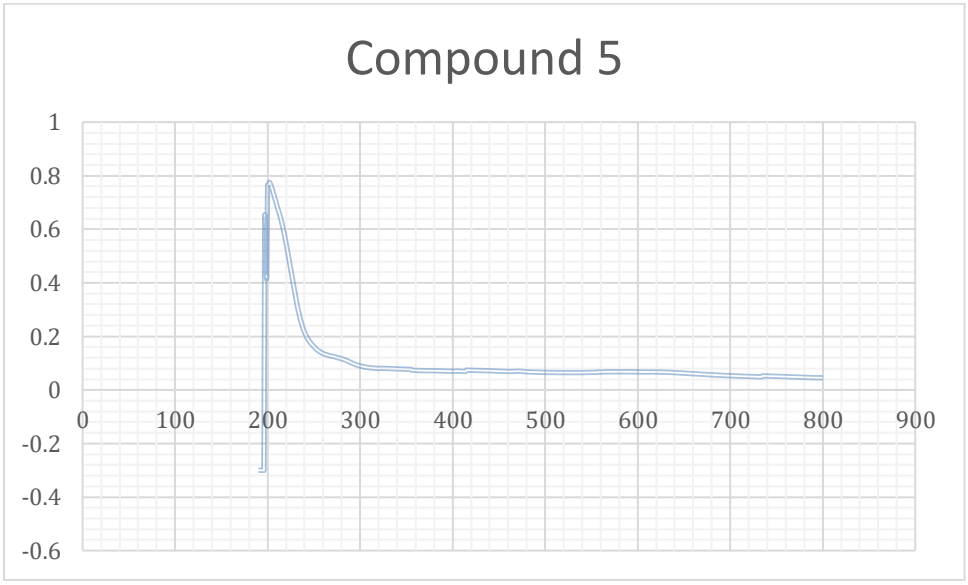

Figure S69. The UV-vis spectrum for compound **5**

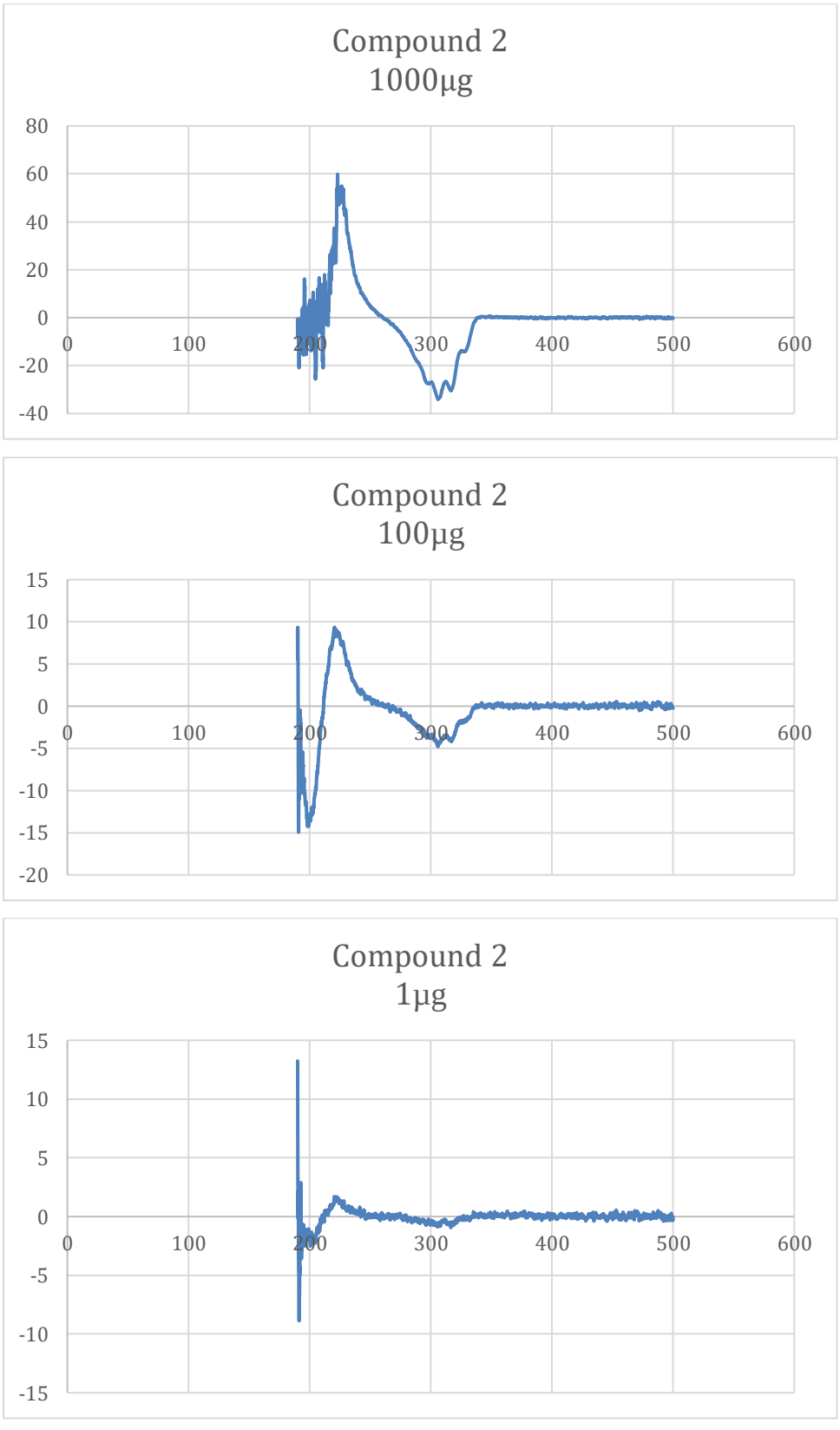

Figure S70. The CD spectrum for compound **2**

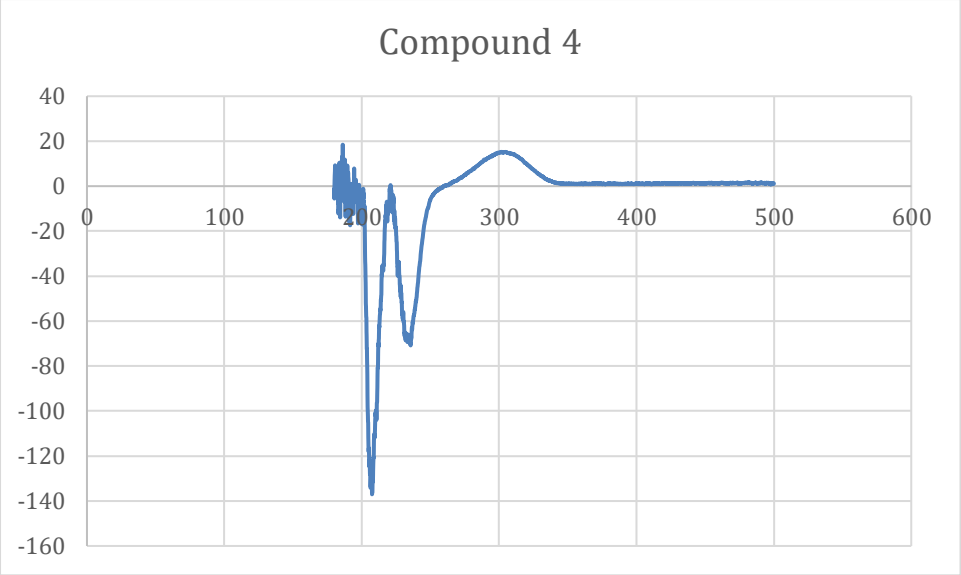

Figure S71. The CD spectrum for compound **4**

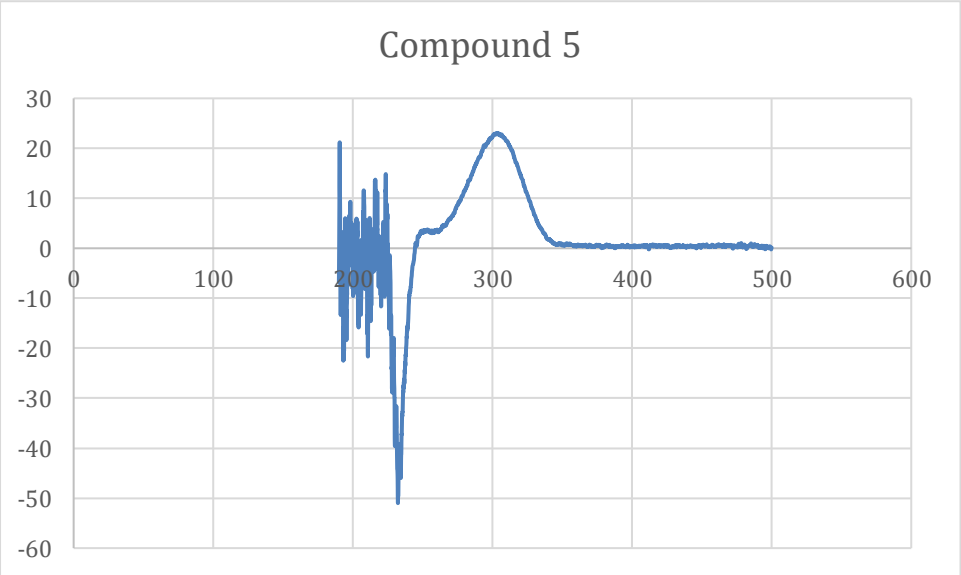

Figure S72. The CD spectrum for compound **5**

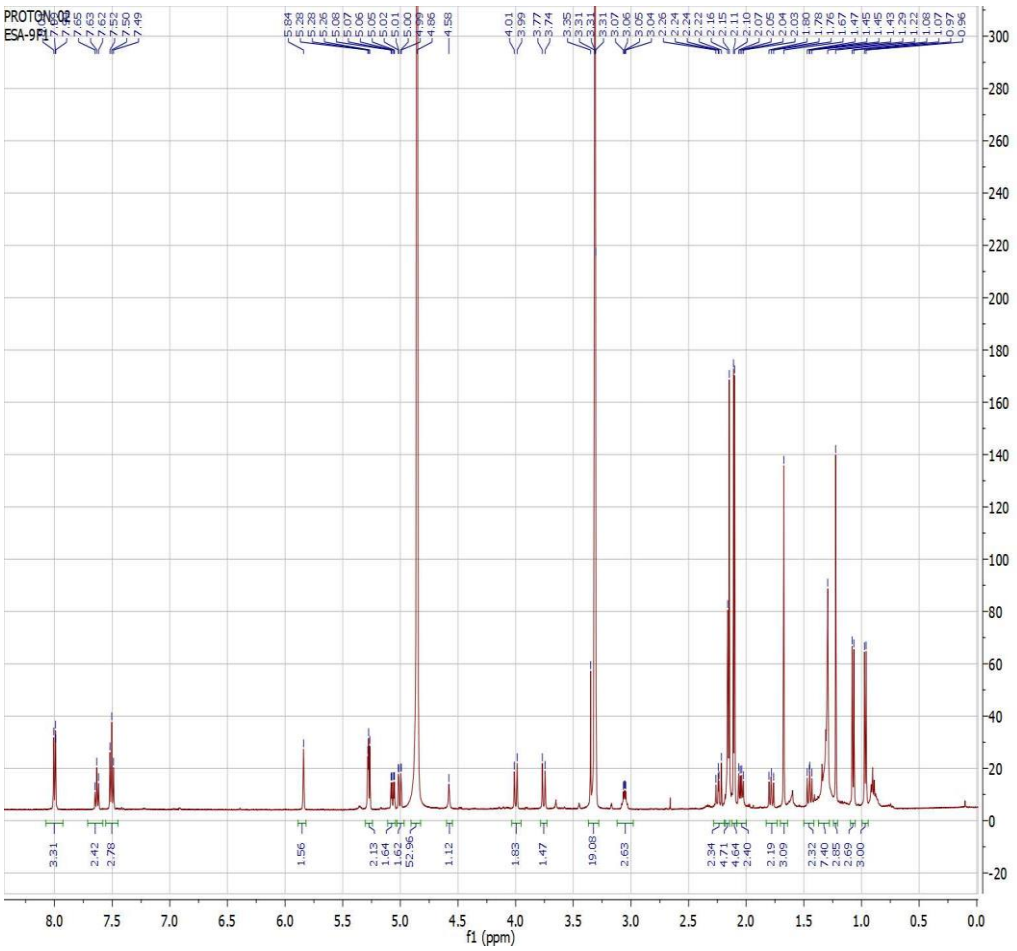

Figure S73. ^{1}H NMR (500 and 125 MHz, CD_3OD) spectra of **6**

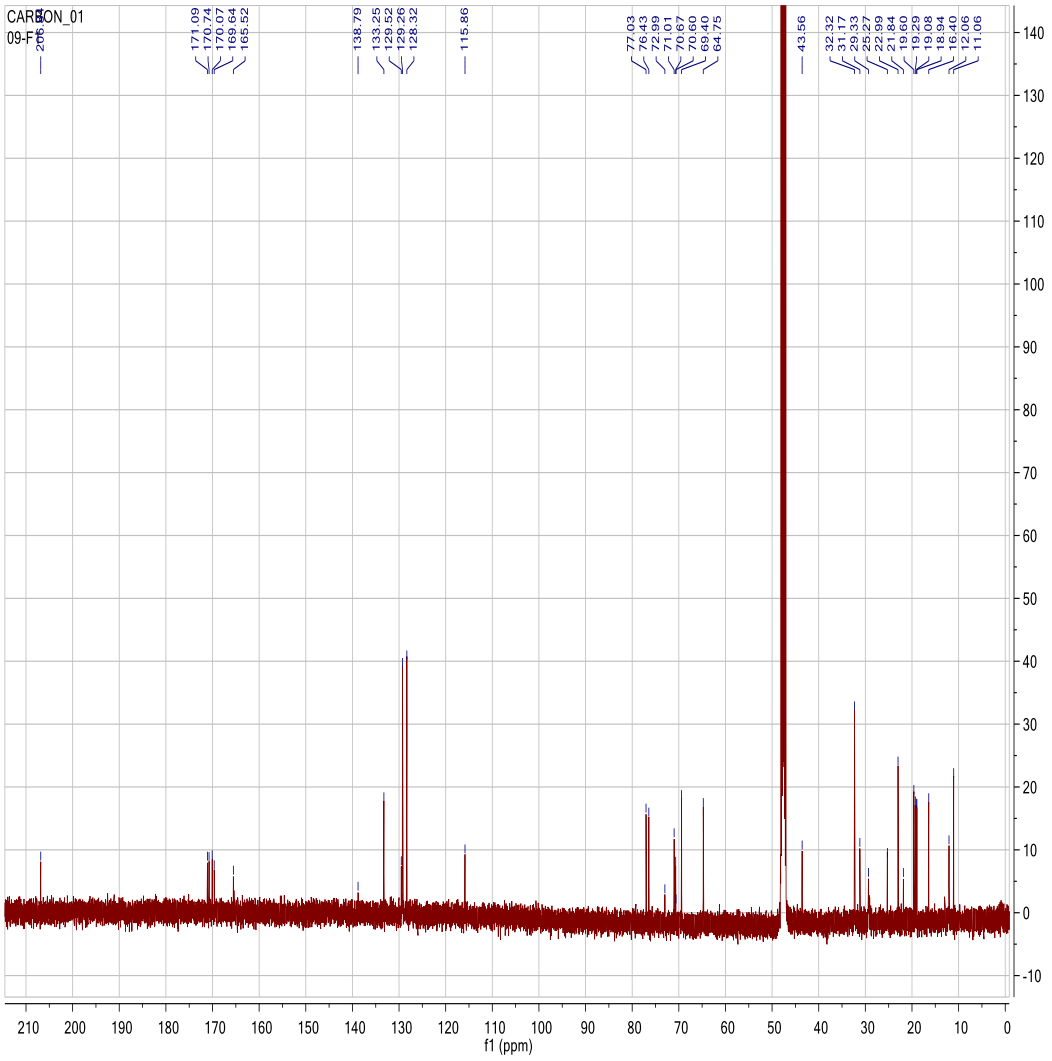

Figure S74. ^{13}C NMR (500 and 125 MHz, CD_3OD) spectra of **6**

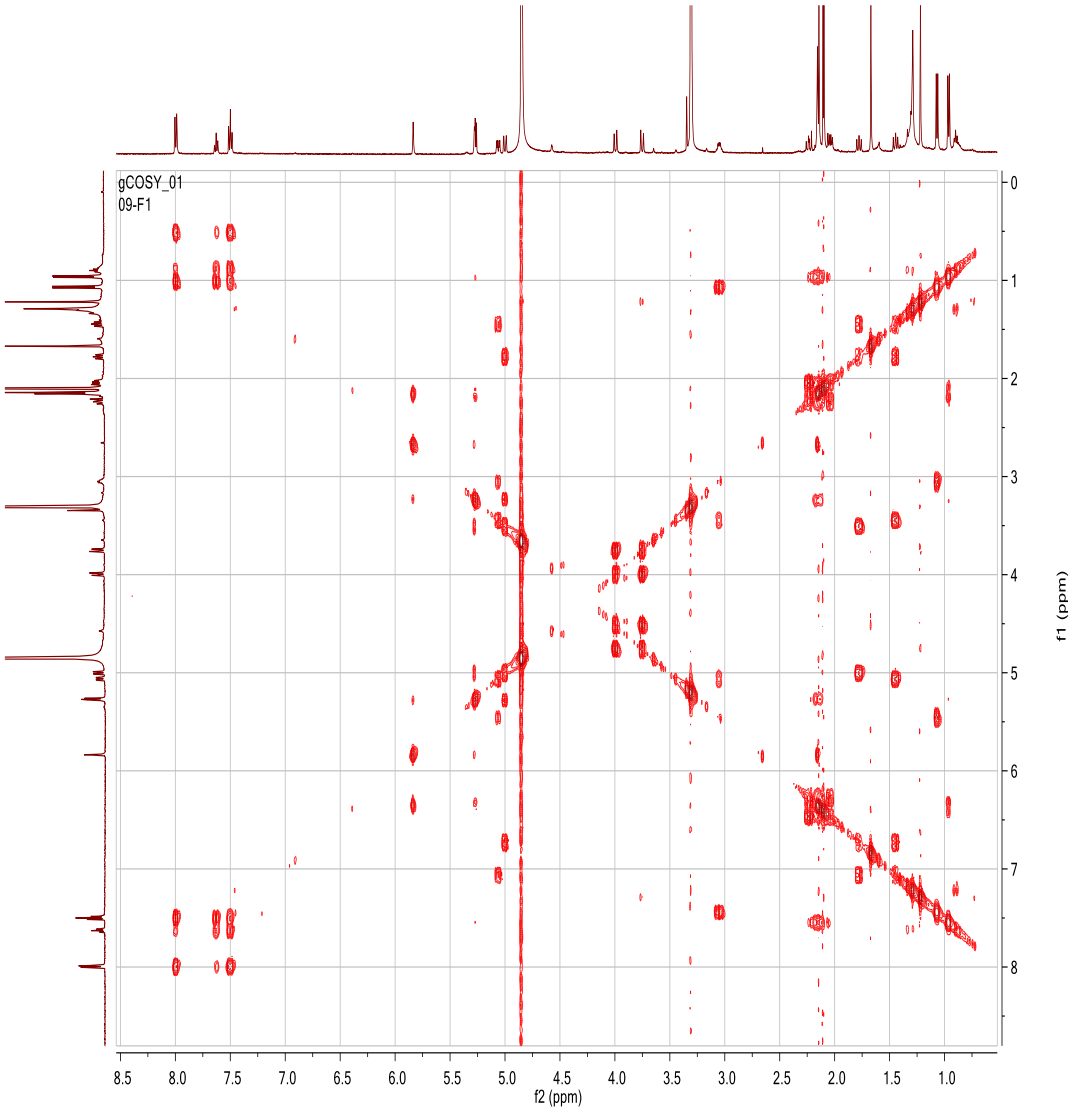

Figure S75. ^{1}H-^{1}H COSY (500 and 125 MHz, CD_3OD) spectra of **6**

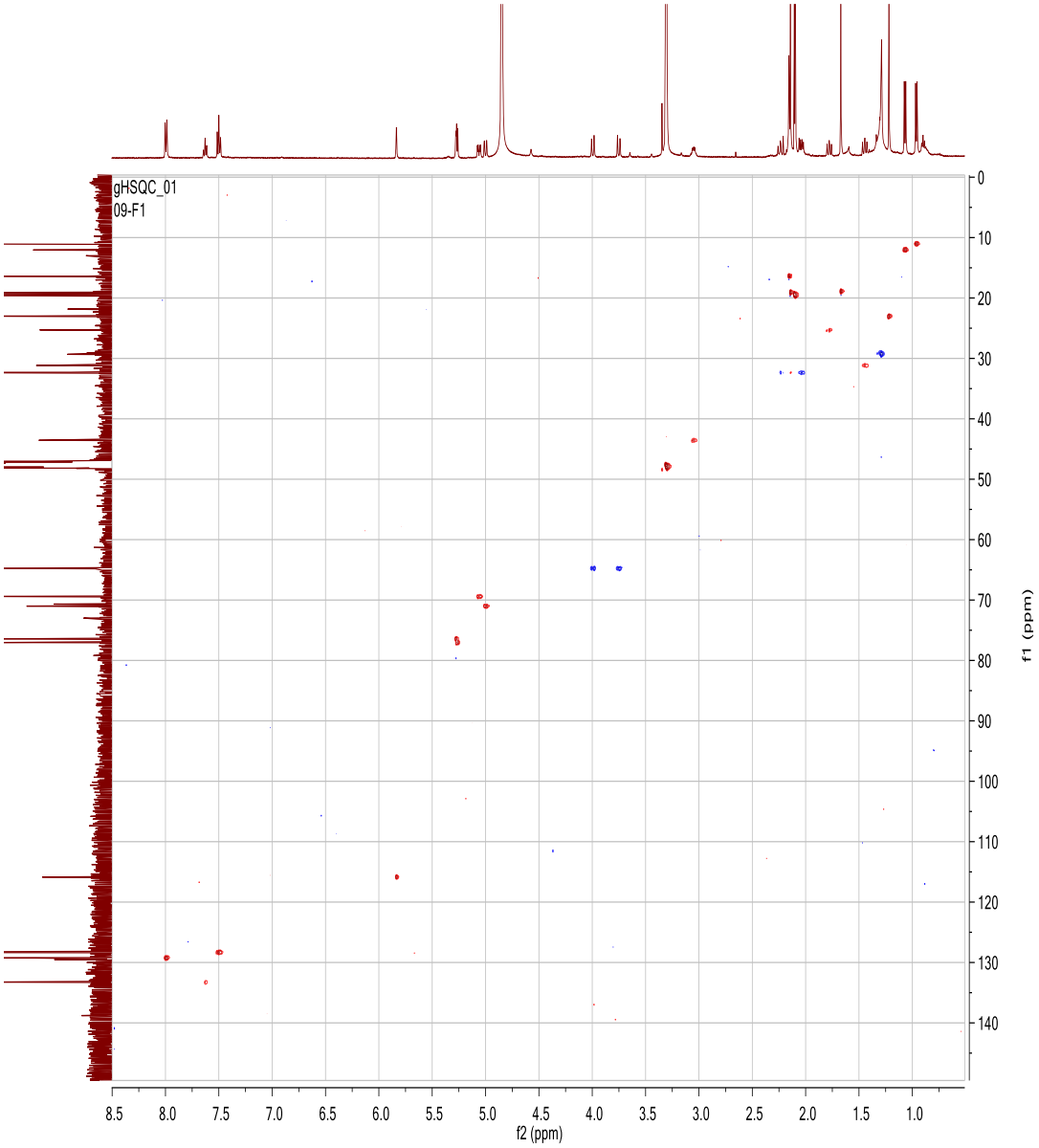

Figure S76. HSQC (500 and 125 MHz, CD_3OD) spectra of **6**

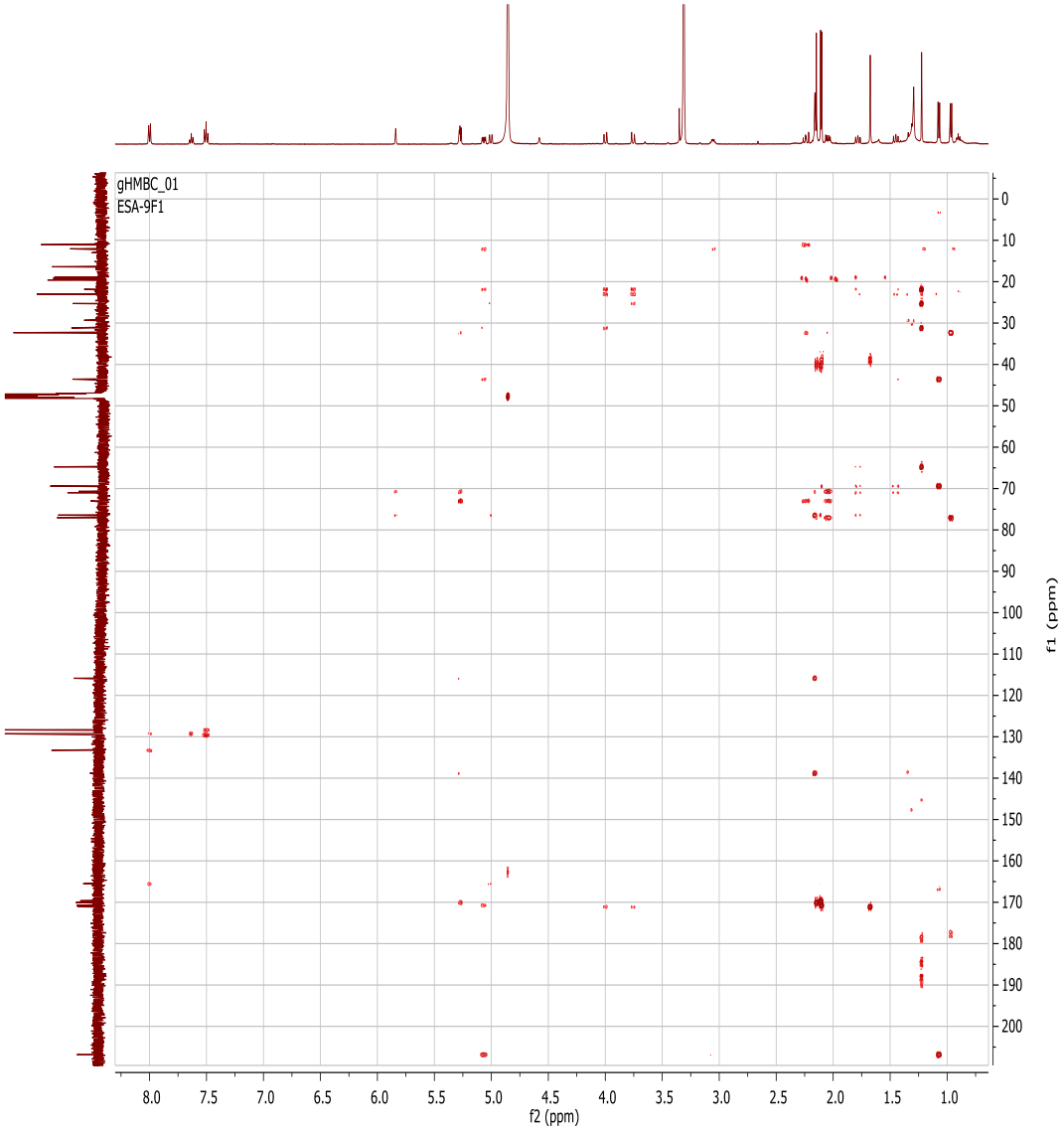

Figure S77. HMBC (500 and 125 MHz, CD_3OD) spectra of **6**

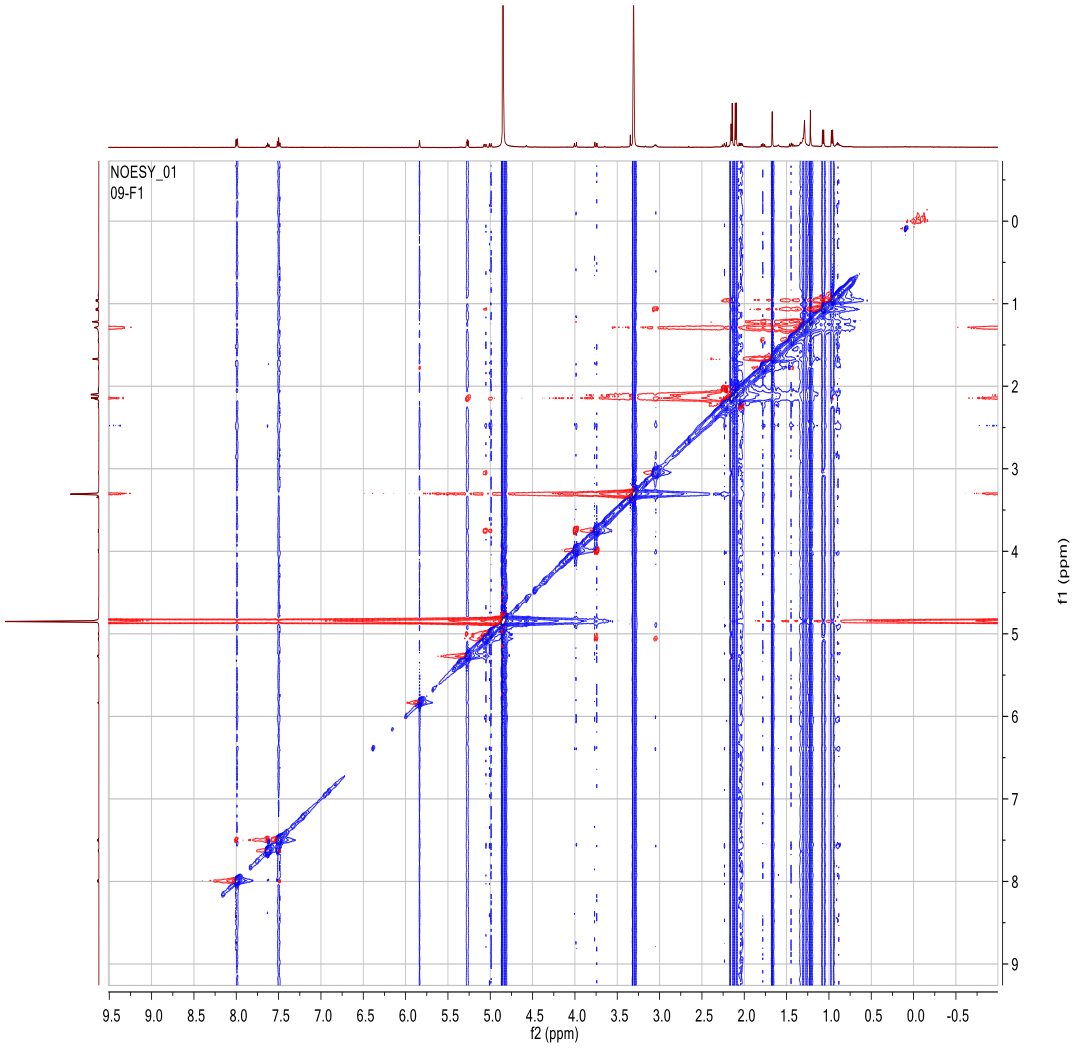

Figure S78. NOESY (500 and 125 MHz, CD_3OD) spectra of **6**

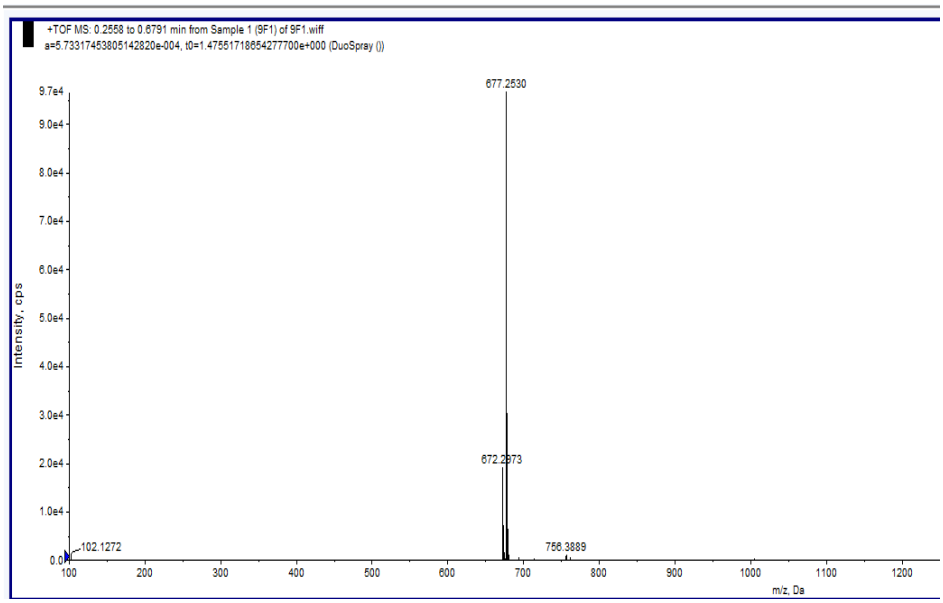

Figure S79. HRESI (+) MS spectra of **6**